USING NONCOVALENT BONDING TO IMPROVE THE INTERFACE BETWEEN GRAPHENE NANOPLATELETS AND AN EPOXY MATRIX

By

Christopher Cugini

A DISSERTATION

Submitted to
Michigan State University
in partial fulfillment of the requirements
for the degree of

Chemical Engineering – Doctor of Philosophy

2022

ABSTRACT

Epoxy polymers offer superior chemical and thermal resistance, mechanical properties, and are easily processable compared to similar performing materials. Graphene nanoplatelets (GnP) added as a nanofiller to a polymer create polymer nanocomposites with multifunctional properties. GnP, few-layer stacks of atomically thin graphene sheets with diameters in the micron range, have excellent mechanical, thermal, and electrical properties. Composite performance depends on the ability of the polymer to interact strongly with the GnP. Due to the platelet morphology and the chemically inert GnP basal plane surface, interactions with the epoxy resin are limited to a few edge sites and weak van der Waals intermolecular interactions with the basal plane. This dissertation investigates improving the noncovalent interfacial interactions between GnP and an epoxy resin through the use of a bi-functional interfacial molecule that can interact simultaneously with the GnP and epoxy polymer.

An interfacial molecule was synthesized to form strong noncovalent interactions with the GnP surface and covalent bonding with the epoxy resin utilizing a condensation reaction between 1-pyrenealdehyde and poly(oxypropylene) diamine. GnP-epoxy nanocomposites were produced using an epoxy/amine polymer matrix. Several model interfacial molecules were used to investigate the effects on the composite properties. A poly(oxypropylene) diamine was adsorbed onto the GnP surface and reacted with the epoxy in the curing process. The resulting composite exhibited reduced flexural modulus and glass transition temperature versus the unmodified GnP composites.

1-pyrenealdheyde was investigated as a molecule that could noncovalently attach to the GnP surface through π-π interactions. Due to the intercalative properties

of 1-pyrenealdehyde, the GnP was exfoliated and exhibited higher GnP concentration at the same loading volume. As a result, flexural modulus increased by 40%. However, due to a negligible change in interfacial interactions, the flexural strength, glass transition temperature, and loss modulus remained similar to the baseline GnP composites.

A third molecule, α-isopropyliminopyrene-ω-amino-poly[oxy(2-methylethylene)] (Py-POP), was synthesized in this research to both noncovalently attach to the GnP basal plane and react into the epoxy matrix. The pyrene end strongly interacts with the GnP surface, and the opposite end of the molecule participates in the epoxy curing mechanism. The length of the polypropylene segment increases the ability of this molecule to connect to the crosslinked epoxy network at a distance away from the GnP basal plane surface. The flexural modulus, flexural strength, and glass transition temperature was improved above the unmodified GnP composites. This signifies improved interfacial interactions between the GnP surface and epoxy matrix. Additionally, significantly increased electrical conductivity represents improved GnP dispersion quality and epoxy adhesion.

Stronger interfacial interactions between the GnP surface basal plane and epoxy polymer have shown to improve the composite multifunctionality. The combination of strong noncovalent interactions with the GnP basal plane along with covalent bonding with the epoxy resin using Py-POP resulted in stronger interfacial interactions compared with the poly(oxypropylene) diamine and 1-pyrenealdehyde. Noncovalent bonding an interfacial molecule onto the GnP basal plane improved the nanocomposite multifunctionality while reserving the excellent GnP properties.

ACKNOWLEDGEMENTS

Earning a PhD is not a small undertaking, and it requires a great deal of support in all aspects. First, I'd like to thank my advisor Dr. Lawrence Drzal for accepting me into his group and giving me the opportunity to grow and learn throughout the years.

I greatly appreciate the guidance from the CMSC staff, Per Askeland, Ed Drown, Brian Rook, and Mike Rich. From equipment training to data comprehension, I am thankful for them answering the countless questions I threw at them.

I want to especially thank my high school chemistry teacher Maggie Jones. She sparked my interest in chemistry and research and made me excited to learn more.

I am grateful for my fellow grad students Erik, Mario, Zeyang, Mariana, and Keith for being there to support my research. Thank you for your companionship that made my time at MSU more enjoyable.

Lastly, I want to thank my family and friends. I appreciate the unwavering support and friendship from Austin, Dustin, and Rachel. My mother Denise has been an invaluable supporter all throughout my life. I want to thank my brothers Michael and Matthew for their encouragement and support.

TABLE OF CONTENTS

LIST OF TABLES

LIST OF FIGURES

CHAPTER 1: INTRODUCTION

1.1 Project Background

Production of polymers and polymer composites is a large industry with widespread areas of application. Polymers have been used for their corrosion resistance, light weight, and ease of processing compared with other materials. Polymer composites provide additional mechanical, thermal, electrical, and gas barrier property enhancements over the base polymer depending on the filler used. Many types of composite fillers exist, though use of nanoscale fillers is of increasing interest as they offer excellent versatility. Nanoscale fillers can achieve multifunctional composite property enhancements due to their small size and high aspect ratio, resulting in a lighter weight composite and can be produced in a simplified process [24]. Additionally, nanofillers that are electrically or thermally conductive or are two dimensional can be tailored to provide desired composite properties.

Graphene nanoplatelets (GnP) have been shown to be attractive as a nanofiller for a wide variety of composite applications. While the edges of graphene nanoplatelet can consist of reactive chemical groups to provide chemical interaction with a polymer, the graphene basal plane surface of GnP, however, is chemically non-reactive and does not interact strongly with many polymers. Consequently, weak interfacial interactions result between the filler and a polymer matrix. To strengthen this interface, GnP has been functionalized covalently and noncovalently. Covalent functionalization of the graphene basal plane is difficult due to its relative chemical inertness [4]. One adverse side effect of covalent functionalization is the breakdown of the graphene structure. Converting the sp^2 carbons to sp^3 hybridization bends the bonds out of the flat plane

and reduces the mechanical, thermal, and electrical properties. Noncovalent functionalization, on the other hand, has the potential to attract molecules via intermolecular interactions, preserving the GnP basal structure and the GnP desirable properties. This noncovalent attached molecule can be selected specifically for the application by utilizing an ‘anchor’ terminal chemical group to strongly interact with the GnP surface and designing the rest of the molecule to be specifically attracted to the polymer matrix. Attaching the desired molecule to the GnP surface noncovalently is a relatively facile process as it relies on intermolecular bonding interactions rather than chemical reactions. As the anchored molecule increases in chain length, it is expected to extend away from the GnP surface. Using a tailored molecule to form strong interactions between the GnP surface and epoxy resin can improve the composite properties.

1.2 Graphene Nanoplatelets

Graphene sheets are atom thick layers of six-membered carbon aromatic rings first isolated in 2004 by Novoselov et al [23]. There are many methods of producing graphene including growth by chemical vapor deposition, growth onto a silicon carbide substrate, mechanical exfoliation of graphite, use of graphite intercalation compounds, and oxidation of graphite to graphene oxide (GO) followed by a chemical reduction step [19]. While some of these methods excel in producing pristine monolayer graphene sheets, they are not suitable for scaling up to large volume processing. Of these, the graphite intercalation and GO methods are scalable approaches for use in composite materials.

1.2.1 Intercalation

Acids have been used to intercalate graphite to create graphite intercalation compounds. This material is comprised of small diameter platelets of graphite (Figure 1.1). By rapidly heating the graphite intercalation compound to a high temperature, the intercalant volatilizes and causes the graphite to expand to 300-500 times its initial volume to form expanded graphite “worms.” Lastly, these graphene nanoplatelets are formed by breaking apart the expanded graphite “worms” through ultrasonication in a liquid. The graphene nanoplatelets (GnP) are high aspect ratio 2D structures of a few layers of graphene (5 – 15 nm in thickness and range from 1 – 25+ μm in diameter). The GnP nanoparticles have exceptional mechanical, thermal, electrical properties and because of their platelet morphology can impart gas and liquid impermeability properties to any polymer into which they are dispersed. The GnP basal plane is a graphene surface free of functional groups, resulting in a chemically inert, hydrophobic surface. As a result of the acid intercalation and thermal exfoliation method, the edges also contain a small fraction of oxygen functional groups. While these are available for reaction, the GnP edge to surface area ratio is very low (~3%), which results in a small site for chemical reaction with a polymer.

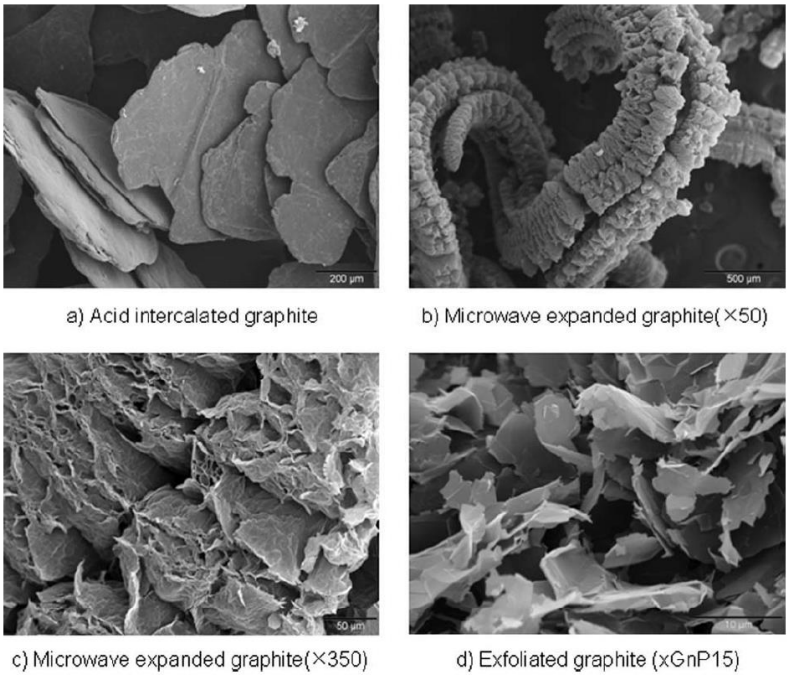

Figure 1.1: Scanning electron microscope images of several stages in the production of graphene nanoplatelets [17].

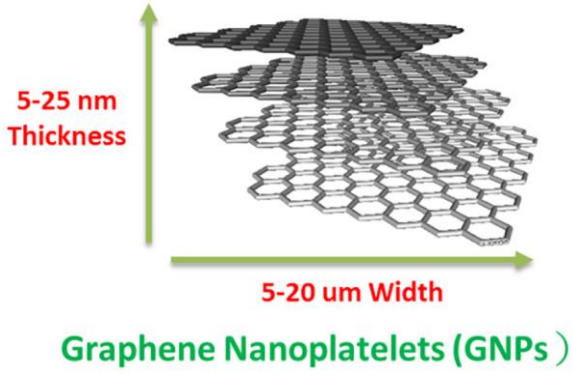

Figure 1.2: Graphene nanoplatelets [1].

1.2.2 Graphene Oxide (GO)

Producing GO involves thoroughly oxidizing GnP using strong mineral acids and oxidizing agents as described in the Hummers method for example [33]. The GO consists of single to few layers of graphene heavily populated with oxygen functional groups. Typically, the basal plane contains epoxy and hydroxyl groups while carboxylic

acid groups exist at the edges. As a result of the conversion of the sp^2 carbons to sp^3 hybridization through oxidation, the flat graphene sheet is transformed into a corrugated structure. Compared with pristine graphene, GO exhibits reduced modulus and strength and is electrically and thermally non-conductive. On the other hand, GO is hydrophilic and has many sites available for functionalization. Chemically reducing GO into reduced GO (rGO) has been found to restore the graphene structure except for the regions where the functional surface groups have been added. Electrical and thermal conductivity are increased. However, the reduction process removes some carbon atoms from the basal plane leaving holes in the basal plane which consequently does not completely recover its mechanical properties.

Because of the multifunctionality of graphene, it has been utilized for various applications. These include electronics, batteries, gas-impermeable membranes, mechanical reinforcement, fire retardancy, sensor technology, and thermally stabilized materials [10], [13], [28]. A common obstacle for incorporating GnP into polymers is the difficulty in achieving high dispersion of the nanoparticles. The highly hydrophobic surface of the basal plane results in poor, nonuniform dispersion as the nanoplatelets, with a tendency to agglomerate, interferes with achieving polymer composites' multifunctionality at low concentrations. The primary cause of this is the relatively chemically inert GnP basal plane, which limits intermolecular interactions with the polymer matrix. While GO is one solution to this issue as its oxygen-functionalized basal plane is hydrophilic and chemically reactive, the two-step chemical reaction process to create GO is time consuming and requires corrosive materials. Additionally, the loss of basal plane carbon atoms makes the GO route less attractive than chemical

intercalation and direct exfoliation.

1.3 Epoxy Resins

Epoxy resins are an important type of thermoset polymer material, commonly cured by polyfunctional primary amines to form a three-dimensional crosslink network. Because of their desirable properties such as chemical and temperature resistance, good mechanical properties and adhesion, epoxies are used in automotives, aerospace, and other high-performance composite materials and adhesives. During the curing process, a primary amine reacts with an epoxy to form a secondary amine, a secondary amine reacts with an epoxy to form a tertiary amine, and a hydroxyl group reacts with an epoxy to form an ether linkage (Figure 1.3). The characteristics of a cured epoxy rely on the stoichiometry between the resin and hardener and the curing cycle.

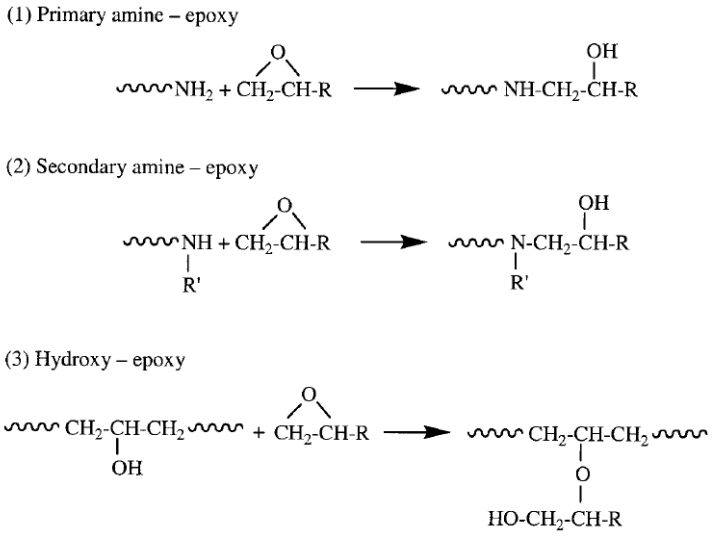

Figure 1.3: Epoxy resin and amine curing reactions [21].

Addition of fillers to epoxy resin further improve the composite properties. Stress is transferred from the epoxy matrix to the filler for additional mechanical support. Especially in the case of nanofillers, the interaction between the filler and epoxy dictates the efficiency of the mechanical stress transfer, thermal and electrical conductivity

improvements, and dispersion quality. Stronger interactions induce better dispersion, stress transfer, and overall properties. The presence of fillers can also hinder crosslink formation during cure, resulting in a lower crosslink density and lower brittleness. Similarly, the reactivity of the filler needs to be considered to understand the property changes. Fillers that will readily react with the epoxy or hardener change the curing stoichiometry, which can significantly affect the epoxy network [9].

1.4 Processing Polymer Nanocomposites

There are several methods that can be used to successfully incorporates GnP into polymers. Melt mixing is a process that thoroughly mixes GnP into thermoplastics. [10], [13]. The polymer is heated to its melting point and the GnP is added while screws mechanically mix the components together. Results of the shear forces applied during this process are exfoliation and size breakdown of the platelets. While a good dispersion can be obtained, introduction of the nanofiller increases the viscosity of the system and hinders the effectiveness of the mixing. Similarly, prolonged mixing times become necessary with higher filler concentration, and subjecting the polymer to high temperatures for long periods may cause deterioration.

Solution mixing is an alternate method for integrating GnP into a thermoplastic polymer [18], [11], [15]. Adding a solvent reduces the viscosity of the system for improved mixing. By dispersing the GnP in a solvent before adding the mixture to the epoxy, the aggregates are broken up for easier dispersion. After the GnP is dispersed in the polymer, via ultrasonication or three-roll milling, the solvent is removed before casting it into a mold. This method is less desirable moving to an industrial scale.

Due to the chemically inert, hydrophobic GnP basal plane surface, many

polymers interact weakly with GnP. Liquid ultrasonication, three-roll milling, and planetary ball milling are processing methods that can produce a composite with a high degree of GnP dispersion. These methods involve a large amount of energy transfer to fragment the GnP agglomerates. Prolonged processing, however, can result in a reduction in platelet size.

1.5 Modifying Graphene Nanoplatelets

Commonly, a major limiting factor in improving composite properties is achieving a high degree of interfacial interaction between the graphene and epoxy resin interface. Weak interfacial interactions result in poor dispersion and GnP agglomeration. Improving this interface contributes to a better dispersed composite and, in turn, a greater improvement in the composite's properties. Unmodified GnP are hydrophobic due their inert basal plane, which does not strongly interact with most epoxies. By attaching a molecule to the GnP surface that interacts favorably with the epoxy, the GnP can disperse well and prevent fracture propagation at the interface.

While covalent bonding to the GnP basal plane is possible, it requires harsh chemical conditions and can reduce the graphene properties [4]. Although there are functional groups available for covalent bonding at the GnP edges, the low volume compared with the platelet limits this effectiveness. Another option is noncovalent bonding, which utilizes intermolecular interactions to attach to the GnP surface. The carbon aromatic structure of GnP exhibits π-π bonding out of plane, allowing for strong intermolecular bonding through π-π stacking. Simulations performed by Li et al. [20] showed that polycyclic aromatic hydrocarbons (PAH) strongly interact with the graphene surface through physisorption. The adsorption energy increases as PAHs increase in

size and hydrophobicity.

1.6 Problem Statement

The research described in this dissertation focuses on improving the interface between the GnP surface and epoxy resin for the purpose of enhancing polymer composite properties by creating an interfacial molecule that will noncovalently interact strongly with the GnP basal plane surface and covalently bond with the epoxy during cure. The objective is to achieve improved mechanical, thermal, electrical, and dispersive properties. Noncovalent interactions would enhance the interaction between the GnP and the polymer without requiring a chemical modification of the GnP basal plane.

1.7 Dissertation Outline

The research presented in this dissertation is divided into four main chapters to describe the results on investigating the interactions between the GnP basal plane and a suitable coupling molecule that can both interact noncovalently with the basal plane and chemically react with the epoxy matrix. Chapter 2 discusses the synthesis of an oligomer with the desired interactivity between both the GnP surface and epoxy. Chapter 3 examines the effects on the GnP nanocomposite by introducing an interfacial molecule that has strong interaction with the epoxy, but weak interaction with the GnP surface. Conversely, the contents of Chapter 4 regard an interfacial molecule that has a strong interaction with the GnP surface and weak interaction with the epoxy resin. Chapter 5 then investigates the affects a strong interaction between both sides of the interface has on GnP nanocomposites.

BIBLIOGRAPHY

[1] Chiou, Yung-Chuan, Hsin-Yin Chou, and Ming-Yuan Shen. "Effects of adding graphene nanoplatelets and nanocarbon aerogels to epoxy resins and their carbon fiber composites." Materials & Design 178 (2019): 107869.

[2] Cho, Jaehyun, et al. "Improving dispersion and barrier properties of polyketone/graphene nanoplatelet composites via noncovalent functionalization using aminopyrene." ACS applied materials & interfaces 9.33 (2017): 27984-27994.

[3] Choi, Wonbong, et al. "Synthesis of graphene and its applications: a review." Critical Reviews in Solid State and Materials Sciences 35.1 (2010): 52-71.

[4] Chua, Chun Kiang, and Martin Pumera. "Covalent chemistry on graphene." Chemical Society Reviews 42.8 (2013): 3222-3233.

[5] Cooper, Daniel R., et al. "Experimental review of graphene." International Scholarly Research Notices 2012 (2012).

[6] Dhand, Vivek, et al. "A comprehensive review of graphene nanocomposites: research status and trends." Journal of Nanomaterials 2013 (2013).

[7] Fendarkar, D. A., et al. "Modification and Functionalization of Graphene/Graphene oxide." Methods 12 (2015): 13.

[8] Guo, Yongqiang, et al. "Factors affecting thermal conductivities of the polymers and polymer composites: A review." Composites Science and Technology 193 (2020): 108134.

[9] Gupta, V. B., et al. "The temperature-dependence of some mechanical properties of a cured epoxy resin system." Polymer Engineering & Science 25.13 (1985): 812-823.

[10] Honaker, K., F. Vautard, and L. T. Drzal. "Investigating the mechanical and barrier properties to oxygen and fuel of high density polyethylene–graphene nanoplatelet composites." Materials Science and Engineering: B 216 (2017): 23-30.

[11] Hu, Guangjun, et al. "Low percolation thresholds of electrical conductivity and rheology in poly (ethylene terephthalate) through the networks of multi-walled carbon nanotubes." Polymer 47.1 (2006): 480-488

[12] Jawaid, Mohammad, Mohamed Thariq, and Naheed Saba, eds. Failure analysis in biocomposites, fibre-reinforced composites and hybrid composites. Woodhead Publishing, 2018.

[13] Jiang, Xian, and Lawrence T. Drzal. "Multifunctional high density polyethylene nanocomposites produced by incorporation of exfoliated graphite nanoplatelets 1:

morphology and mechanical properties." Polymer Composites 31.6 (2010): 1091-1098.

[14] Karkanas, Panagiotis I., and Ivana K. Partridge. "Cure modeling and monitoring of epoxy/amine resin systems. I. Cure kinetics modeling." Journal of applied polymer science 77.7 (2000): 1419-1431.

[15] Kilic, Ugur, Muhammad M. Sherif, and Osman E. Ozbulut. "Tensile properties of graphene nanoplatelets/epoxy composites fabricated by various dispersion techniques." Polymer Testing 76 (2019): 181-191.

[16] Kim, Hyunwoo, Ahmed A. Abdala, and Christopher W. Macosko. "Graphene/polymer nanocomposites." Macromolecules 43.16 (2010): 6515-6530.

[17] Kim, Sumin, Inhwan Do, and Lawrence T. Drzal. "Thermal stability and dynamic mechanical behavior of exfoliated graphite nanoplatelets-LLDPE nanocomposites." Polymer composites 31.5 (2010): 755-761.

[18] Lavoratti, Alessandra, Ademir José Zattera, and Sandro Campos Amico. "Mechanical and dynamic-mechanical properties of silane-treated graphite nanoplatelet/epoxy composites." Journal of Applied Polymer Science 135.45 (2018): 46724.

[19] Lee, Xin Jiat, et al. "Review on graphene and its derivatives: Synthesis methods and potential industrial implementation." Journal of the Taiwan Institute of Chemical Engineers 98 (2019): 163-180.

[20] Li, Bing, et al. "Polycyclic aromatic hydrocarbons adsorption onto graphene: a DFT and AIMD study." Materials 11.5 (2018): 726.

[21] Liu, Heping, et al. "Influence of substituents on the kinetics of epoxy/aromatic diamine resin systems." Journal of Polymer Science Part A: Polymer Chemistry 42.13 (2004): 3143-3156.

[22] Mittal, Garima, et al. "A review on carbon nanotubes and graphene as fillers in reinforced polymer nanocomposites." Journal of Industrial and Engineering Chemistry 21 (2015): 11-25.

[23] Novoselov, Kostya S., et al. "Electric field effect in atomically thin carbon films." science 306.5696 (2004): 666-669.

[24] Potts, Jeffrey R., et al. "Graphene-based polymer nanocomposites." Polymer 52.1 (2011): 5-25.

[25] Preghenella, Michele, Alessandro Pegoretti, and Claudio Migliaresi. "Thermo-mechanical characterization of fumed silica-epoxy nanocomposites." Polymer 46.26 (2005): 12065-12072.’

[26] Shokrieh, M. M., et al. "Effect of Graphene Nanosheets (GNS) and Graphite Nanoplatelets (GNP) on the Mechanical Properties of Epoxy Nanocomposites." Science of Advanced Materials 5 (2013): 1-7.

[27] Smith, Ieuan T. "The mechanism of the crosslinking of epoxide resins by amines." Polymer 2 (1961): 95-108.

[28] Szeluga, Urszula, et al. "Effect of graphene filler structure on electrical, thermal, mechanical, and fire retardant properties of epoxy-graphene nanocomposites-a review." Critical Reviews in Solid State and Materials Sciences 46.2 (2021): 152-187.

[29] Terrones, Mauricio, et al. "Interphases in graphene polymer-based nanocomposites: achievements and challenges." Advanced Materials 23.44 (2011): 5302-5310.

[30] Thalib, Nur Bazilah, et al. "Tailoring graphene reinforced thermoset and biothermoset composites." Reviews in Chemical Engineering 36.5 (2020): 623-652.

[31] Umboh, Markus Karamoy, et al. "Mechanical properties of nano-silica particulate-reinforced epoxy composites considered in terms of crosslinking effect in matrix resins." Journal of Materials Science 48.15 (2013): 5148-5156.

[32] Wang, Fuzhong, et al. "Mechanical properties and thermal conductivity of graphene nanoplatelet/epoxy composites." *Journal of materials science* 50.3 (2015): 1082-1093.

[33] Yu, Wang, et al. "Progress in the functional modification of graphene/graphene oxide: A review." RSC advances 10.26 (2020): 15328-15345.

CHAPTER 2: SYNTHESIS OF PYRENE TERMINATED POLY(OXYPROPYLENE) DIAMINES

2.1 Abstract

Noncovalent bonding to the graphene nanoplatelet (GnP) basal plane surface is a potential method to increase GnP interaction with polymers and introduce composite multifunctionality. Pyrene shares the six-membered carbon aromatic ring structure with graphene which allows for strong intermolecular bonding through π – π stacking. Optimal design of using pyrene as a coupling agent for GnP in an epoxy matrix would be achieved by adding pyrene to one end of poly(oxypropylene) diamine. A Schiff base condensation reaction was investigated as the approach to achieve this desired structure. The pyrene terminated monofunctional poly(oxypropylene) amine (Py-POP) product was successfully synthesized in acceptable purity. In addition, there was negligible evidence that a molecule with a pyrene moiety terminating both ends was produced by carefully controlling the stoichiometry and reaction procedure.

2.2 Introduction

Graphene nanoplatelets (GnP) consist of several stacked layers of graphene with diameters in the micron range. GnP consists of an uninterrupted six-membered carbon aromatics ring structure which enables strong intermolecular bonding through π – π stacking. Polycyclic aromatic hydrocarbons (PAH) have the same structure of GnP but at a fraction of the size. Therefore, PAHs can noncovalently bond to the GnP surface through π – π bonding interactions without altering the GnP structure. Maintaining the GnP structure retains its desired mechanical, thermal, and electrical properties. Several studies, [2], [5], [6], [8], [9], [16], [17], show that PAHs readily adsorbed to the

GnP surface through π – π stacking. Similarly, Li et al [8] performed simulations that showed adsorption energy increased with number of carbons present, i.e., the larger the PAH is, the higher adsorption energy. The various adsorption configurations were found to have similar adsorption energies, enabling the PAHs to rotate and move along the GnP surface without outside interaction. Because of the similar hydrophobicity of PAHs and GnP, adsorption can be expedited by using a polar solvent. Conditions necessary to induce adsorption are a polar solvent, dispersed GnP, and prolonged mixing time at room temperature.

Because of this interaction, PAHs can be used to anchor tailored molecules for desired properties. In this way, the PAH holds the molecule at the GnP surface, altering its intermolecular interactions and reactivity with chemical systems, such as an epoxy matrix. In this study, pyrene was the chosen PAH to act as an anchor for Jeffamine D2000, a poly(oxypropylene) diamine. To attach a pyrene moiety to the Jeffamine D2000, a Schiff base condensation reaction was utilized between 1-pyrenealdehyde and the primary amines at the ends of the polymer. In particular, the desired product was a Jeffamine D2000 molecule with one pyrene terminated end and a primary amine at the other. The reaction between the aldehyde and primary amine produces an imine bond and a water molecule. As this a reversible reaction, presence of water in the mixture will reduce the yield. Because of the symmetry of the D2000 molecule, there is no preference for which end the 1-pyrenealdehyde will bond with. However, using a stoichiometric amount of each reactant and adding the 1-pyrenealdehyde stepwise is expected to reduce the amount of difunctional D2000 products.

As the pyrene attaches to the GnP surface, the polymer chain can extend out

and be available for reaction. This modified GnP will be used in an epoxy resin and primary amine curing agent system to be discussed in later chapters. The D2000 amine is expected to be involved in the curing mechanism by reacting with the epoxy resin. This product will be used to noncovalently couple to the GnP surface and crosslink into the epoxy matrix in order to improve the dispersion and adhesion of the GnP and the resulting composite properties.

2.3 Materials and Methods

2.3.1 Materials

1-pyrenealdehyde, toluene, and ethanol were purchased from Sigma Aldrich, used as received. Poly(oxypropylene) diamine known by its trade name Jeffamine D2000 (Hunstman) has an average molecular weight of 2000 g/mol and amine hydrogen equivalent weight of 514 g/eq.

2.3.2 Schiff Base Condensation Reaction

In this process, the reaction mixture was heated to reflux in an oil bath and mechanically stirred with a stir bar. A Dean-Stark apparatus and condenser were used to separate the water formed during the reaction from the toluene solvent. To produce the single pyrene functionalized Jeffamine D2000, α-isopropyliminopyrene-ω-amino-poly[oxy(2-methylethylene)] (Py-POP), a 1.1:1 molar ratio of 1-pyrenealdehyde to Jeffamine D2000 was used. First, Jeffamine D2000 was dissolved in toluene in a round-bottom flask and heated to reflux at ~160 °C. Separately, 1-pyrenealdehyde was dissolved in toluene and added stepwise to the reflux mixture every 20 minutes. After the reaction was completed, the remaining solvent was removed via the Dean-Stark apparatus at elevated temperature. The residual solvent remaining was removed in a

vacuum oven overnight at room temperature.

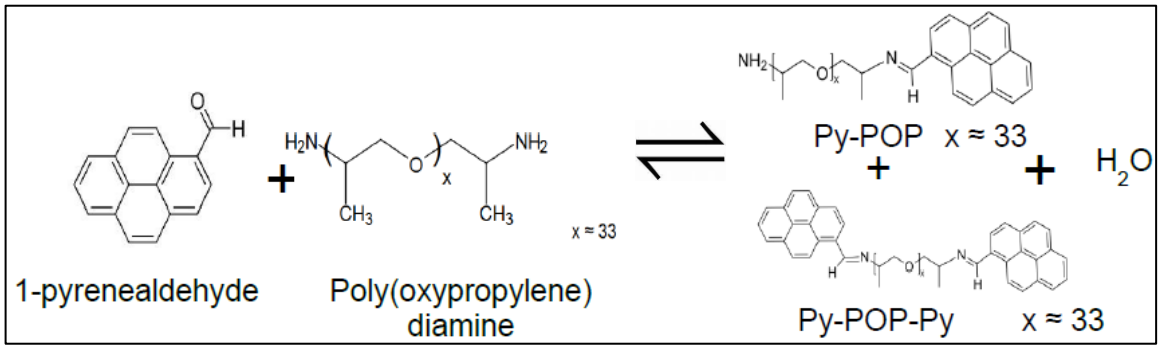

Figure 2.1: Condensation reaction between 1-pyrenealdehyde and Jeffamine D2000.

2.3.3 Characterization Techniques

The Jasco FT/IR-4600 was used to perform Fourier-transform infrared spectroscopy (FTIR) to analyze the synthesized molecules. These samples are in liquid form, so they were sandwiched between two pellets of compressed potassium bromide for analysis. The absorbance spectra were measured from 400 – 4000 cm^{-1}.

The TA Instruments TGA Q500 was used for thermogravimetric analysis (TGA) of the samples' thermal stability. Heating rate was set at 10 °C/min to 500 °C in a nitrogen atmosphere. The TA Universal Analysis program was used to collect weight % measurements and derivative of weight changes. Decomposition onset temperature was determined using ASTM E2550.

Reaction products were analyzed through fluorescent spectroscopy using the Photon Technology International Fluorometer. Pyrene is the only significantly fluorescent component in this system, and peak shifts relate to chemical changes. Samples were diluted in pure ethanol at a concentration of 5 µg/mL. Analysis conditions were set to excitation wavelength at 350 nm and measured the emission over a range of 365 – 600 nm.

A Waters Xevo G2-XS UPLC/MS/MS machine utilizing a quadrupole time-of-flight method to measure molecule weight distribution. Samples were diluted in methanol and ionized by electrospray ionization in positive ion mode. Singly charged ion distributions were used to calculate the molecular weight distribution.

2.4 Results and Discussion

2.4.1 Reagent Characterization

1-pyrenealdehyde and Jeffamine D2000 were analyzed individually. FTIR absorbance shows peaks of prominent bonds present in each molecule. For 1-pyrenealdehyde, the peaks of interest are as follows. The aldehyde functional group is shown through a carbonyl peak, C=O (1680 cm^{-1}), and C-H bonds (2715, 2864 cm^{-1}). The aromatic nature of 1-pyrenealdehyde, which is not present in Jeffamine D2000, is characteristic of the molecule. Aromatic C-H bonds form peaks at 700-900 cm^{-1} and at 3039 cm^{-1}. Jeffamine D2000, a poly(oxypropylene) diamine, shows a strong ether peak, C-O, at 1105 cm^{-1} since it is contained in the repeating unit. Peaks formed due to primary amine N-H occur at 1550-1700 and 3100-3500 cm^{-1}. Lastly, sp^3 hybridized C-H bonds form strong peaks at 1372, 1450, and 2800-3000 cm^{-1}.

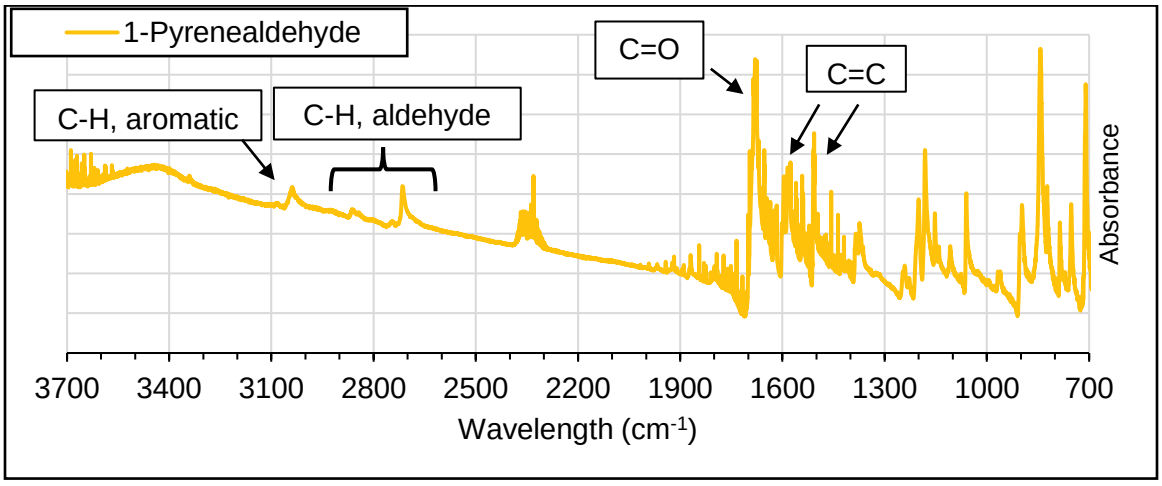

Figure 2.2: FTIR spectra for 1-pyrenealdehyde and Jeffamine D2000.

Figure 2.2 (cont'd)

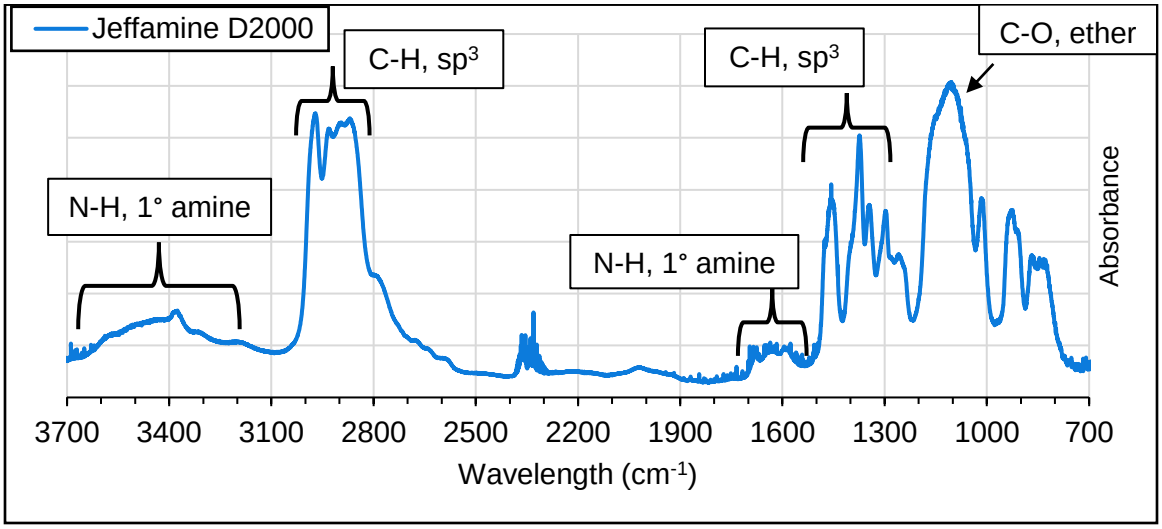

Thermogravimetric analysis was used to determine the decomposition onset temperature and the temperature at the largest loss in weight %. 1-pyrenealdehyde shows its highest loss of weight % at 278 °C, and Jeffamine D2000 at 348 °C. Decomposition onset temperature is found in Table 2.1.

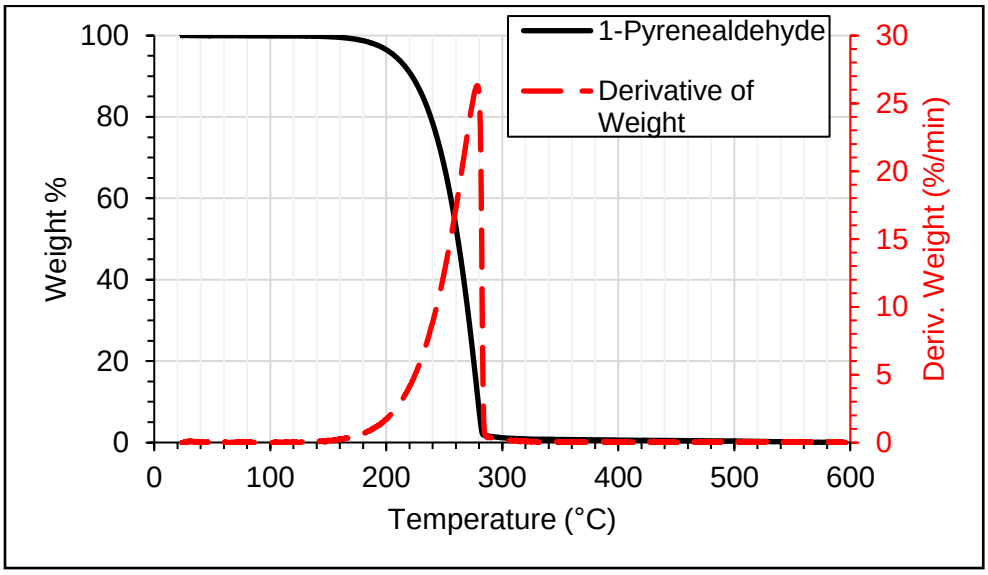

Figure 2.3: Weight loss decomposition data for 1-pyrenealdehyde and Jeffamine D2000.

Figure 2.3 (cont'd)

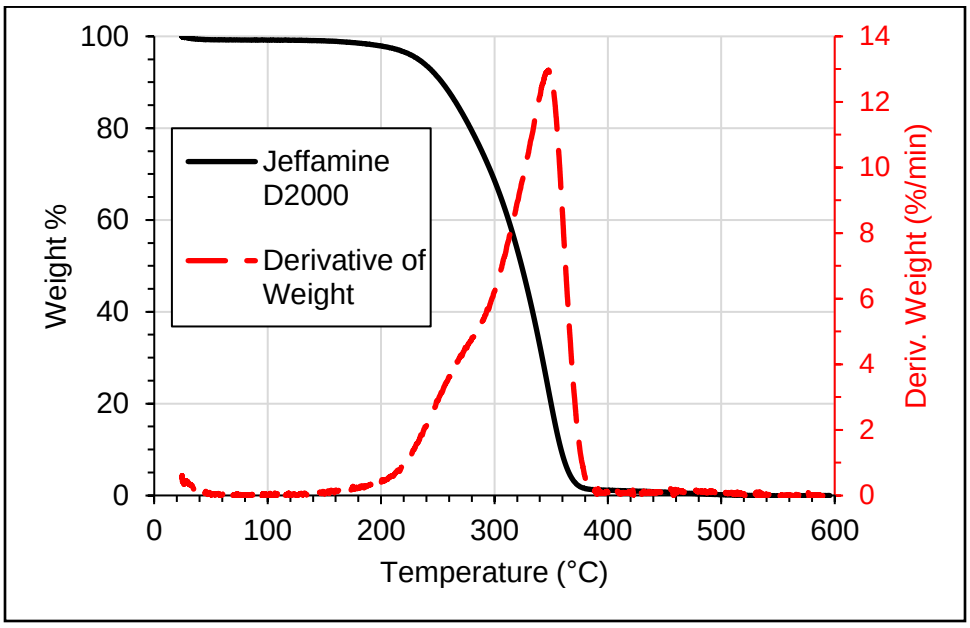

Table 2.1: Decomposition onset temperatures.

Sample	**Decomposition Onset Temp (°C)**
1-Pyrenealdehyde	131
Jeffamine D2000	101

Mass spectrometry determines the molecular weight of 1-pyrenealdehyde to be 231 g/mol, which also matches the NIST reference [12]. Jeffamine D2000, however, is represented by a molecular weight distribution. Based on the data, the most common molecular weight is 1875 g/mol which corresponds with 31 repeating units in a range of 1300 – 2400 g/mol.

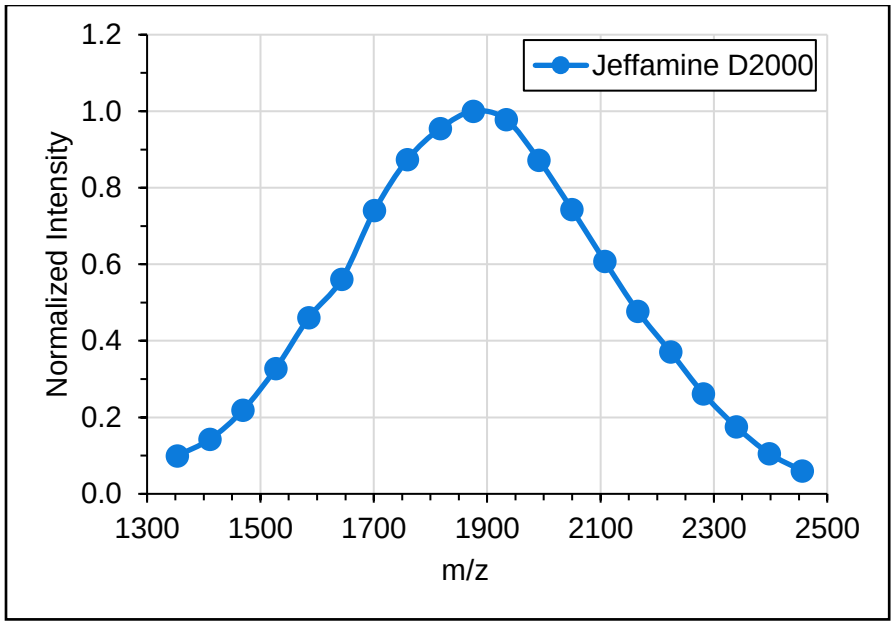

Figure 2.4: Mass spectrometry data for Jeffamine D2000 showing molecular weight distribution.

Aromatic organic molecules tend to exhibit fluorescence. Since pyrene is a known fluorescent molecule, fluorescence spectroscopy was used to analyze changes in molecular structure in the imine product. Figure 2.5 shows the normalized fluorescence spectra for 1-pyrenealdehyde and Jeffamine D2000. Using an excitation wavelength of 350 nm, 1-pyrenealdehyde exhibited a strong peak at 446 nm. Jeffamine D2000 was very weakly fluorescent in this range and showed two peaks at 391 and 425 nm. These samples were dispersed in ethanol, which does not contribute any fluorescence. An equimolar mixture of 1-pyrenealdehyde and Jeffamine D2000 showed the same peak as 1-pyrenealdehyde at 446 nm and a weak shoulder peak at ~390 nm due to the presence of Jeffamine D2000. Therefore, the intermolecular interactions between these two molecules do not significantly affect the fluorescence of the 1-pyrenealdehyde.

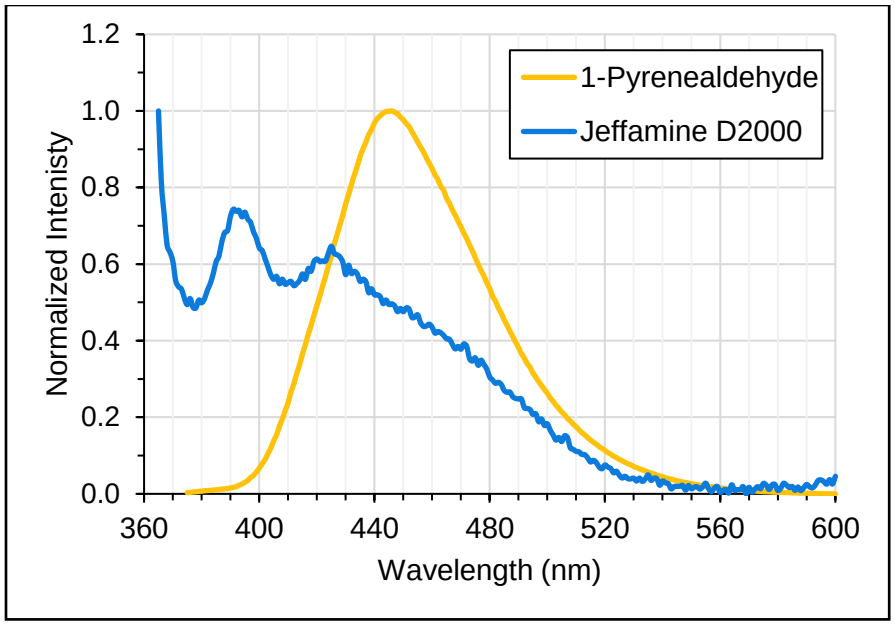

Figure 2.5: Normalized fluorescence spectra for 1-pyrenealdehyde and Jeffamine D2000.

2.4.2 Product Characterization

The product, Py-POP, was characterized to ensure it did not contain excess reagents or undesired products. Due to the similarity in structure of Py-POP to Jeffamine D2000, the FTIR spectra showed small changes. The primary interest was to determine the formation of an imine bond, C=N, that appears in the peak range of 1640 – 1690 cm^{-1} [10]. Despite the presence of primary amine N-H peaks from 1550 – 1700 cm^{-1}, there is a clear increase in peak intensity in this range that signifies the presence of the imine bond. Although the pyrene moiety is in relatively small concentration compared with the poly(oxypropylene) chain, the aromatic C-H peaks are apparent. The peaks at 3039 cm^{-1} and ~850 cm^{-1} are representative of the pyrene C-H bonds. Similarly, the lack of a prominent aldehyde C=O peak at 1680 cm^{-1} and aldehyde C-H at 2715 cm^{-1} are indicators of the conversion of the aldehyde to an imine. Further, the ether C-O and sp^3 carbon C-H peaks are maintained in the spectra for Py-POP, which

indicates that the poly(oxypropylene) backbone is not affected in this reaction.

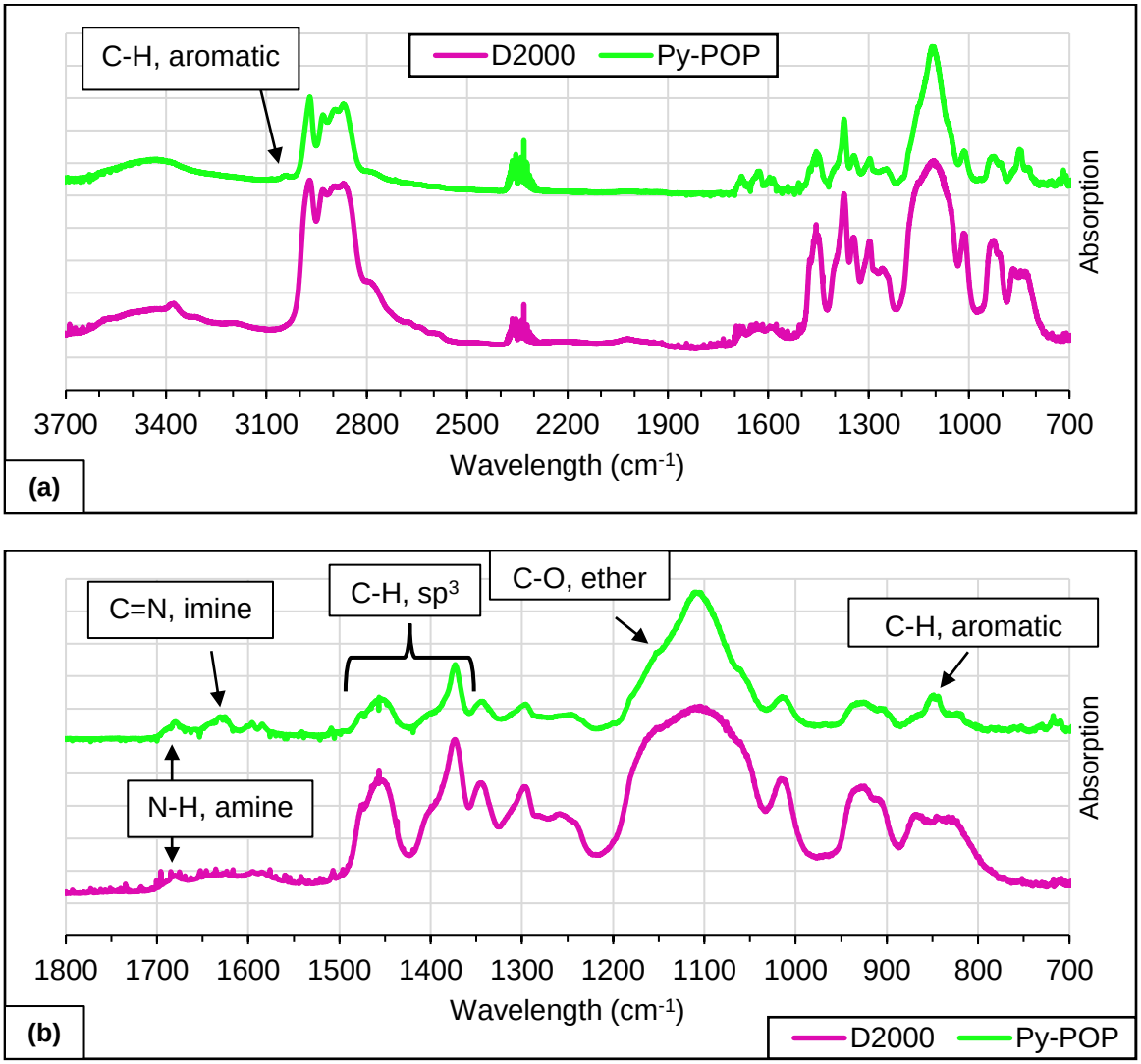

Figure 2.6: FTIR spectra for Py-POP and Jeffamine D2000.

The decomposition of the product was also utilized to verify reaction conversion. The decomposition onset temperature for Py-POP shifted to 150 °C, 20 and 50 °C higher than 1-pyrenealdehyde and Jeffamine D2000, respectively. Due to the similarity in the polymer backbone of Py-POP and Jeffamine D2000, the temperature at the peak decomposition rate did not change significantly. However, it is 71 °C higher than 1-pyrenealdehyde at 349 °C. These changes in decomposition properties indicates that

the structure of the molecule was altered but did not affect the D2000 backbone.

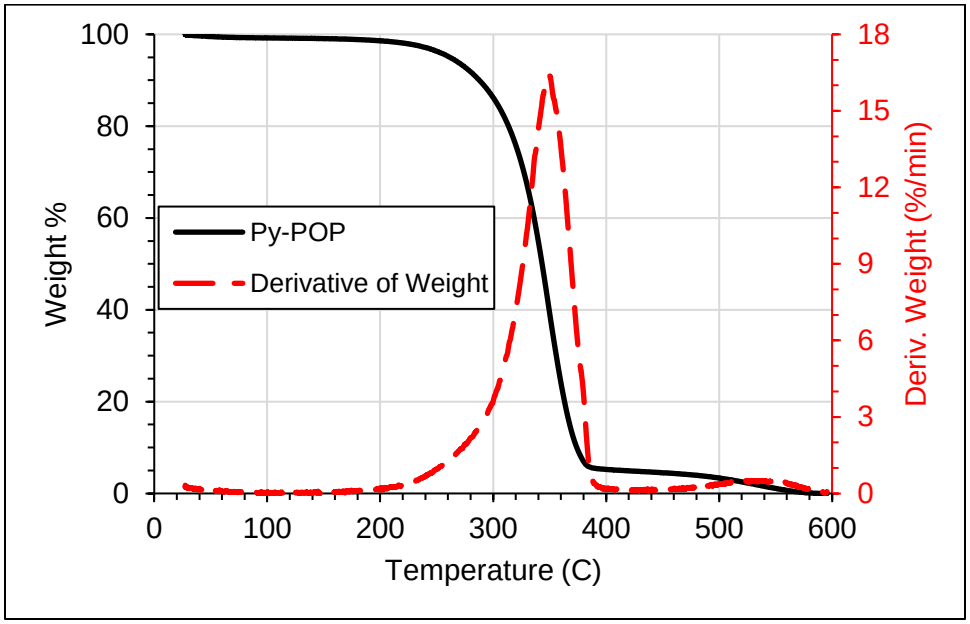

Figure 2.7: Decomposition weight loss analysis data for Py-POP.

Mass spectrometry is a useful technique to analyze molecular weights and molecular weight distribution of various materials. Data from the reagents 1-pyrenealdehyde and Jeffamine D2000 can be used for direct comparison to indicate the components present in the products. For Py-POP, the molecular weight distribution spans from 1600 to 2600 g/mol with a peak at 2029 g/mol which corresponds to 30 repeat units. This distribution follows the weight change with Jeffamine D2000 terminated with one pyrene moiety.

To ensure a mostly pure product, molecular weight distributions for Jeffamine D2000 and Py-POP-Py were found within this data as shown in Figure 2.8. The difunctional Py-POP-Py molecule was present in a very low concentration and was considered negligible. While Jeffamine D2000 was present in a slightly higher concentration, its maximum normalized intensity was below 20%. Combined with its lower potential to adsorb to the GnP surface than the pyrene functionalized molecules,

its presence was also considered to have a negligible effect. Similarly, the 1-pyrenealdehyde peak was at a significantly lower intensity than the rest of the components. As a result, the Py-POP product was used without any further separation.

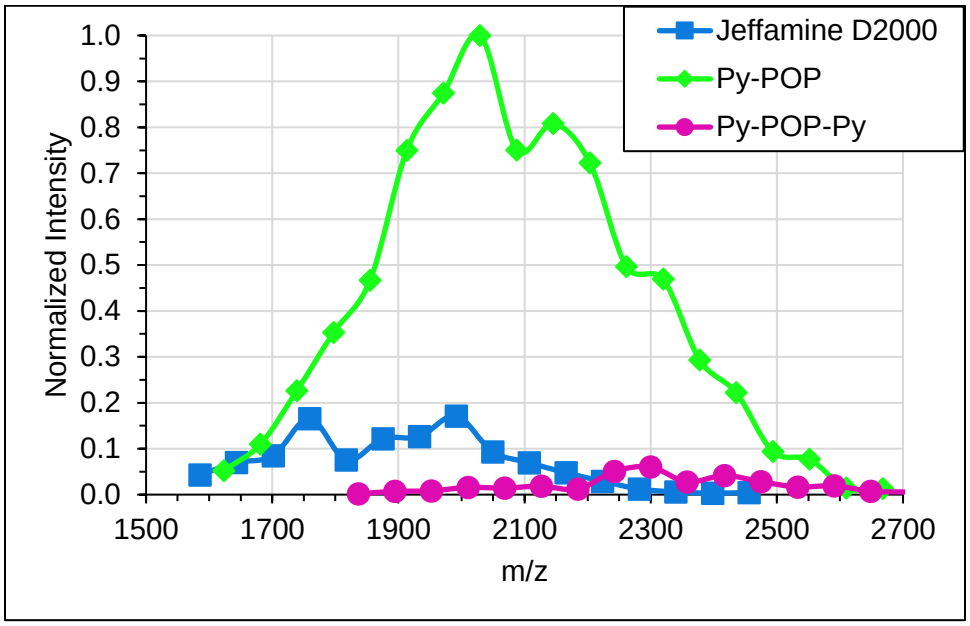

Figure 2.8: Component concentration for Py-POP reaction product.

Fluorescence spectroscopy was also used to qualitatively determine the reaction conversion. Since pyrene and its derivatives are the only fluorescent components, the change in peak locations are indications of altered molecular structure. The pyrene functionalized Jeffamine D2000 molecules showed a shift in their peaks. Although pyrene is a strongly fluorescent molecule, there is a small volume of pyrene moieties relative to the Jeffamine D2000, leading to low intensity peaks. Py-POP and Jeffamine D2000 exhibited one common peak at ~390 nm. However, Py-POP had another peak at 415 nm, shifted 10 nm lower than Jeffamine D2000. In addition, there was no strong 1-pyrenealdehyde peak present.

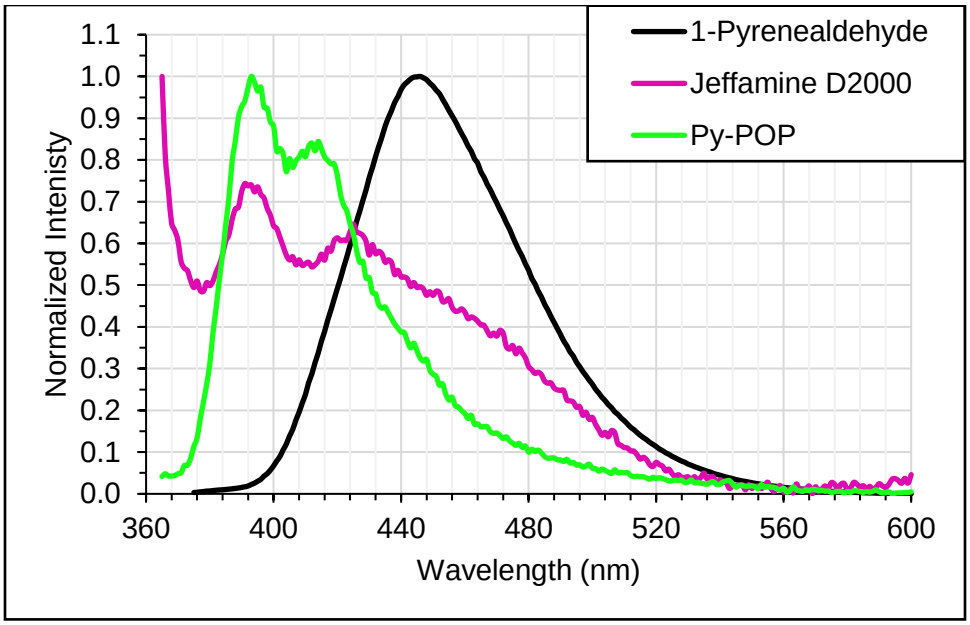

Figure 2.9: Fluorescent spectroscopy spectra for Py-POP, 1-pyrenealdehyde, and Jeffamine D2000.

2.5 Conclusion

A pyrene molecule can interact strongly to the GnP surface through noncovalent bonding as a result of π – π stacking interaction between the pyrene and GnP surface. In order to utilize this interaction in an epoxy matrix composite, a pyrene modified reactive amine was synthesized by utilizing the reaction between aldehyde and primary amine containing polymer. Utilizing an equimolar ratio between the reactants 1-pyrenealdehyde and Jeffamine D2000 produced a molecule with a primary amine on one end and a pyrene moiety on the other. FTIR and mass spectrometry confirmed the molecular structure. In addition, mass spectrometry verified that the mono-pyrene configuration was the main product. As a result, the Py-POP product was utilized to determine the effects of an adsorbate noncovalently bonded with the GnP surface and covalently bonding with an epoxy during the curing process.

BIBLIOGRAPHY

[1] Adachi, Kyoko, and Norio Ichinose. "Fluorescent high-performance liquid chromatographic determination of primary aromatic amines by formation of Schiff base." Fresenius' Journal of Analytical Chemistry 338.3 (1990): 265-268.

[2] Adeola, Adedapo O., and Patricia BC Forbes. "Optimization of the sorption of selected polycyclic aromatic hydrocarbons by regenerable graphene wool." Water Science and Technology 80.10 (2019): 1931-1943.

[3] ASTM Standard E2550, 2021, “Standard Test Method for Thermal Stability by Thermogravimetry,” ASTM International, West Conshohocken, PA, 2021, DOI: 10.1520/D0790-17, www.astm.org.

[4] Babgi, Bandar A., and Asma Alzahrani. "Optical sensing properties of pyrene-Schiff bases toward different acids." Journal of fluorescence 26.4 (2016): 1415-1419.

[5] Björk, Jonas, et al. "Adsorption of aromatic and anti-aromatic systems on graphene through π− π stacking." The Journal of Physical Chemistry Letters 1.23 (2010): 3407-3412.

[6] Choi, Eun Yeob, Lak Won Choi, and C. K. Kim. "Noncovalent functionalization of multi-walled carbon nanotubes with hydroxyl group-containing pyrene derivatives for their composites with polycarbonate." Carbon 95 (2015): 91-99.

[7] Hwang, T. K., et al. "Determination of primary amines by means of fluorescent schiff base derivatives." Analytica Chimica Acta 99.2 (1978): 305-315.

[8] Li, Bing, et al. "Polycyclic aromatic hydrocarbons adsorption onto graphene: a DFT and AIMD study." *Materials* 11.5 (2018): 726.

[9] Liu, Jingquan, et al. "Thermosensitive graphene nanocomposites formed using pyrene-terminal polymers made by RAFT polymerization." Journal of Polymer Science Part A: Polymer Chemistry 48.2 (2010): 425-433.

[10] Mishra, Aswini K., et al. "FT-IR and XPS studies of polyurethane-urea-imide coatings." Progress in organic coatings 55.3 (2006): 231-243.

[11] Niko, Yosuke, et al. "Fundamental photoluminescence properties of pyrene carbonyl compounds through absolute fluorescence quantum yield measurement and density functional theory." Tetrahedron 68.31 (2012): 6177-6185.

[12] NIST Mass Spectrometry Data Center, William E. Wallace, director, "Mass Spectra" in NIST Chemistry WebBook, NIST Standard Reference Database Number 69, Eds. P.J. Linstrom and W.G. Mallard, National Institute of Standards and Technology, Gaithersburg MD, 20899, https://doi.org/10.18434/T4D303.

[13] Potts, Jeffrey R., et al. "Graphene-based polymer nanocomposites." Polymer 52.1 (2011): 5-25.

[14] Chaiyakun, S., et al. "Preparation and characterization of graphene oxide nanosheets." Procedia Engineering 32 (2012): 759-764.

[15] Sahoo, Gobinda Prasad, et al. "Morphology directing synthesis of 1-pyrene carboxaldehyde microstructures and their photo physical properties." RSC Advances 4.21 (2014): 10903-10911.

[16] Wang, Jun, Zaiming Chen, and Baoliang Chen. "Adsorption of polycyclic aromatic hydrocarbons by graphene and graphene oxide nanosheets." Environmental science & technology 48.9 (2014): 4817-4825.

[17] Xu, Liyan, and Xiaoning Yang. "Molecular dynamics simulation of adsorption of pyrene–polyethylene glycol onto graphene." Journal of colloid and interface science 418 (2014): 66-73.

CHAPTER 3: CHANGES IN COMPOSITE MULTIFUNCTIONALITY USING JEFFAMINE D2000 AS AN ADSORBATE ONTO GNP-M25

3.1 Abstract

Adsorption of a molecule that has the ability to both chemically react with the epoxy network and simultaneously be strongly attracted to the graphene nanoplatelet (GnP) basal plane surface through noncovalent interactions has been investigated as a method to improve the resulting composite properties. Jeffamine D2000, a poly(oxypropylene) diamine, was adsorbed onto the GnP basal plane through van der Waals forces to create an interfacial layer which could also react with the epoxy resin through reaction with its amine group. The composite mechanical properties were not significantly improved compared with the composite without the presence of the Jeffamine D2000. The interfacial layer containing the Jeffamine D2000 at the GnP surface exhibited a lower modulus than the bulk epoxy. As a result, the flexural modulus was lowered for GnP-M25-D2000 composites below 4 vol%. In addition, the glass transition temperature for the GnP-M25-D2000 composites were lowered compared with the unmodified GnP-M25. Similarly, the loss modulus curves showed an increase in chain mobility versus unmodified GnP-M25. However, cross-sectional image processing indicated that the adsorbed Jeffamine D2000 improved the GnP dispersion at higher concentrations. As a result, the electrical conductivity of 4 vol% GnP-M25-D2000 increased by over 3000% compared with GnP-M25/epoxy composite without Jeffamine D2000.

3.2 Introduction

The GnP basal plane, a structure of six-membered carbon aromatic rings, adheres poorly to epoxy resins because of the inability to form chemical bonds with this

surface. In this chapter, Jeffamine D2000, a poly(oxypropylene) diamine, was investigated as a potential adsorbate capable of interacting via van der Waals intermolecular forces with the GnP-M25 surface in order to produce a GnP surface that is more attractive to an epoxy resin without altering its chemical structure. While Jeffamine D2000 was not expected to adhere strongly to the GnP, it was important to understand how the polymer interacts to compare with the Py-POP adsorbate.

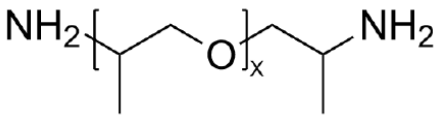

Figure 3.1: Molecular structure of Jeffamine D2000. X ~ 33.

Due to the electronegative structure of the GnP surface and the high concentration of hydrogen atoms along its backbone, Jeffamine D2000 could interact with the graphene nanoplatelets basal plane through van der Waals forces. Additionally, the primary amines present are available to react with the epoxy during the composite curing process. Coupled with entangling effects, the interfacial strength between the epoxy and the GnP could be improved by the Jeffamine D2000 acting as a coupling agent at the interphase between the epoxy network and the surface. However, a high concentration of D2000 at the GnP surface could create an interphase having a lower modulus than the bulk epoxy and as a result could decrease the adhesion and composite properties.

3.3 Materials and Methods

3.3.1 Materials

Graphene nanoplatelets, product name GnP-M25 (d = 25 μm, t ~ 7 nm, 5-10 layers) was provided by XG Sciences. Poly(oxypropylene) diamine known by its trade

name Jeffamine D2000 (Hunstman) has an average molecular weight of 2000 g/mol and amine hydrogen equivalent weight of 514 g/eq. Bisphenol A diglycidyl ether (DGEBA), known by trade name Epon 828 was purchased from Miller-Stephenson. Meta-phenylene diamine (mPDA) and isopropanol were purchased from Sigma Aldrich, used as received. PELCO Conductive Liquid Silver Paint was used to create electrical contact points for electrical conductivity measurements.

3.3.2 Adsorption Method

GnP-M25 was ultrasonicated in isopropanol for 10 minutes in an ice bath to break up agglomerates. An excess of Jeffamine D2000 was added to the mixture and mechanically stirred overnight via a stir bar. The mixture was then vacuum filtered through a 0.22 µm filter paper (PTFE) to remove the solvent and excess Jeffamine D2000. The GnP-M25-D2000 was dried in a vacuum oven to remove the residual solvent.

3.3.3 Composite Preparation Method

Four concentrations of GnP-M25 were used: 0, 3, 5, and 8 weight % (0, 1.5, 2.5, 4 volume %). The GnP-M25-D2000 sample was added to isopropanol and ultrasonicated for 10 minutes in an ice bath. DGEBA was added to the mixture, mechanically stirred to dissolve, and ultrasonicated 10 minutes in an ice bath while stirring with a stir bar. The isopropanol was removed from the mixture in a vacuum oven at 80 °C. After the solvent was removed, mPDA (14.5:100 weight ratio to DGEBA) was added at 75 °C to the GnP-M25-D2000/DGEBA mixture and stirred thoroughly. After degassing, the mixture was poured into flexural coupon silicone molds and cured using a cycle of 2 h at 75 °C then 2 h at 125 °C. The cured composites were polished to a flat

surface before testing. All data will reference the GnP-M25 concentration for clarity, and it is noted that the addition of the adsorbates will increase the volume % of additives.

3.3.4 Characterization

Laser Raman spectroscopy was used to analyze the structure of GnP-M25 before and after adsorption of Jeffamine D2000 using the LabRAM Aramis (Horiba). Laser wavelength was 532 nm. Spectra were recorded in two parts (1000 – 2000 cm^{-1} and 2000 – 3000 cm^{-1}) to reduce oxidation of the material.

Composite flexural coupons were tested using a three-point bending method according to the standard ASTM D790 using a Universal Testing System (Instron). Rectangular specimens were supported 2 inches apart, then force was applied to the middle of the specimen at a strain rate of 0.01 mm/mm/min until failure. Force applied and extension of deflection measured were used to calculate flexural modulus and flexural strength.

The TA Instruments TGA Q500 machine was used for thermogravimetric analysis (TGA) of the samples' thermal stability. Heating rate was set at 10 °C/min to 500 °C in a nitrogen atmosphere. Decomposition onset temperature was determined using ASTM E2550.

Dynamic mechanical analysis (DMA) was performed using a TA DMA Q800 machine. Testing conditions were single-cantilever method, temperature ramp to 200 °C at a rate of 3 °C/min, set at a frequency of 1 Hz, and set at an amplitude of 30 μm. Glass transition temperature was defined as the temperature at the peak of the tan δ curve. Polymer density was measured according to the standard ASTM D792.

A Carl Zeiss Auriga Dual Column FIB scanning electron microscope was used to

capture cross-sectional images of polymer composites. These images were used to qualitatively analyze GnP dispersion. Using the image processing software ImageJ, a quantitative measurement of dispersion and agglomeration was calculated.

Flexural testing coupons were used to measure electrical conductivity via a Four-point probe method. Coupons were cut to 30 mm in length, polished surfaces to be flat, and oxygen plasma treated for 10 minutes at 300 W. Opposite ends were coated in a layer of silver paint. Two contacts points were placed using silver paint 15 mm apart in the middle of the composite coupon surface. A heat gun was used to dry the silver paint. A Keithley 2000 multimeter was used to apply a 1 μA current from one end to the opposite end of the sample. Voltage was measured between the two contact points.

Thermal conductivity was calculated by measuring the composites thermal diffusivity and heat capacity. The thermal diffusivity was measured via laser flash method using a Netzsch LFA 447 according to ASTM 1461-13. Flexural coupon samples were cut to fit in the machine, surfaces polished flat, and coated with a graphite layer. A TA DSC Q2000 was used to measure heat capacity according to ASTM E1269-11. Samples were ramped to -10 °C at 20 °C/min, held isothermally for 5 minutes, ramped to 50 °C at 20 °C/min, and held isothermally for 5 minutes. Heat capacity was taken at 25 °C.

3.4 Results and Discussion

3.4.1 Adsorption of Jeffamine D2000 onto GnP-M25

Laser Raman spectroscopy was used to analyze the adsorption of Jeffamine D2000 onto GnP-M25. Changes in the D peak (~1350 cm^{-1}) and the I_D:I_G peak intensity ratio represent changes in the structure of the GnP surface [6]. The D peak is caused

due to the scattering of a charge carrier at a defect in the graphene crystal structure. For example, the D peak will increase with more chemical bonding to the surface. Figure 3.2 and Table 3.1 demonstrate that Jeffamine D2000 does not chemically change the graphene surface but rather adsorbs through physical interactions. Consequently, the strongest interactions between Jeffamine D2000 and the GnP surface are van der Waals intermolecular forces.

Interestingly, there is a significant increase in the 2D peak (~2700 cm^{-1}) and I_{2D}:I_G peak intensity ratio. The interpretation of this data is that the D2000 acts as an intercalant to fully or partially exfoliate the GnP. This is due to the 2D peak representing the number of layers of the GnP, where a larger peak ratio indicates a smaller number of layers.

Table 3.1: Laser Raman peak intensity ratios.

Peak Intensity Ratios	**GnP-M25**	**GnP-M25-D2000**
D:G	0.01	0.019
2D:G	0.0016	0.27

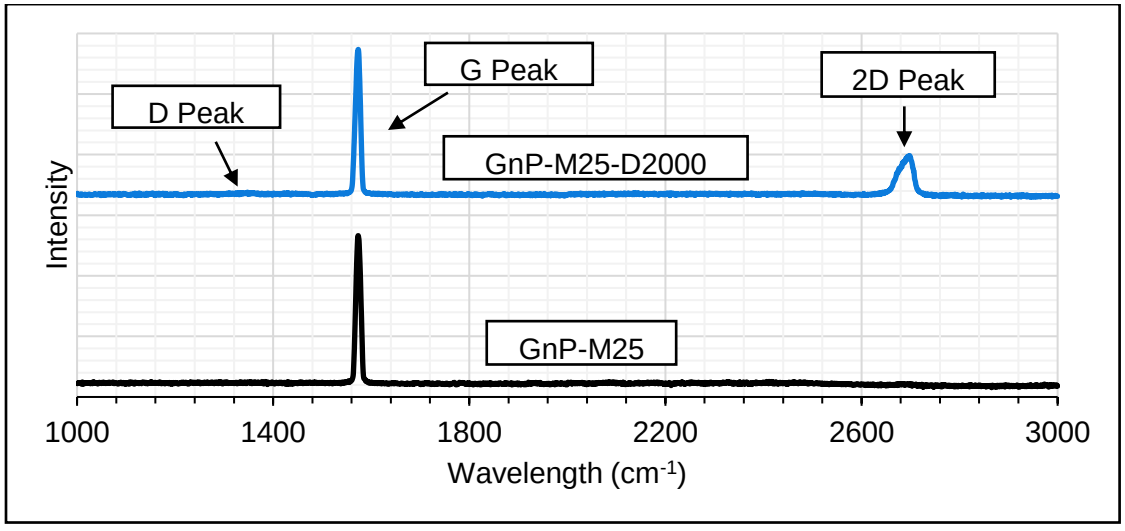

Figure 3.2: Laser Raman Spectra for GnP-M25 (bottom) and GnP-M25-D2000 (top).

The GnP-M25 did not experience significant weight loss below its decomposition temperature (~500 - 600 °C). Therefore, the weight lost in the GnP-M25-D2000 sample is expected to be entirely Jeffamine D2000 and is further supported through the Laser Raman data. From this the amount adsorbed was calculated as 455 mg Jeffamine D2000/g GnP-M25. For a better understanding, this amount can be compared with the adsorbed quantity of Py-POP. Since there is a simple molar relationship between the pyrene moieties and moles of each molecule, this was converted to mg pyrene moieties/g GnP-M25. Using a 1:1 molar ratio of pyrene to Jeffamine D2000 to directly compare this with Py-POP, the results are 52 mg pyrene moieties/g GnP-M25. This value is 31% less than the adsorbed content of Py-POP from Chapter 5 (75 mg pyrene moieties/g GnP-M25). As a result, the amount of Jeffamine D2000 adsorbed was a significantly smaller amount than Py-POP. Without a pyrene end group, the forces of attraction attracting the D2000 and keeping the molecules on the surface were weaker.

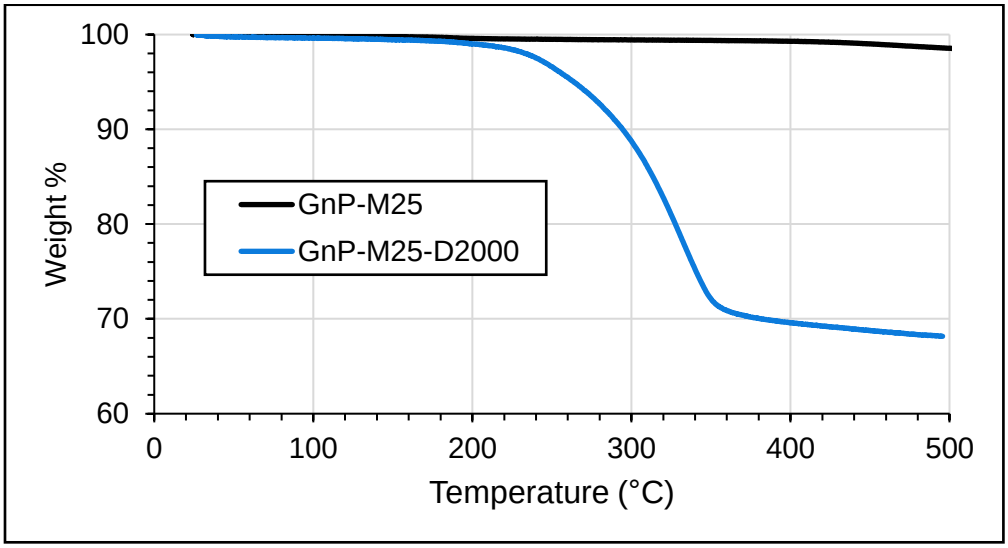

Figure 3.3: Weight loss analysis through TGA on GnP-M25 and GnP-M25-D2000 in a N_2 atmosphere.

3.4.2 GnP Dispersion

Cured composite samples were sectioned and cross-sectional images of each material were obtained to determine the dispersion of the GnP in the epoxy. The white lines and groups in Figure 3.4 represent the GnP platelets. Qualitatively, increasing the GnP concentration increased the number of platelets in the cross-section. Tyson et al. [17] developed a method for determining a dispersion and agglomeration percent using image analysis. In this approach, dispersion % represents the uniformity of the distance between platelets. A higher dispersion % implies more evenly dispersed GnP. On the other hand, agglomeration % represents the uniformity of the size of platelets. Lower agglomeration % means that the platelet sizes are more uniform.

Figure 3.6 shows the plotted data for dispersion and agglomeration %. GnP-M25-D2000 exhibits a relatively consistent dispersion % across each concentration. Because of a higher agglomeration effect, dispersion % was expected to decrease with concentration as is shown for the unmodified GnP-M25. Agglomeration % increased for GnP-M25 going from 2.5 to 4 vol%, but the GnP-M25-D2000 increased only a fraction of the amount. The GnP-M25-D2000 exhibit slightly better overall dispersion at 4 vol% due to more consistently sized GnP while at the same dispersion %. Due to the layered structure of D2000, the platelets are less likely to restack and maintain the GnP sizes and dispersion.

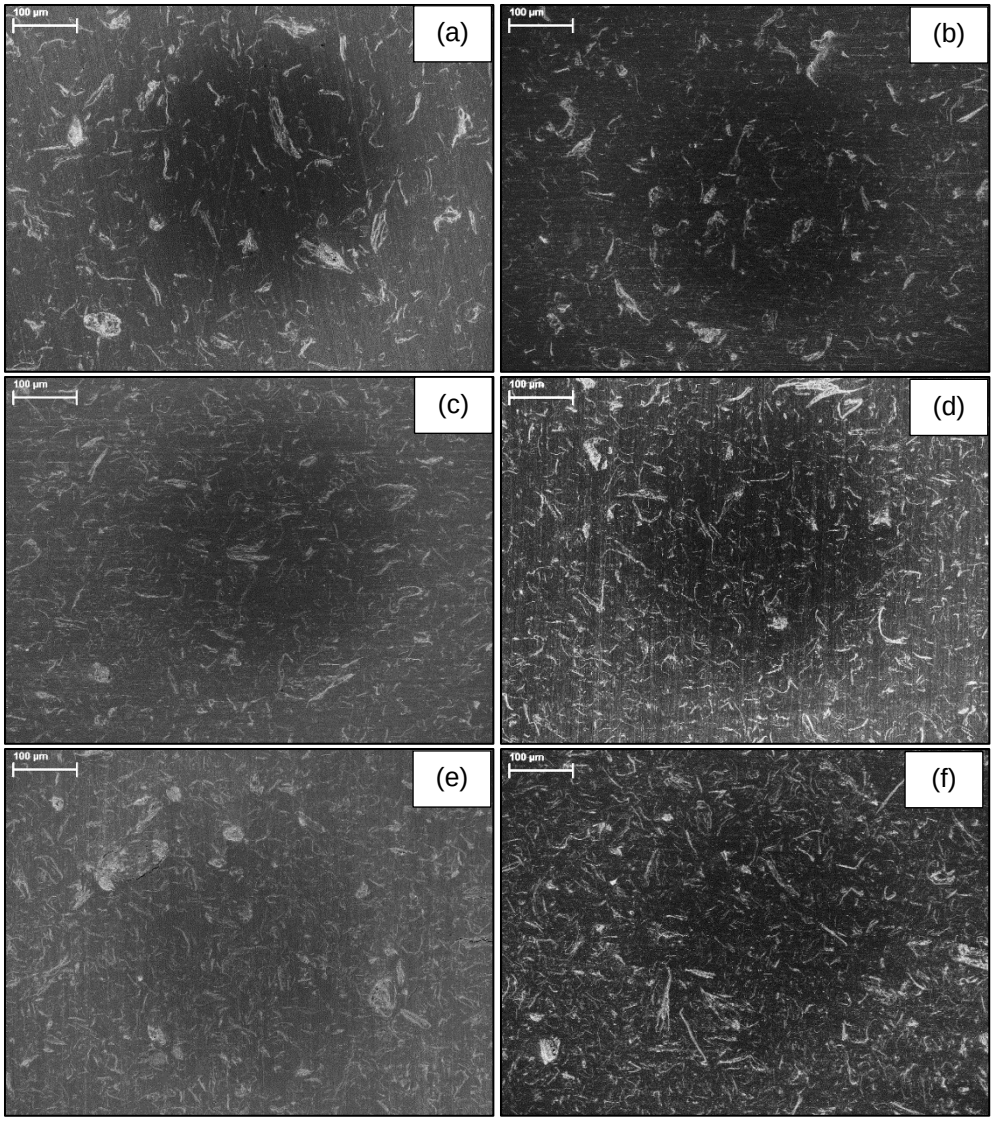

Figure 3.4: SEM cross sectional images for GnP-M25 composites at (a) 1.5 vol%, (c) 2.5 vol%, and (e) 4 vol%, and GnP-M25-D2000 composites at (b) 1.5 vol%, (d) 2.5 vol%, and (f) 4 vol%.

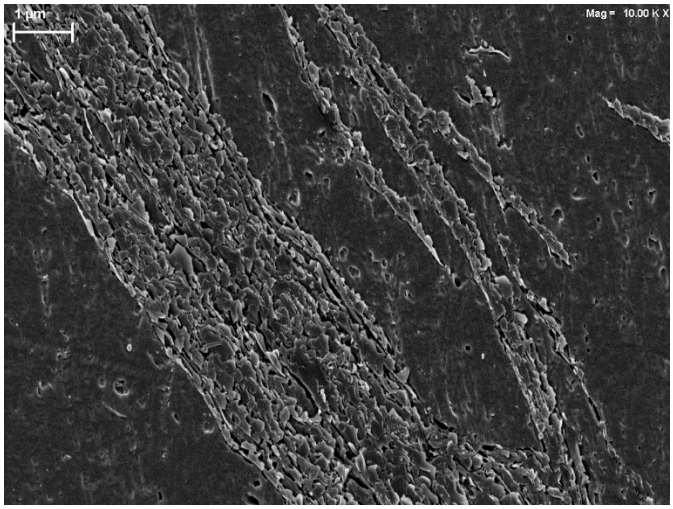

Figure 3.5: 1.5 vol% GnP-M25 cross-sectional image.

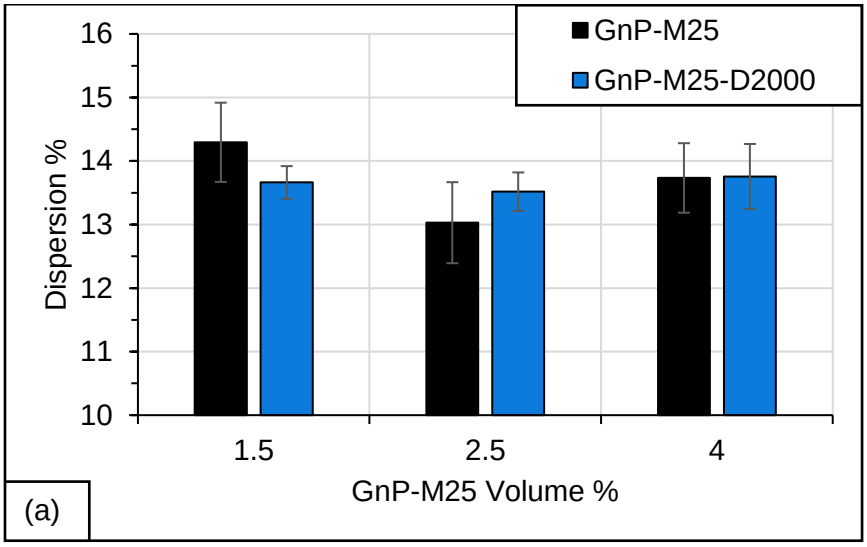

Figure 3.6: (a) Dispersion % and (b) agglomeration % calculated from SEM cross-sectional images.

Figure 3.6 (cont'd)

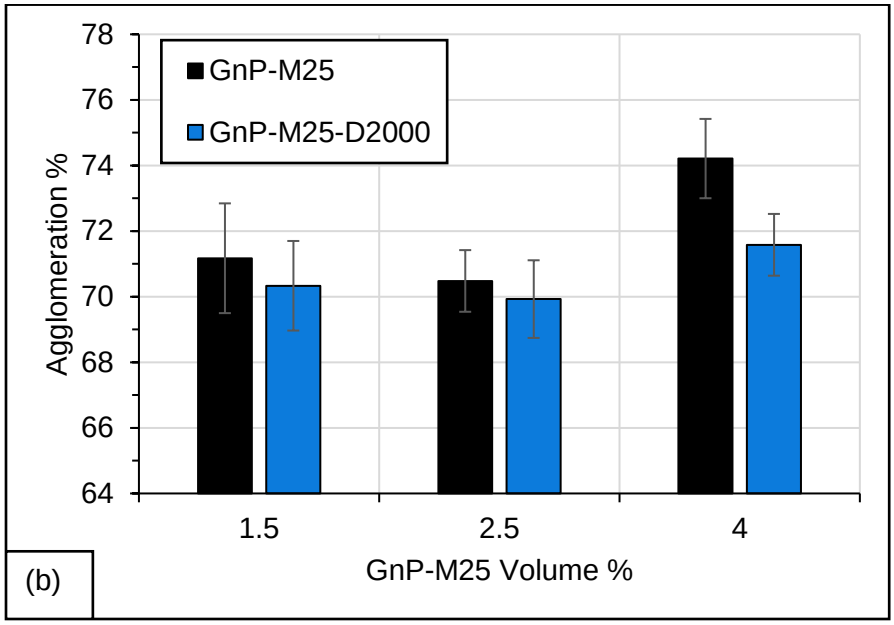

3.4.3 Jeffamine D2000 Effect on Epoxy Matrix Properties

In order to determine the effect of the addition of Jeffamine D2000 on epoxy properties, epoxy samples containing Jeffamine D2000 without GnP-M25 were tested. The mass of Jeffamine D2000 used corresponds to 20, 50, and 100% of the experimental adsorption onto 4 vol% GnP-M25 from Section 3.4.1. The data collected allowed for better understanding of the adsorbate's effects on the composite properties as an interfacial layer on GnP and as an untethered filler.

Comparing the glass transition temperatures (T_g) for the 20, 50, and 100% D2000 composites showed an average of 5 °C difference. As a result, the 100% D2000 value was used for analysis. At this concentration, the T_g increased 33% over the neat DGEBA/mPDA. Since the D2000 has a relatively long polymer chain, it can entangle with the epoxy, which assists in restricting the composite chain movement. The D2000 was expected to participate in the epoxy curing process. As a result, the amine parts by weight per hundred parts of the epoxy resin (phr) was increased from stoichiometry at

14.5 to 14.7. One study [8] investigated the ratio of mPDA with epoxy resin and found that the modulus of the epoxy increases when the mPDA content increases above 20 phr (curing agent parts per one hundred parts of epoxy resin by weight). Therefore, this increase in amine phr should not considerably affect the modulus.

Normalized loss modulus curves (E''/E''_{Peak}) plotted against normalized temperature ($T - T_{Peak}$) and increasing temperature were utilized to directly compare changes in the peaks' shapes [7]. The normalized loss modulus curve for neat DGEBA/mPDA was subtracted from each sample material as well (labeled Sub in Figure 3.7) for direct analysis in peak shape changes. An interesting effect on the loss modulus curves occurred at 20 and 50% D2000 loading. Both experience multiple distinct peaks in the curves. One similarity between the three concentrations is a broadening effect 10 °C above the peak. This broadening indicates that the D2000 is reducing the epoxy chain mobility, resulting in less uniform chain movement. The 100% D2000 composite shows the smallest change above T_{Peak}, presumably due to more even distribution of the D2000 in the material.

Figure 3.7b illustrates this phenomenon more clearly by showing the shifts in the peak temperature. All three concentrations have a peak ~135 °C, but both 20 and 50% D2000 have peaks at lower temperatures closer in value to the neat epoxy. The peak that overlaps for each curve represents a more homogeneous mixture and the extra peaks in 20 and 50% represent the D2000 poor sections.

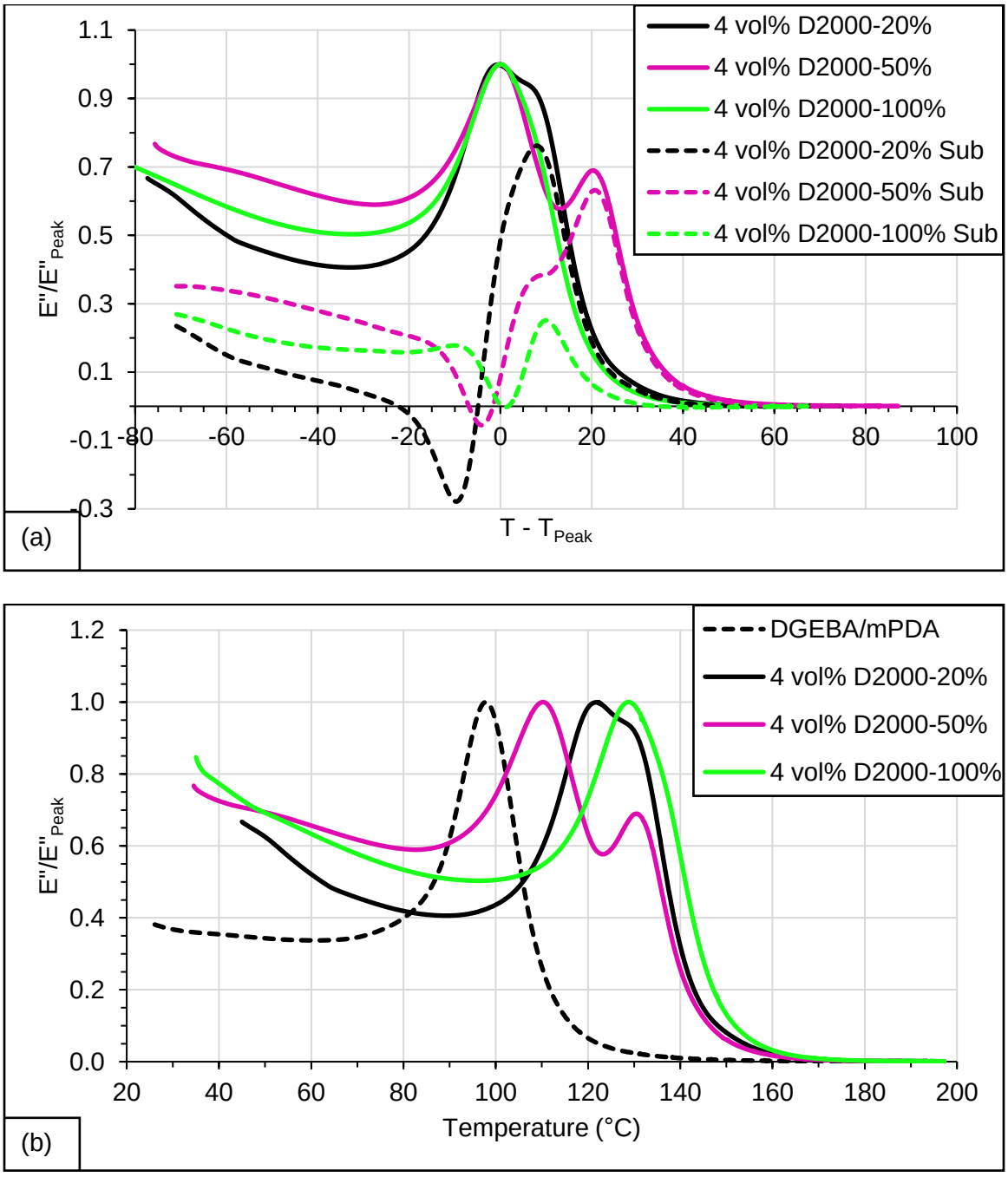

Figure 3.7: Normalized loss modulus curves of Jeffamine D2000 composites (a) versus normalized temperature and (b) versus increasing temperature.

The measurement of electrical conductivity through 4-point probe testing found that addition of 20, 50, and 100% D2000 did not change the electrical conductivity of the composite.

The 100% D2000 composite showed an increase in thermal conductivity of 32% above the neat epoxy.

Table 3.2: Thermal conductivity.

Samples	**Thermal Cond. (W/m*K)**	**Thermal Cond. Error (W/m*K)**
Neat DGEBA/mPDA	0.213	0.027
100% D2000	0.281	0.044
4 vol% GnP-M25	0.971	0.120

3.4.4 Mechanical Properties

The effects on flexural modulus due to adsorbed Jeffamine D2000 onto GnP-M25 are summarized in Figure 3.8. Due to the adsorbate's interactions with the epoxy, the flexural modulus of the composites is reduced by 3.8 and 5.4% at 1.5 and 2.5 vol% GnP-M25-D2000, respectively. At the surface of the GnP, there is an interfacial layer of D2000 that is adsorbed on the GnP and covalently bonded with the epoxy resin. This layer consisting primarily of D2000 has a lower modulus than the mPDA/epoxy since the D2000 is at its highest concentration at the GnP surface. As a result, the overall flexural modulus of this interphase is decreased compared to the bulk epoxy/mPDA matrix. At 4 vol% GnP-M25-D2000, there is a 4% increase above the unmodified GnP-M25 composite. Figure 3.9 compares the Halpin-Tsai model with the experimental flexural modulus data. The GnP-M25-D2000 follows the model closely across all concentrations. If the GnP-M25 composites did not experience agglomeration at 4 vol%, it is expected that its flexural modulus would be closer to 4 vol% GnP-M25-D2000.

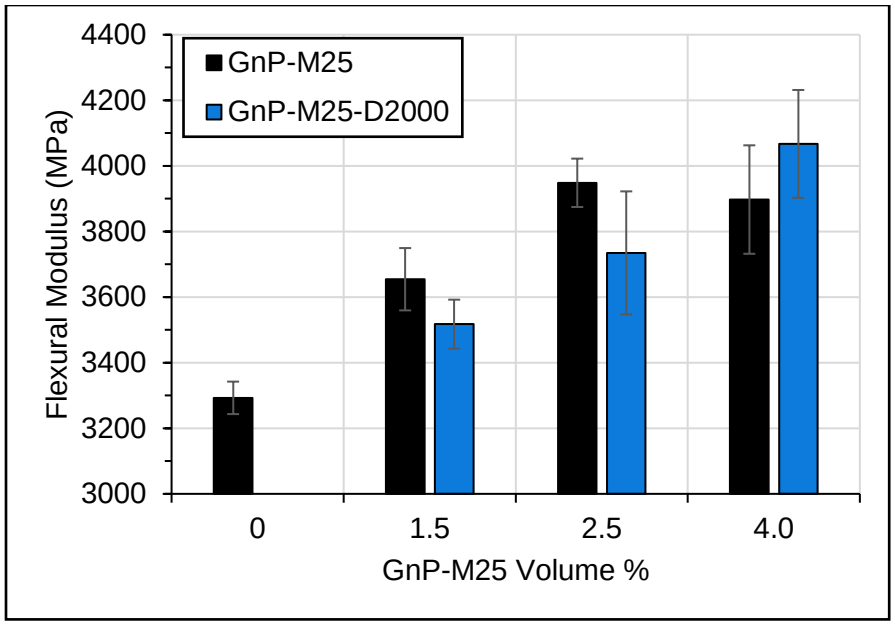

Figure 3.8: Flexural modulus for GnP-M25 and GnP-M25-D2000 composites.

Further evidence for the presence of D2000 can be seen with molecular weight between crosslinks (MW_C) data. At all concentrations, the GnP-M25-D2000 composites show a higher MW_C than the unmodified GnP-M25. This increase is because of the addition of the D2000 chain to the crosslink matrix. In addition, the MW_C at each concentration of GnP-M25-D2000 is virtually the same value within error. Despite this, the flexural modulus increases with GnP volume, indicating a larger effect resulting from the better dispersion of the GnP.

Table 3.3: Flexural modulus percent increase over neat DGEBA/mPDA.

Composite Filler	**1.5 vol%**	**2.5 vol%**	**4 vol%**
GnP-M25	11.0	19.9	18.4
GnP-M25-D2000	6.8	13.4	23.5

Table 3.4: Molecular weight between crosslinks calculated experimentally.

	Molecular Weight between Crosslinks (g/mol)		
Filler Concentration (vol%)	GnP-M25	GnP-M25-D2000	D2000
0	335 ± 66	335 ± 66	-
1.5	260 ± 1.1	272 ± 38	-
2.5	255 ± 0.54	268 ± 7.7	-
4	232 ± 57	268 ± 17	308 ± 9.9

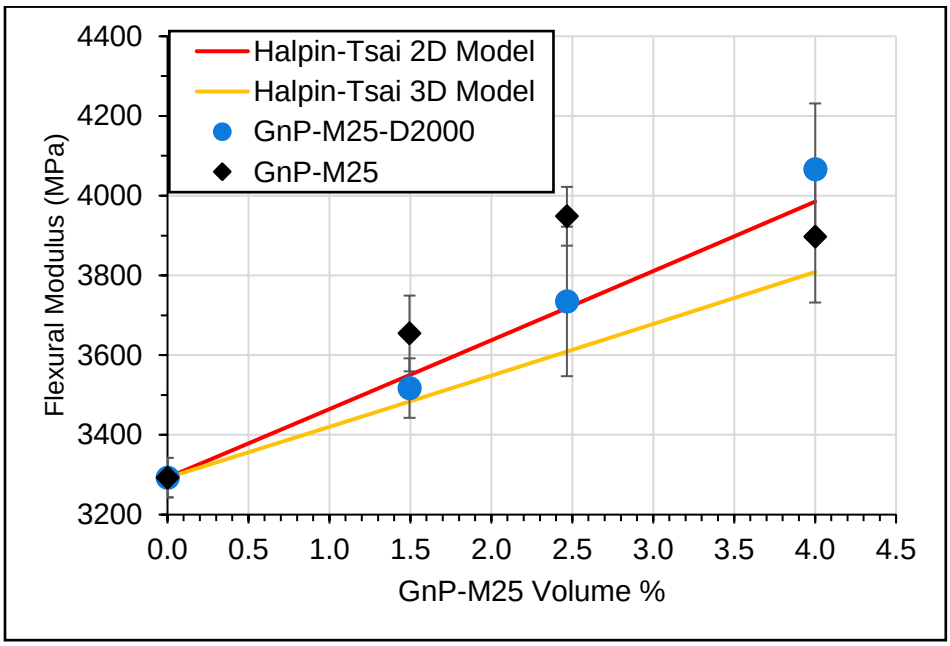

Figure 3.9: Halpin-Tsai model for flexural modulus.

The flexural strength of the GnP-M25-D2000 composites is very similar to the unmodified GnP-M25 composites across all concentrations. Flexural strength is determined by the interfacial strength between the GnP and epoxy. Since there is not a significant improvement in the interface, adsorption of D2000 was not expected to improve the flexural strength. As the volume of D2000 increased to 4 vol% GnP-M25, slight improvement was found mostly due to an increase in GnP surface area from fewer agglomerates.

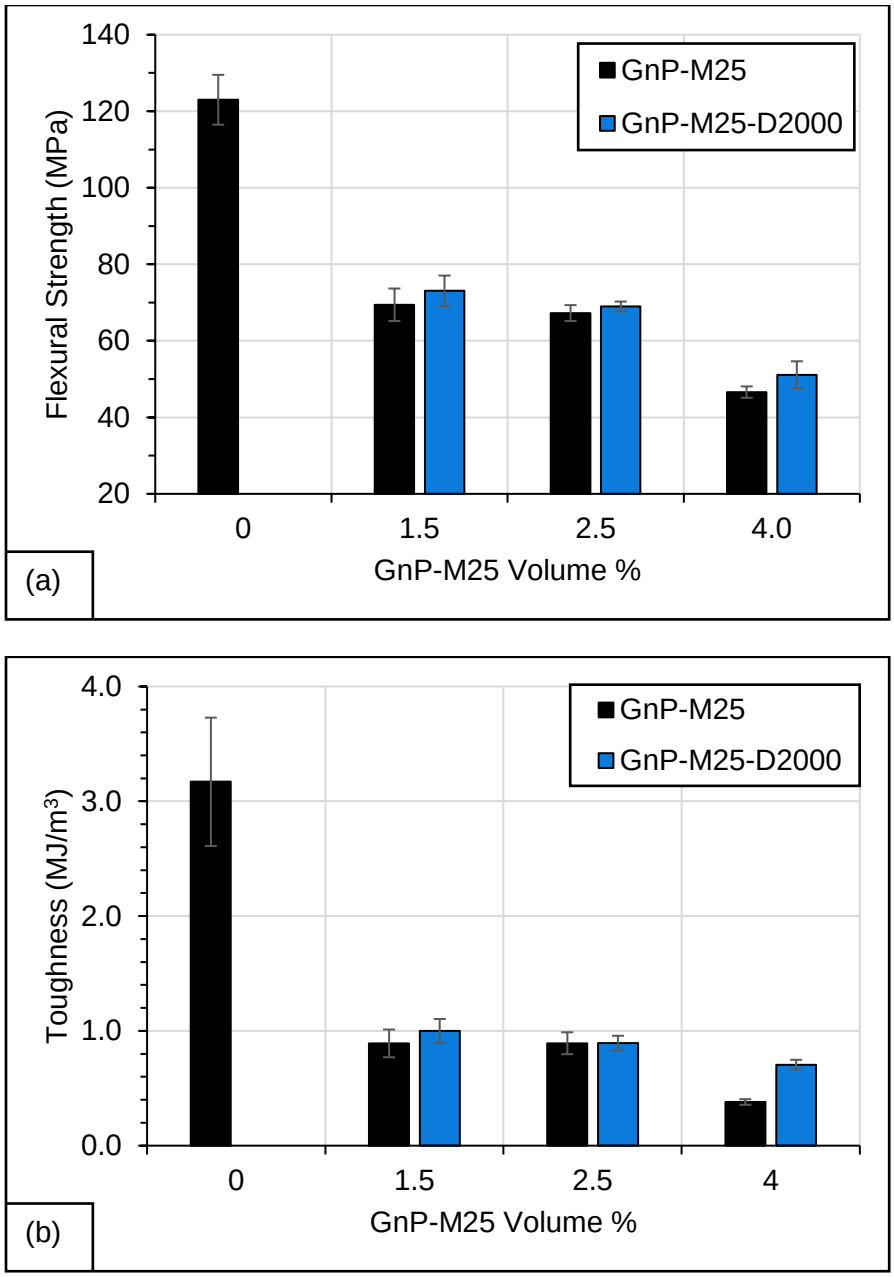

Figure 3.10: (a) Flexural strength and (b) toughness for GnP-M25 and GnP-M25-D2000 composites.

Since Jeffamine produces a lower modulus layer at the GnP surface, the toughness at 4 vol% is 85% higher than unmodified GnP-M25.

3.4.5 Thermal Properties

At 1.5 and 2.5 vol% GnP-M25, the samples with and without adsorbed Jeffamine D2000 show a large increase (54 °C) in glass transition temperature (T_g) over the neat epoxy. However, at 4 vol% GnP, the unmodified GnP composite has a T_g similar to the neat epoxy. Also, the 4 vol% GnP-M25-D2000 shows a T_g 15 °C lower than the GnP-M25 sample. Interestingly, the T_g for the 100% D2000 sample without GnP is 33% higher than the neat material. This difference indicates that the reduction in T_g for the GnP-M25-D2000 material is due to a poor interface. The interfacial layer of D2000 generated a lower modulus at the GnP surface which allowed the epoxy chains to move more freely rather than being restricted by the platelets. Additionally, the interfacial strength with the GnP was not significantly improved with the adsorption of D2000. Because the D2000 was more evenly dispersed within the epoxy for the 100% D2000 material, there was a higher probability for entanglement to restrict the epoxy chain movement, increasing the T_g.

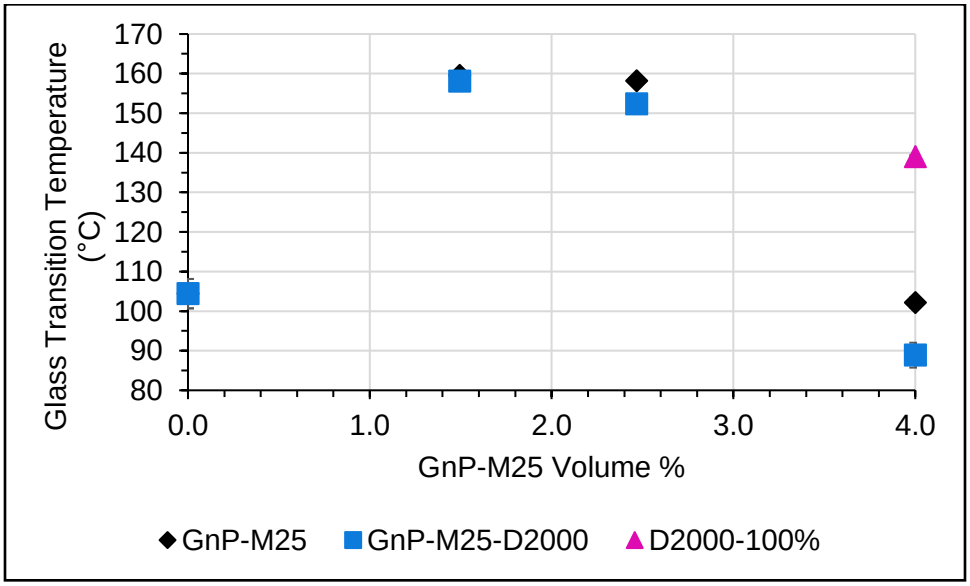

Figure 3.11: Glass transition temperature of composites using GnP-M25 (diamond), GnP-M25-D2000 (circle), and 100% Jeffamine D2000 (triangle).

Further insight on the GnP/epoxy interface can be seen through the tan δ peak magnitude [18]. The height of the tan δ peak in representative of the amount of stress transferred to the GnP. A lower peak height demonstrates more stress transfer as the GnP is experiencing the load rather than the epoxy. At 1.5 and 2.5 vol%, the GnP-M25-D2000 does not differ from the unmodified GnP. Similarly, there is a small increase at 4 vol% over GnP-M25, but both materials decrease ~50% below the values at 2.5 vol%. Due to the high concentration and surface area of GnP at 4 vol%, the tan δ peak decreased significantly for each material. The 100% D2000 has a peak slightly higher than the other samples at 4 vol% but is due to restriction of epoxy chains through entanglement.

The loss modulus curve represents energy dissipated as heat caused by the friction between the GnP and epoxy. The loss modulus peak widens with incorporation of GnP as the platelets restrict chain movement. At the same concentration, the material with a better GnP/epoxy interface will have a larger full width half maximum (FWHM) loss modulus peak. At 1.5 and 2.5 vol% GnP-M25-D2000, the FWHM is smaller than unmodified GnP-M25 due to the lower modulus D2000 layer reducing the friction. 4 vol% GnP-M25-D2000 composites show an increase of 7% over the unmodified GnP-M25 material. The increase in FWHM is mostly likely caused by the reduced agglomeration which resulted in a higher GnP concentration.

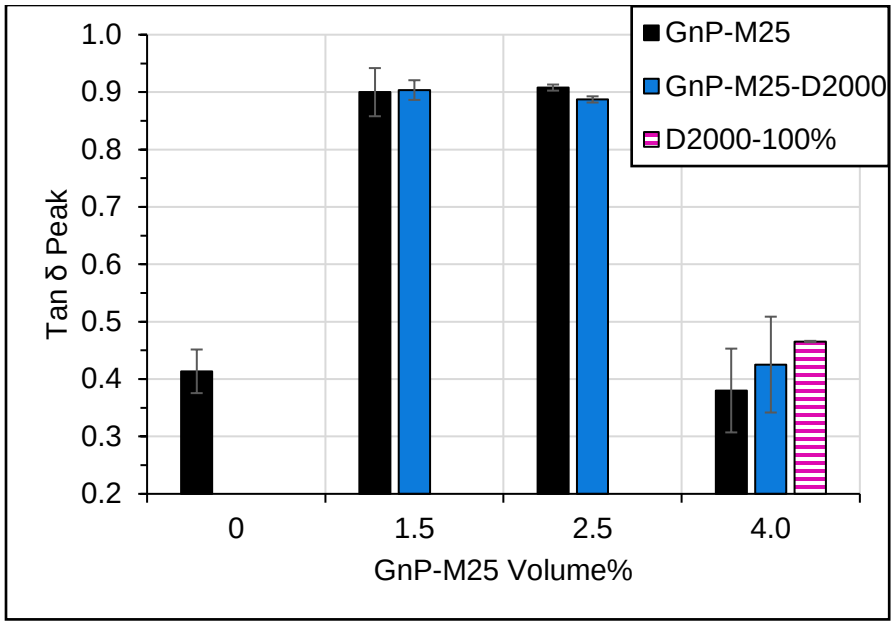

Figure 3.12: Tan δ peak magnitudes.

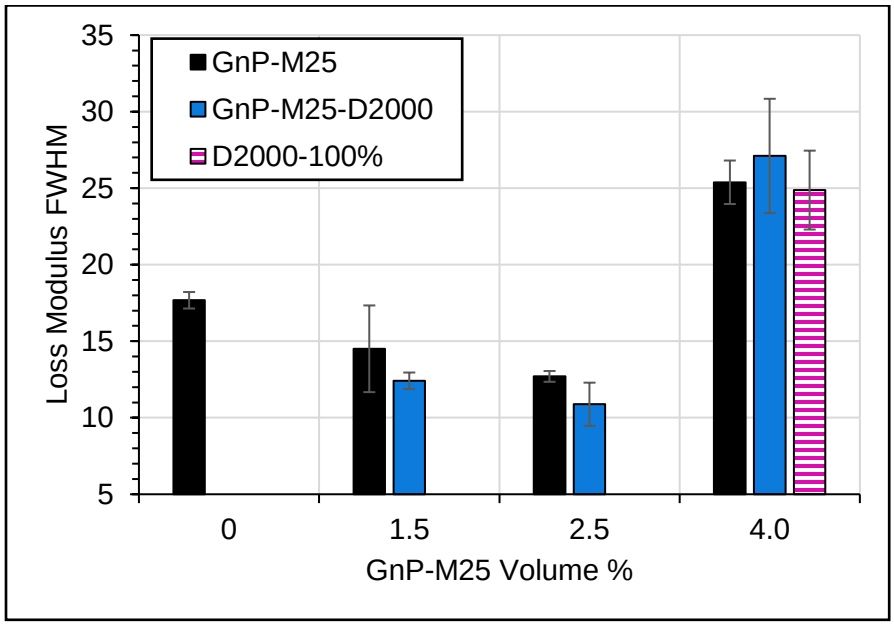

Figure 3.13: Full width half maximum of loss modulus peaks for GnP-M25 and GnP-M25-D2000 composites.

The normalized loss modulus (E"/E"$_{Peak}$) curves were plotted versus normalized temperature (T – T$_{Peak}$) for an easier depiction of the effects of each filler. In Figure 3.14a, the subtracted curves for all three materials follow a similar trend at temperatures

below the peak. However, the 100% D2000 subtracted curve shows a small increase 10 degrees below the peak. Because this is not followed by the GnP-M25-D2000, it shows that the D2000 does not substantially affect the GnP/epoxy interface. Above T_{Peak}, each material exhibits a broadening of the E" curve. The GnP-M25 and GnP-M25-D2000 broaden the curve to a similar temperature, while the 100% D2000 shifts towards a higher temperature. Where the GnP samples are decreasing the uniformity of the chain movement through the presence of stiff platelets, the 100% D2000 does the same with only entanglement effects.

Plotting normalized loss modulus versus temperature shows how the peaks shift over a temperature range. The location of the peak represents the temperature needed to stimulate bulk chain movement. The GnP-M25-D2000 composites follow a trend indicating that increasing the concentration decreases T_{Peak}. This follows the similar trend as unmodified GnP-M25, but the presence of a D2000 interfacial layer decreases T_{Peak}. Figure 3.14c shows this effect. The lower modulus D2000 layer at the GnP surface lets the GnP move more easily, decreasing the temperature needed to initiate bulk chain movement. Without the GnP trapping the volume of D2000, the polymer can entangle with the epoxy chains and contribute a more restricting effect.

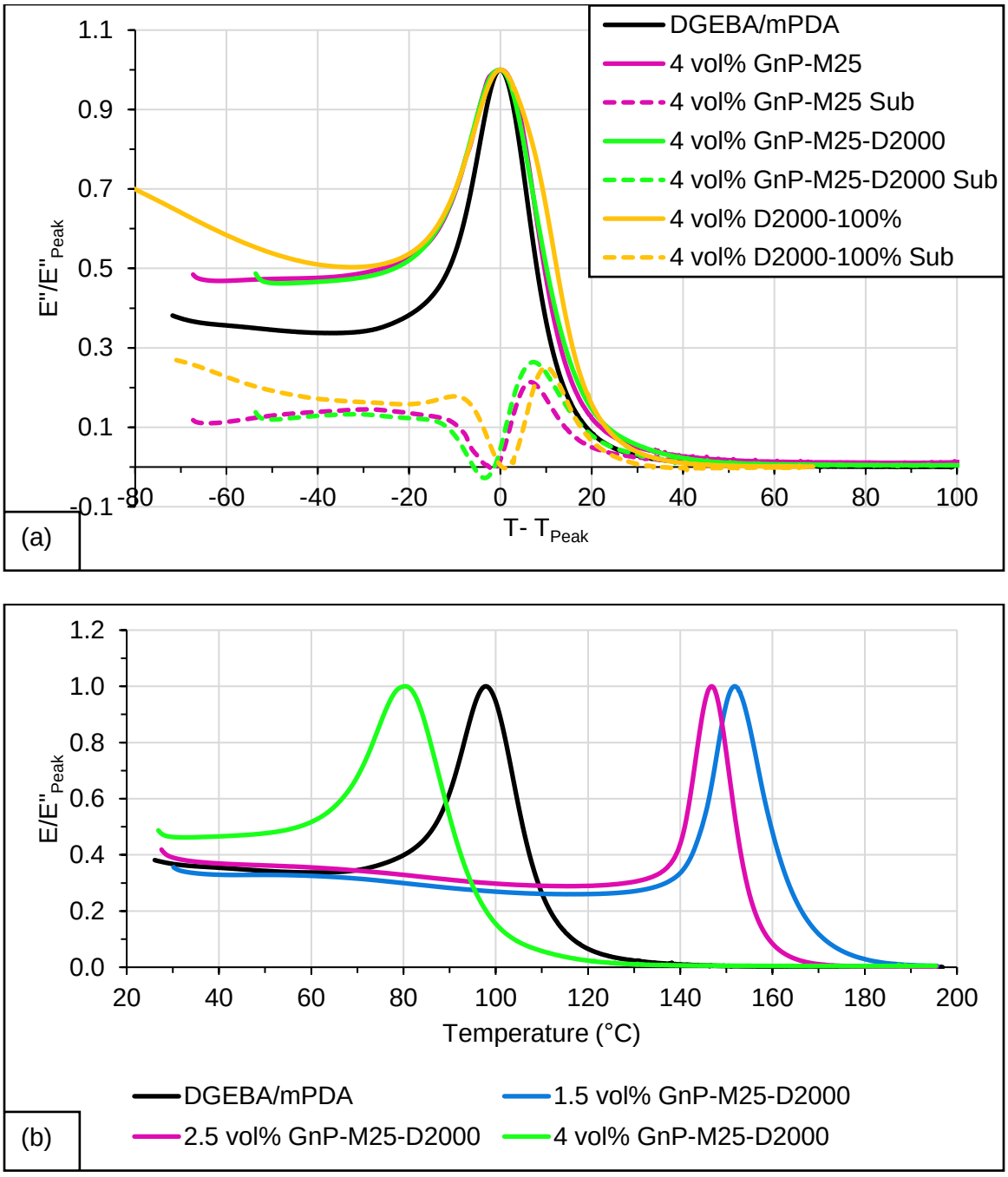

Figure 3.14: Normalized loss modulus curves for GnP-M25, GnP-M25-D2000, and 100% D2000 composites.

Figure 3.14 (cont'd)

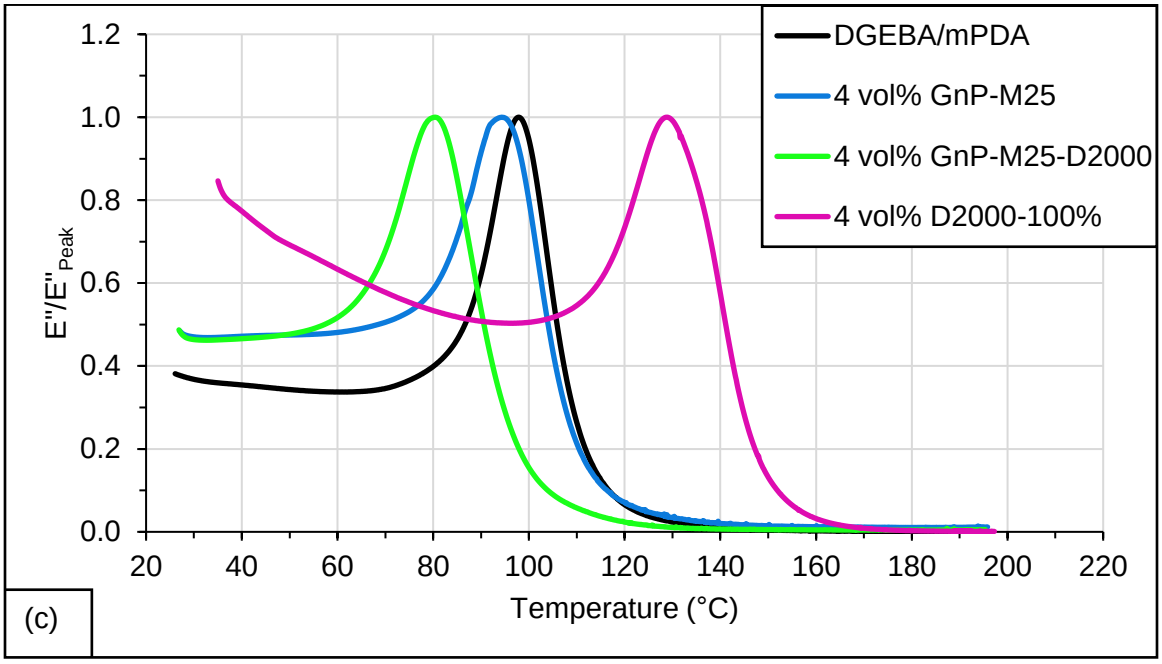

3.4.6 Electrical and Thermal Conductivity

Due to the inherently high thermal conductivity of GnP-M25, the resulting nanocomposites are expected to exhibit increased thermal conductivity. The data shown in Figure 3.15 follows this assertion. Increasing GnP concentration also increases thermal conductivity of the composite. Additionally, the layer of D2000 on GnP only noticeably affects this property at 1.5 vol%. When comparing the GnP materials with the 100% D2000 result, the D2000 does not cause a significant change in thermal conductivity of the epoxy.

One prominent factor that affects the thermal conductivity of a GnP nanocomposite is the interfacial thermal resistance between the graphene basal plane and epoxy matrix [10]. Improving the surface interaction between the GnP and epoxy matrix is expected to increase the composite thermal conductivity. However, surface modification tends to increase phonon scattering on the GnP basal plane. As a result of

increased phonon scattering, the thermal conductivity of the GnP composite decreases. Another factor is the dispersion quality of the GnP within the epoxy matrix. More uniform dispersion results in a higher surface area of GnP which increases the composite thermal conductivity. The intercalation effect of D2000 increases the GnP surface area at the same volume fraction by exfoliating the platelets. While this is expected to improve the thermal conductivity, the surface interaction between the GnP basal plane and D2000 can increase the phonon scattering at that interface, decreasing the composite thermal conductivity. The combination of these two effects results in minimal change between the GnP-M25-D2000 and GnP-M25 composites thermal conductivity.

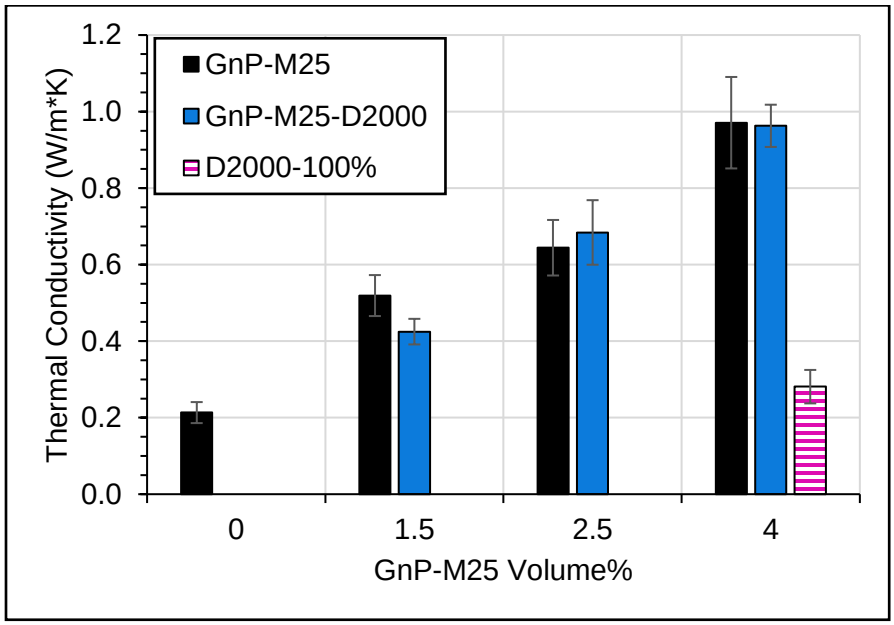

Figure 3.15: Thermal conductivity of GnP-M25 and GnP-M25-D2000 composites.

Similar to thermal conductivity, increasing the concentration of GnP in a composite is expected to increase electrical conductivity [14]. Unmodified GnP-M25 follows this trend, with a large jump between 1.5 and 2.5 vol%. As expected, GnP-M25-D2000 also follows this trend. However, its electrical conductivity is 298% above unmodified GnP-M25 at 2.5 vol% and 3210% at 4 vol%. As a result of the GnP-M25-

D2000 experiencing a lower agglomeration %, the electrical conductivity is increased. Looking at the percolation threshold (Table 3.6), there is no appreciable difference between the two materials. This result further supports that the D2000 was not adsorbed more strongly or differently than the epoxy resin.

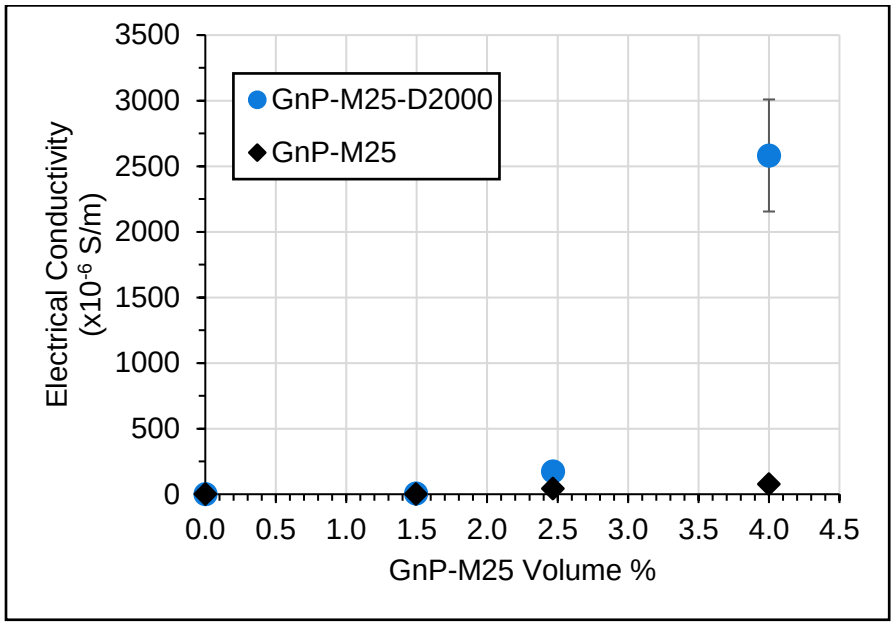

Figure 3.16: Electrical conductivity of GnP-M25 and GnP-M25-D2000 composites.

Table 3.5: Electrical conductivity measurements for GnP-M25 and GnP-M25-D2000 composites.

	Electrical Conductivity (x10^{-6} S/m)	
Filler Concentration (vol%)	GnP-M25	GnP-M25-D2000
0	1.86 ± 0.07	1.86 ± 0.07
1.5	1.95 ± 0.09	5.55 ± 2.66
2.5	43.8 ± 5.26	174 ± 23.5
4	78.0 ± 13.4	2582 ± 427

Table 3.6: Electrical percolation threshold for GnP-M25 and GnP-M25-D2000 composites.

Composite Filler	**Percolation Threshold (vol %)**
GnP-M25	1.41
GnP-M25-D2000	1.49

3.5 Conclusion

Through various characterization techniques, the effects of the adsorption of Jeffamine D2000 on GnP-M25 was investigated. GnP-M25-D2000 presented a lower flexural modulus at 1.5 and 2.5 vol% than unmodified GnP-M25. At 4 vol%, GnP-M25-D2000 had a 4% higher flexural modulus. At this concentration, the GnP-M25 composite was affected by agglomeration, where the adsorbed D2000 acted as a deterrent to this effect. Similarly, D2000 was shown to exhibit intercalative properties through Laser Raman spectroscopy, which can exfoliate the GnP increasing the number of nanoplatelets for the same bulk volume fraction which will also assist in increasing effective GnP loading. Flexural strength is an indication of the interfacial strength between the GnP surface and epoxy, and it was shown that there was no significant difference between the two materials. However, the toughness of the GnP-M25-D2000 at 4 vol% increased by 85% due to the lower modulus layer of D2000.

Through the incorporation of Jeffamine D2000 in the cured network of the epoxy matrix, the MW_C at the GnP surface was increased. As a result, the T_g was lower for the GnP-M25-D2000 composites compared with unmodified GnP-M25. The interfacial strength between the GnP and epoxy did not change significantly with the addition of D2000. The normalized loss modulus data supports this. The GnP-M25-D2000 follows the same trends as without D2000. However, the lower modulus D2000 layer

exacerbates these effects, allowing for more chain movement.

Thermal conductivity was unchanged between the two materials over each concentration. Surface adsorption negatively affects composite thermal conductivity by increasing phonon scattering. In combination with an increase in thermal conductivity due to an increase in GnP surface area through nanoplatelet exfoliation, there is a minimal net change in the composite thermal conductivity compared with the GnP-M25 composite. However, the electrical conductivity of GnP-M25-D2000 showed an improvement over GnP-M25 by producing a more uniform dispersion with less agglomeration which induces increased electrical conductivity.

BIBLIOGRAPHY

[1] ASTM Standard E1269, 2011, “Standard Test Method for Determining Specific Heat Capacity by Differential Scanning Calorimetry,” ASTM International, West Conshohocken, PA, 2011, DOI:10.1520/E1269-11R18, www.astm.org.

[2] ASTM Standard E1461, 2013, “Standard Test Method for Thermal Diffusivity by the Flash Method,” ASTM International, West Conshohocken, PA, 2013, DOI:10.1520/E1461-13R22, www.astm.org.

[3] ASTM Standard E2550, 2021, “Standard Test Method for Thermal Stability by Thermogravimetry,” ASTM International, West Conshohocken, PA, 2021, DOI: 10.1520/D0790-17, www.astm.org.

[4] ASTM Standard D790, 2017, “Standard Test Methods for Flexural Properties of Unreinforced and Reinforced Plastics and Electrical Insulating Materials,” ASTM International, West Conshohocken, PA, 2021, DOI:10.1520/E2550-21, www.astm.org.

[5] ASTM Standard D792, 2020, “Standard Test Methods for Density and Specific Gravity (Relative Density) of Plastics by Displacement,” ASTM International, West Conshohocken, PA, 2020, DOI: 10.1520/D0792-20, www.astm.org.

[6] Childres, Isaac, et al. "Raman spectroscopy of graphene and related materials." New developments in photon and materials research 1 (2013): 1-20.

[7] Eitan, A., et al. "Reinforcement mechanisms in MWCNT-filled polycarbonate." Composites Science and Technology 66.9 (2006): 1162-1173.

[8] Gupta, V. B., et al. "The temperature-dependence of some mechanical properties of a cured epoxy resin system." Polymer Engineering & Science 25.13 (1985): 812-823.

[9] Halpin, JC, and J. L. Kardos. "The Halpin-Tsai equations: a review." Polymer Engineering & Science 16.5 (1976): 344-352.

[10] Huang, Xingyi, et al. "Thermal conductivity of graphene-based polymer nanocomposites." Materials Science and Engineering: R: Reports 142 (2020): 100577.

[11] King, Julia A., et al. "Mechanical properties of graphene nanoplatelet/epoxy composites." Journal of applied polymer science 128.6 (2013): 4217-4223.

[12] King, Julia A., et al. "Mechanical properties of graphene nanoplatelet/epoxy composites." Journal of Composite Materials 49.6 (2015): 659-668.

[13] Li, Bing, et al. "Polycyclic aromatic hydrocarbons adsorption onto graphene: a DFT and AIMD study." *Materials* 11.5 (2018): 726.

[14] Li, Yan, et al. "Mechanical, electrical and thermal properties of in-situ exfoliated graphene/epoxy nanocomposites." Composites Part A: Applied Science and Manufacturing 95 (2017): 229-236.

[15] Liu, Jia Daniel, et al. "Effect of crosslink density on fracture behavior of model epoxies containing block copolymer nanoparticles." Polymer 50.19 (2009): 4683-4689.

[16] Liu, Jingquan, et al. "Thermosensitive graphene nanocomposites formed using pyrene-terminal polymers made by RAFT polymerization." Journal of Polymer Science Part A: Polymer Chemistry 48.2 (2010): 425-433.

[17] Tyson, Bryan M., et al. "A quantitative method for analyzing the dispersion and agglomeration of nano-particles in composite materials." Composites Part B: Engineering 42.6 (2011): 1395-1403.

[18] Vennerberg, Danny, Zach Rueger, and Michael R. Kessler. "Effect of silane structure on the properties of silanized multiwalled carbon nanotube-epoxy nanocomposites." Polymer 55.7 (2014): 1854-1865.

[19] Wang, Jun, Zaiming Chen, and Baoliang Chen. "Adsorption of polycyclic aromatic hydrocarbons by graphene and graphene oxide nanosheets." Environmental science & technology 48.9 (2014): 4817-4825.

[20] Xu, Liyan, and Xiaoning Yang. "Molecular dynamics simulation of adsorption of pyrene–polyethylene glycol onto graphene." Journal of colloid and interface science 418 (2014): 66-73.

[21] Zaman, Izzuddin, et al. "Epoxy/graphene platelets nanocomposites with two levels of interface strength." Polymer 52.7 (2011): 1603-1611.

[22] Zaman, Izzuddin, et al. "Interface modification of clay and graphene platelets reinforced epoxy nanocomposites: a comparative study." Journal of materials science 49.17 (2014): 5856-5865.

[23] Zheng, Wenge, Bin Shen, and Wentao Zhai. "Surface functionalization of graphene with polymers for enhanced properties." New progress on graphene research 10 (2013): 50490.

CHAPTER 4: CHANGES IN COMPOSITE MULTIFUNCTIONALITY USING 1-PYRENEALDEHYDE AS AN ADSORBATE ONTO GNP-M25

4.1 Abstract

Improving the graphene nanoplatelet/epoxy matrix interface through a non-covalent pathway is one method to enhance composite properties. Using 1-pyrenealdehyde as an adsorbate in which the pyrene group would interact with the basal plane of GnP-M25 via π-π stacking and the aldehyde group introduces hydrogen bonding interactions with the epoxy, the resulting composites were investigated for changes in the composite's properties. Through flexural modulus and strength, data showed that although flexural modulus improved 40% over unmodified GnP-M25 composites, flexural strength did not change. Though there is an addition of hydrogen bonding intermolecular forces, the interfacial improvement did not significantly affect the composite properties, as shown in thermomechanical data such as T_g, loss modulus and tan δ. However, the composite electrical conductivity did increase with respect to unmodified GnP-M25 composites. The resulted property improvements are attributed to an improvement in dispersion, agglomeration, and increased GnP concentration.

4.2 Introduction

Non-covalently modifying the graphene nanoplatelet (GnP) basal plane can influence its interaction with an epoxy matrix, resulting in a change in composite properties. In Chapter 5, the change in composite properties due to a pyrene-capped poly(oxypropylene) amine (Py-POP) is discussed. Similarly, 1-pyrenealdehyde – one reactant used to produce Py-POP – was also chosen as an adsorbate for GnP-M25. While Py-POP strongly adheres noncovalently to the GnP surface and covalently bonds with the epoxy resin, 1-pyrenealdehyde only exhibits strong interactions with the

graphene basal plane. 1-Pyrenealdehyde's structure is very similar to graphene albeit a fraction of the size, both containing a network of conjugated cyclic hydrocarbons. Consequentially, 1-pyrenealdehyde readily adsorbs to the GnP surface via π-π stacking, a strong intermolecular bonding interaction [18]. Additionally, the aldehyde functional group sterically prevents tight arrangement to create an unbroken monolayer of pyrene but does not disrupt the adsorption mechanism.

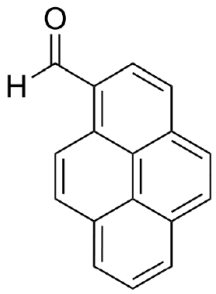

Figure 4.1: Molecular structure of 1-pyrenealdehyde.

The only reactive functional group within 1-pyrenealdehyde is an aldehyde. Similarly, GnP contains oxygen functional groups on its edges such as hydroxyl, ether, and carboxylic acid groups. Due to the very low fraction of edge to surface area, there is a relatively low chance for these to chemically interact and would result in minimal effects. The presence of an aldehyde introduces the possibility for reactions with the epoxy and primary amines. In order for the aldehyde to react with the epoxy, typically a catalyst is necessary along with the proper solvent [7], [17]. Similarly, one study found that an imine is produced from an aldehyde and epoxy in the presence of aqueous ammonia [8]. Without these conditions, yield of any reaction will be low.

There is a possible reaction between the aldehyde and the primary amine curing agent. Generally, this reaction utilizes an acid catalyst to produce high yields. However, it is possible for another primary amine to facilitate the proton transfer in place of a

catalyst or protic solvent [23]. As a result, it is likely for the 1-pyrenealdehyde and m-phenylene diamine to produce in imine, particularly in the elevated temperatures of the curing process. Secondary and tertiary amines require a catalyst in order to react with an aldehyde [24]. Therefore, once the amines begin curing with the epoxy, the rate of imine formation decreases significantly. Because the amount of adsorbed 1-pyrenealdehyde is small compared to the quantity of primary amines, it is not expected to negatively affect the epoxy-amine ratio. However, a covalent interaction with the adsorbate is expected to improve the composite properties.

The adsorption of 1-pyrenealdehyde to the GnP surface is expected to have a small effect on its intermolecular interaction with the epoxy resin due to the small fraction of aldehyde oxygens on the surface. The increased presence of oxygen would create a more hydrophilic surface compared to the hydrophobic graphene basal plane.

4.3 Materials and Methods

4.3.1 Materials

Graphene nanoplatelets, product name GnP-M25 (d = 25 μm, t ~ 7 nm, 5-10 layers) was provided by XG Sciences. 1-pyrenealdehyde and isopropanol were purchased from Sigma Aldrich, used as received. Bisphenol A diglycidyl ether (DGEBA), known by trade name Epon 828 was purchased from Miller-Stephenson. Meta-phenylene diamine (mPDA) was purchased from Sigma Aldrich. PELCO Conductive Liquid Silver Paint was used to create electrical contact points for electrical conductivity measurements.

4.3.2 Adsorption Method

GnP-M25 was ultrasonicated in isopropanol for 10 minutes in an ice bath to

break up agglomerates. An excess of 1-pyrenealdehyde was added to the mixture and mechanically stirred overnight via a stir bar. The mixture was then vacuum filtered through a 0.22 µm filter paper (PTFE) to remove the solvent and excess 1-pyrenealdehyde. The GnP-M25-Pyrenealdehyde was dried in a vacuum oven to remove the residual solvent.

4.3.3 Composite Preparation Method

Four concentrations of GnP-M25 were used: 0, 3, 5, and 8 weight % (0, 1.5, 2.5, 4 volume %). The GnP-M25-Pyrenealdehyde sample was added to isopropanol and ultrasonicated for 10 minutes in an ice bath. DGEBA was added to the mixture, mechanically stirred to dissolve, and ultrasonicated 10 minutes in an ice bath while stirring with a stir bar. The isopropanol was removed from the mixture in a vacuum oven at 80 °C. After the solvent was removed, mPDA (14.5:100 weight ratio to DGEBA) was added at 75 °C to the GnP-M25-Pyrenealdehyde/DGEBA mixture and stirred thoroughly. After degassing, the mixture was poured into flexural coupon silicone molds and cured using a cycle of 2 h at 75 °C then 2 h at 125 °C. The cured composites were polished to a flat surface before testing. All data will reference the GnP-M25 concentration for clarity, and it is noted that the addition of the adsorbates will increase the volume % of additives.

4.3.4 Characterization

Laser Raman spectroscopy was used to analyze the structure of GnP-M25 before and after adsorption of 1-pyrenealdehyde using the LabRAM Aramis (Horiba). Laser wavelength was 532 nm. Spectra were recorded in two parts (1000 – 2000 cm^{-1} and 2000 – 3000 cm^{-1}) to reduce oxidation of the material.

Composite flexural coupons were tested using a three-point bending method according to the standard ASTM D790 using a Universal Testing System (Instron). Rectangular specimens were supported 2 inches apart, then force was applied to the middle of the specimen at a strain rate of 0.01 mm/mm/min until failure. Force applied and extension of deflection measured were used to calculate flexural modulus and flexural strength.

The TA Instruments TGA Q500 machine was used for thermogravimetric analysis (TGA) of the samples' thermal stability. Heating rate was set at 10 °C/min to 500 °C in a nitrogen atmosphere. Decomposition onset temperature was determined using ASTM E2550.

Dynamic mechanical analysis (DMA) was performed using a TA DMA Q800 machine. Testing conditions were single-cantilever method, temperature ramp to 200 °C at a rate of 3 °C/min, set at a frequency of 1 Hz, and set at an amplitude of 30 μm. Glass transition temperature was defined as the temperature at the peak of the tan δ curve. Polymer density was measured according to the standard ASTM D792.

A Carl Zeiss Auriga Dual Column FIB scanning electron microscope was used to capture cross-sectional images of polymer composites. These images were used to qualitatively analyze GnP dispersion. Using the image processing software ImageJ, a quantitative measurement of dispersion and agglomeration was calculated.

Flexural testing coupons were used to measure electrical conductivity via a Four-point probe method. Coupons were cut to 30 mm in length, polished surfaces to be flat, and oxygen plasma treated for 10 minutes at 300 W. Opposite ends were coated in a layer of silver paint. Two contacts points were placed using silver paint 15 mm apart in

the middle of the composite coupon surface. A heat gun was used to dry the silver paint. A Keithley 2000 multimeter was used to apply a 1 μA current from one end to the opposite end of the sample. Voltage was measured between the two contact points.

Thermal conductivity was calculated by measuring the composites thermal diffusivity and heat capacity. The thermal diffusivity was measured via laser flash method using a Netzsch LFA 447 according to ASTM 1461-13. Flexural coupon samples were cut to fit in the machine, surfaces polished flat, and coated with a graphite layer. A TA DSC Q2000 was used to measure heat capacity according to ASTM E1269-11. Samples were ramped to -10 °C at 20 °C/min, held isothermally for 5 minutes, ramped to 50 °C at 20 °C/min, and held isothermally for 5 minutes. Heat capacity was taken at 25 °C.

4.4 Results and Discussion

4.4.1 Adsorption of 1-Pyrenealdehyde onto GnP-M25

Adsorption of 1-pyrenealdehyde was analyzed through Laser Raman spectroscopy and TGA. As shown in Figure 4.2 and Table 4.1, the D peak (~1350 cm^{-1}) and I_D:I_G peak intensity ratio for GnP-M25-Pyrenealdehyde show virtually no change with respect to the unmodified GnP-M25. The D peak is caused due to the scattering of a charge carrier at a defect in the graphene crystal structure. The intensity of the D peak represents the disruption of the graphene structure throughout the basal plane due to reactions converting the sp^2 carbons to sp^3 hybridization [8]. Therefore, the adsorbed 1-pyrenealdehyde does not chemically bond with the graphene surface as there is no increase in the I_D:I_G peak intensity ratio. All interactions are confined to π-π stacking between the GnP and 1-pyrenealdehyde.

For GnP-M25, the 2D peak (~2700 cm^{-1}) is negligible and the I_{2D}:I_G peak intensity ratio is also very small, an indication of several layers of stacked graphene sheets. Conversely, the 2D peak for GnP-M25-Pyrenealdehyde is significantly larger and the I_{2D}:I_G peak intensity ratio is two orders of magnitude larger than the unmodified GnP-M25. Because this peak references the number of stacked graphene layers, it is likely that the 1-pyrenealdehyde intercalates the GnP and exfoliates some layers [22].

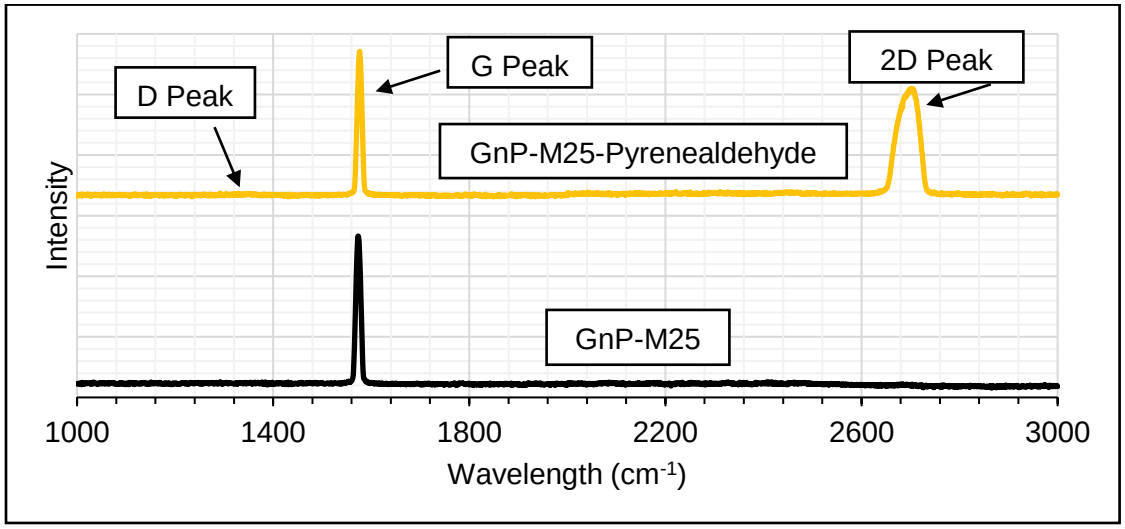

Figure 4.2: Laser Raman Spectra for GnP-M25 (bottom) and GnP-M25-Pyrenealdehyde (top).

Table 4.1: Laser Raman peak intensity ratios.

Peak Intensity Ratios	**GnP-M25**	**GnP-M25-Pyrenealdehyde**
D:G	0.01	0.012
2D:G	0.0016	0.74

From the Laser Raman data, 1-pyrenealdehyde is presumed to be entirely physically adsorbed. Thus, the weight loss below the decomposition temperature for graphene (~500 - 600 °C) can be attributed entirely to the adsorbate, 1-pyrenealdehyde. Based on the surface area of the GnP, the theoretical maximum monolayer adsorption of pyrene onto GnP-M25 is 248 mg pyrene/g GnP-M25. The data from Figure 4.3 shows

that the adsorption is 22% lower than the theoretical maximum at 194 mg 1-pyrenealdehyde/g GnP-M25. Due to the steric effects of the aldehyde group, a close packed monolayer is not likely and therefore the amount adsorbed was expected to be lower than the theoretical monolayer maximum.

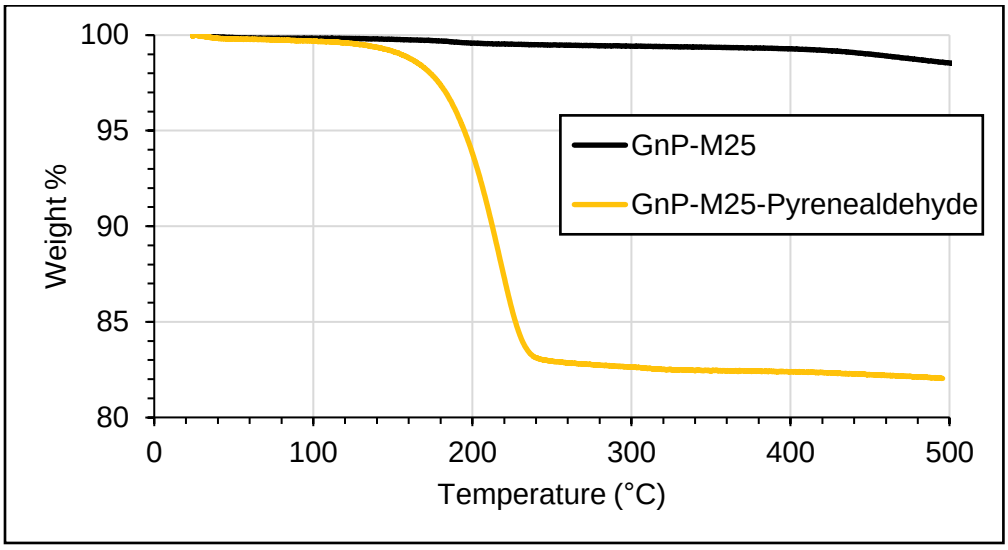

Figure 4.3: Weight loss analysis through TGA on GnP-M25 and GnP-M25-Pyrenealdehyde in a N_2 atmosphere.

4.4.2 GnP Dispersion

Figure 4.4 compares cross-section images of GnP-M25 and GnP-M25-Pyrenealdehyde composites at each concentration. In these images, the white lines and groups represent the GnP. Qualitatively, increasing GnP concentration is apparent. For a more quantitative approach, each material was analyzed using image processing software to measure dispersion and agglomeration percent.

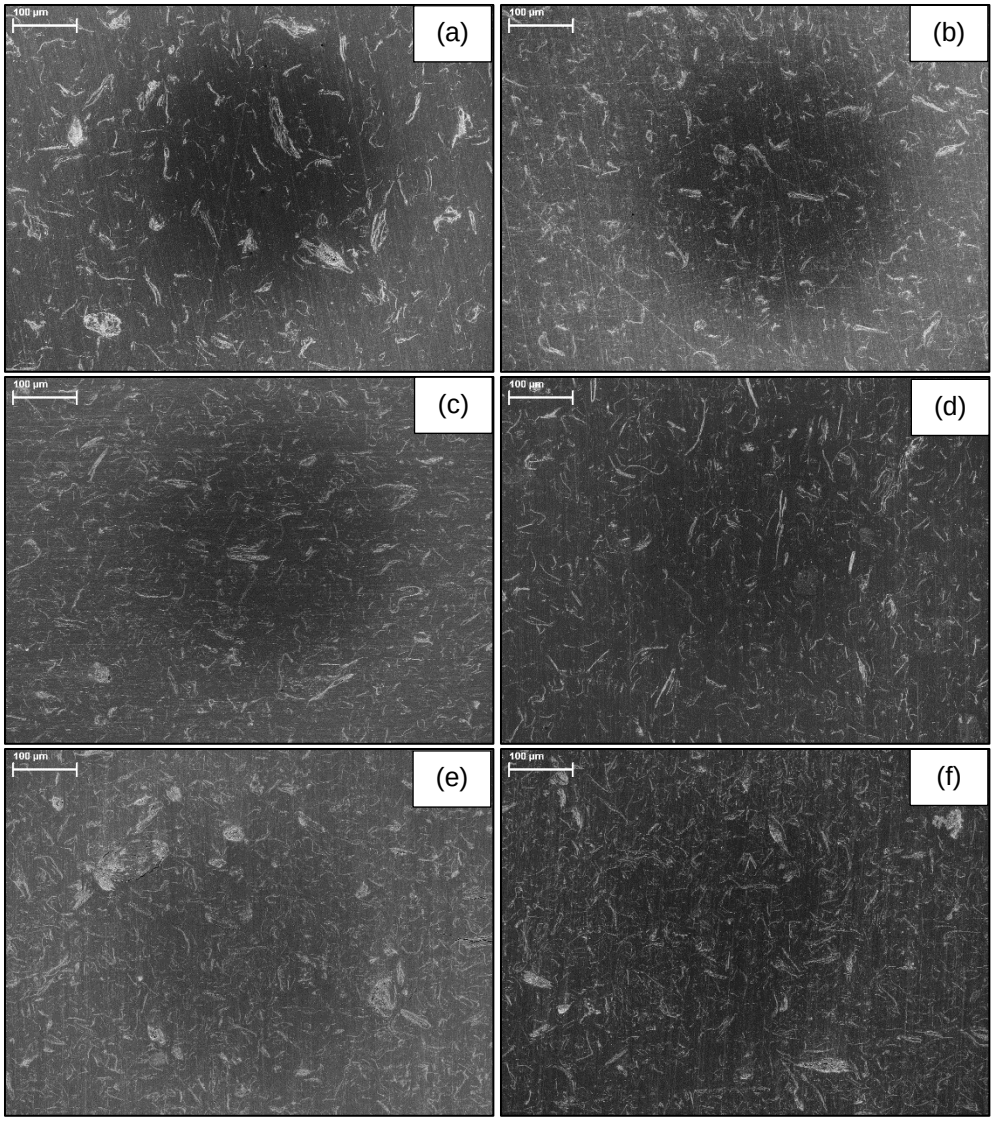

Figure 4.4: SEM cross sectional images for GnP-M25 composites at (a) 1.5 vol%, (c) 2.5 vol%, and (e) 4 vol%, and GnP-M25-Pyrenealdehyde composites at (b) 1.5 vol%, (d) 2.5 vol%, and (f) 4 vol%.

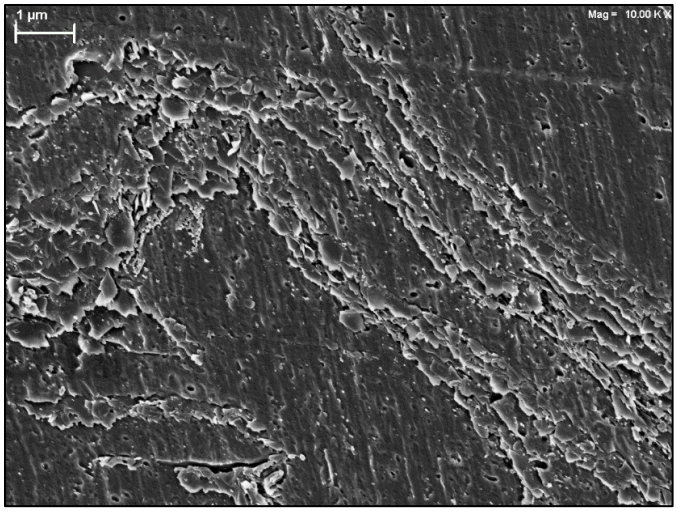

Figure 4.5: 2.5 vol% GnP-M25-Pyrenealdehyde cross-sectional image.

Using the method demonstrated by Tyson et al. [25], the dispersion and agglomeration percent were calculated. Dispersion % measures the distribution of the distances between the platelets, where a higher value indicates a more uniform dispersion. GnP-M25 composites show a trend of decreasing in dispersion % as concentration increases. This follows as higher concentrations result in higher probability of agglomeration. On the other hand, the dispersion % for GnP-M25-Pyrenealdehyde composites remain relatively equal throughout all concentrations.

For a complete picture, agglomeration % is also considered. As expected, the highest concentration for both materials is also the highest agglomeration %. In this case, agglomeration is measured as the uniformity of platelet group thickness. For clarity, a higher agglomeration % refers to more widely distributed agglomerate sizes. The GnP-M25-Pyrenealdehyde composites' agglomeration % increases with concentration but remains lower than GnP-M25. As a result, the GnP-M25-Pyrenealdehyde demonstrates a slightly better overall dispersion due to more uniform platelet/agglomerate sizes with roughly equivalent dispersion %.

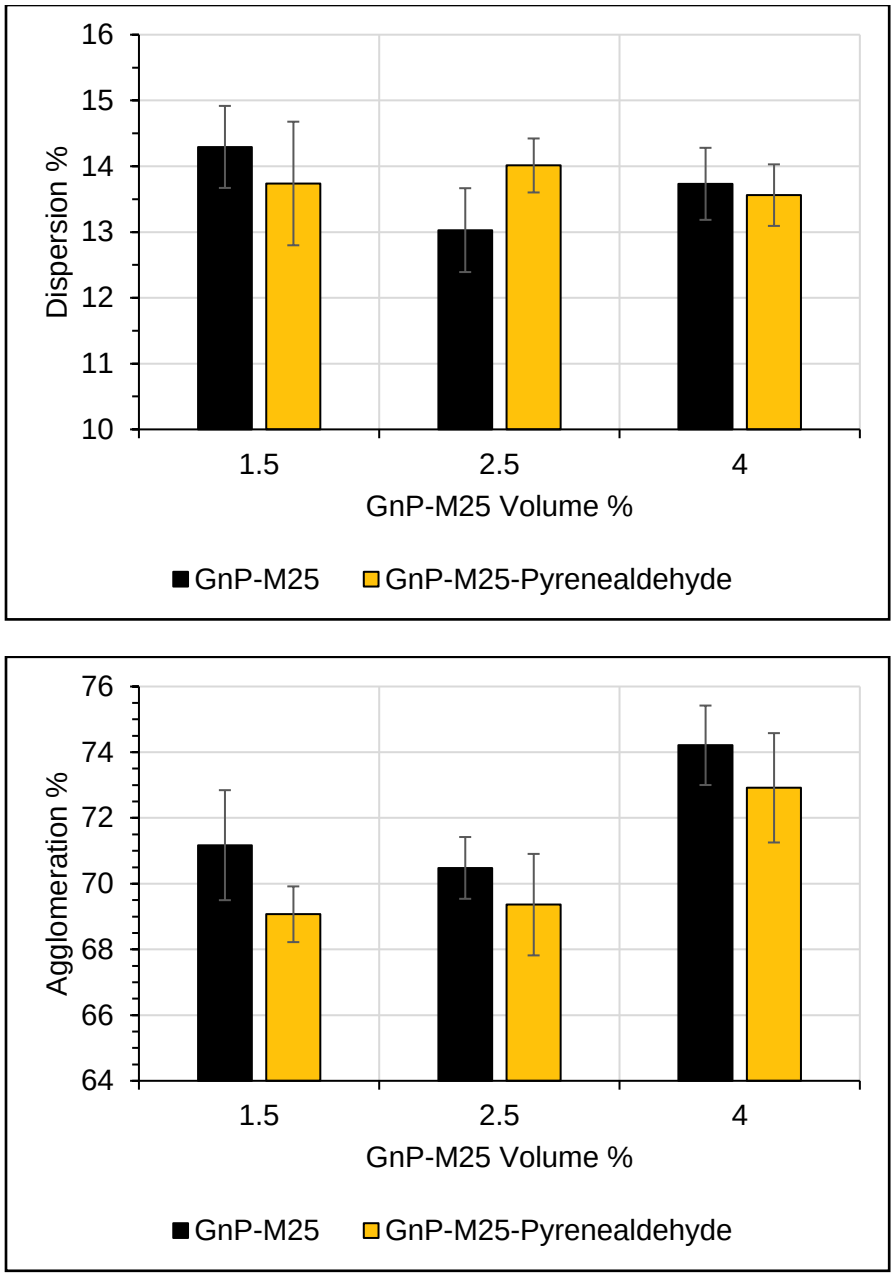

Figure 4.6: Dispersion percent, (a), and agglomeration percent, (b), calculated from SEM cross-sectional images.

4.4.3 1-Pyrenealdehyde Effect on Epoxy Matrix Properties

For further understanding on the interaction of 1-pyrenealdehyde with the DGEBA/mPDA system, composites were tested using the adsorbate without GnP-M25. The mass of 1-pyrenealdehyde used corresponds to 20, 50, and 100% of the

experimental adsorption onto 4 vol% GnP-M25 from Section 4.4.1.

Interestingly, the glass transition temperatures did not change significantly for composites including 20, 50, and 100% adsorbed 1-pyrenealdehyde – only an average of 5 °C between the three sample materials. So, the 100% 1-pyrenealdehyde value was used for analysis. The 100% 1-pyrenealdehyde composite resulted in a 38% increase in Tg over the neat epoxy from ~104 to ~144 °C. This data shows that the 1-pyrenealdehyde participates in inhibiting the movement of the epoxy chains. The 1-pyrenealdehyde acts as a barrier for chain growth to this effect. Additionally, the aldehyde can react with the mPDA, which assists in creating a larger molecule that can act as a chain movement inhibitor. The added aldehyde corresponds to at most 2.5% of the available mPDA amines. Therefore, the ratio between DGEBA and mPDA was not significantly altered to affect the properties.

Normalized loss modulus curves (E''/E''_{Peak}) viewed with respect to normalized temperature ($T - T_{Peak}$) and increasing temperature gives valuable insight into the effects of 1-pyrenealdehyde on the composite system [11]. In Figure 4.7a, the curve shapes of the 1-pyrenealdehyde composites are compared with neat DGEBA/mPDA. Included in this plot are curves where the normalized loss modulus curve is subtracted from the curves for each 1-pyrenealdehyde material. This method of visualization shows where the adsorbate composites differ from the neat epoxy. All three concentrations show similar subtracted curves (labeled Sub in Fig. 4.7a). The 20 and 50% loss modulus curves show a constant lower modulus at temperatures below the peak. At temperatures within 20 degrees above the peak, all three curves are narrower than the neat epoxy. This signifies an increase in chain mobility and a more homogeneous

movement of the chains.

The greatest difference between these materials is that the 100% 1-pyrenealdehyde composite increases and slightly broadens the loss modulus curve below the peak temperature. So, the highest concentration of 1-pyrenealdehyde – which corresponds to the amount adsorbed on 4 vol% GnP-M25-Pyrenealdehyde – improves the elastic properties a small amount. Figure 4.7b depicts the shifts in the loss modulus peaks. As all adsorbate concentrations shift the temperature upward, they all contribute a chain movement inhibition effect, requiring a higher temperature to initiate bulk chain movement. An interesting note is that increasing the 1-pyrenealdehyde concentration lowers the loss modulus peak temperature, although slightly.

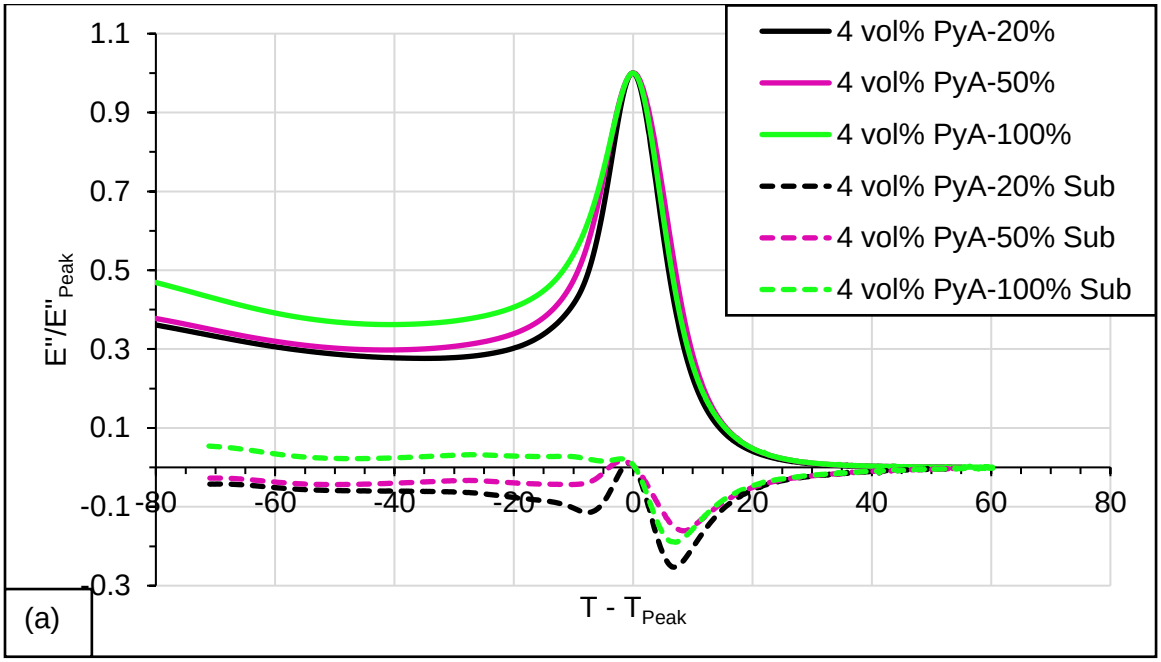

Figure 4.7: Normalized loss modulus curves of 1-Pyrenealdehyde (PyA) composites (a) versus normalized temperature and (b) versus increasing temperature.

Figure 4.7 (cont'd)

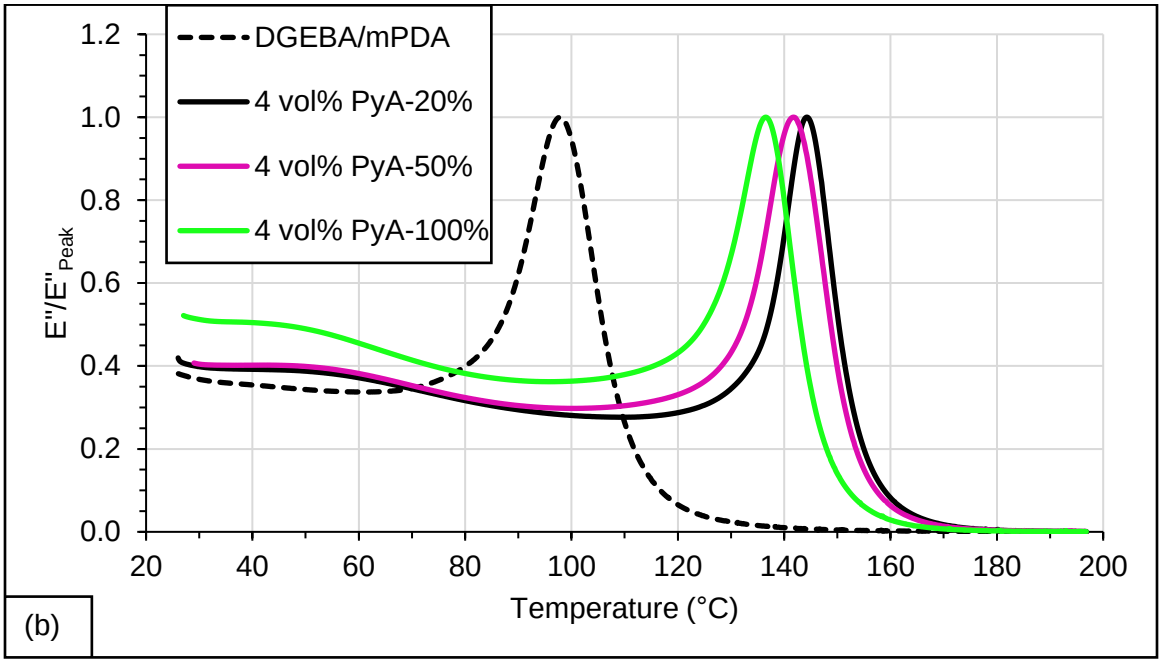

Another characteristic that was measured was electrical conductivity. The 1-pyrenealdehyde at all concentrations did not significantly affect this property. A limit of the multimeter used is that over a certain electrical resistivity, the measured voltage drop is maximized. Because of this, the measured electrical conductivity of the materials measured do not accurately represent the material. However, the outcome is maintained that 1-pyrenealdehyde at these concentrations does not cause a noticeable effect on the composite electrical conductivity.

This adsorbate's effect on thermal conductivity was also considered. The 100% 1-pyrenealdehyde composite increased the thermal conductivity 18% above the neat epoxy. As a comparison, 4 vol% GnP-M25 showed an increase of 355%. So, the 1-pyrenealdehyde affects this property minimally.

Table 4.2: Thermal conductivity.

Samples	**Thermal Cond. (W/m*K)**	**Thermal Cond. Error (W/m*K)**
Neat DGEBA/mPDA	0.213	0.027
100% Pyrenealdehyde	0.252	0.012
4 vol% GnP-M25	0.971	0.120

4.4.4 Mechanical Properties

The flexural modulus data for both GnP-M25 and GnP-M25-Pyrenealdehyde composites is shown in Figure 4.8. The unmodified GnP-M25 composites show a flexural modulus that increases with concentration until a plateau at 4 vol% GnP most likely due to agglomeration effects reducing the effective GnP concentration. The flexural modulus for GnP-M25-Pyrenealdehyde composites increases with concentration as well. While at 1.5 vol%, the GnP-M25-Pyrenealdehyde flexural modulus is lower than the unmodified GnP-M25 composites, there is an increase of 40% at 4 vol% GnP.

Of the factors that dictate changes in mechanical properties, the exfoliation factor and subsequent increase in effective GnP concentration due to intercalation of 1-pyrenealdehyde is expected to be the major reason. Thus, there is a higher concentration and surface area of GnP-M25-Pyrenealdehyde than GnP-M25 at 4 vol% resulting in a clear increase in flexural modulus. An additional factor is the chemical bonding of mPDA with the 1-pyrenealdehyde. As the 1-pyrenealdehyde is adsorbed to the GnP surface, a covalent bond with the adsorbate creates a stronger connection with the epoxy matrix. Due to the similarity in structure of 1-pyrenealdehyde and graphene, the sole variation in intermolecular bonding with the epoxy is the addition of hydrogen bonding due to the aldehyde group. As hydrogen bonding is stronger than van der

Waals forces, the biggest effects expected are improved dispersion of the platelets and a stronger interfacial layer at the GnP surface.

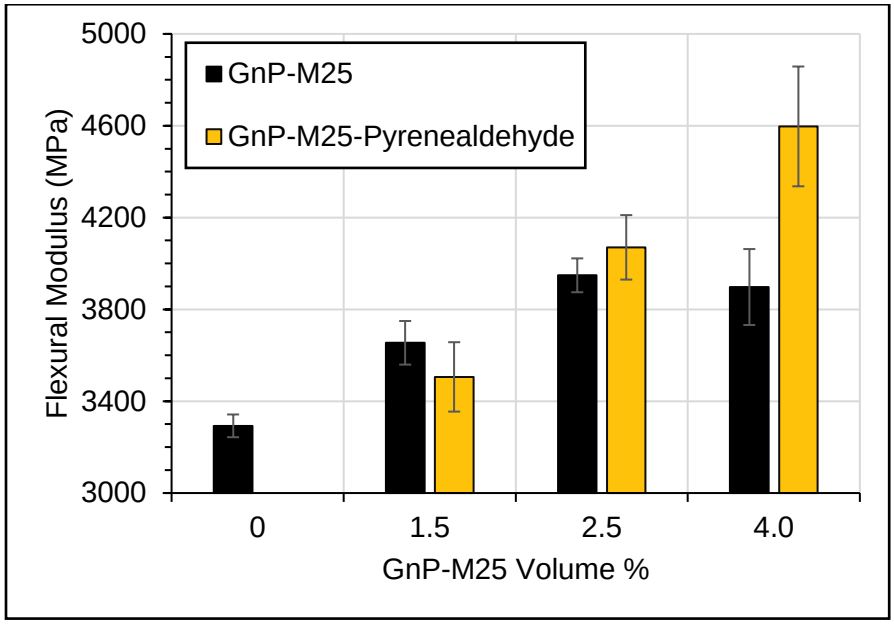

Figure 4.8: Flexural modulus for GnP-M25 and GnP-M25-Pyrenealdehyde composites.

Table 4.3: Flexural modulus percent increase over neat DGEBA/mPDA.

Composite Filler	1.5 vol%	2.5 vol%	4 vol%
GnP-M25	11.0	19.9	18.4
GnP-M25-Pyrenealdehyde	6.5	23.6	39.6

Examining the molecular weight between crosslinks (MW_C) grants further understanding on the interactions occurring in the material systems. Shown in Table 4.4, addition of GnP reduces the MW_C, as expected due to blocking chain diffusion and growth during curing. The MW_C for GnP-M25-Pyrenealdehyde follows this same trend until 4 vol%, where it is 33% higher than GnP-M25 at the same concentration. A higher MW_C relates to a lower crosslink density, which indicates that the epoxy chains can move more easily and are less inhibited by the GnP, especially at elevated temperatures. The Laser Raman data showed that there was some partial to full

exfoliation of the platelets. That would result in a higher effective GnP concentration within the composite, leading to a lower MW_C with good dispersion. This calculation uses DMA measurements to determine the ease of chain movement. 4 vol% GnP-M25-Pyrenealdehyde and 100% 1-pyrenealdehyde both contain the same quantity of 1-pyrenealdehyde. The MW_C for both are very similar and higher than the unmodified GnP-M25 composite, which indicates that the epoxy matrix is including the 1-pyrenealdehyde.

Figure 4.9 shows the Halpin-Tsai model for predicting flexural modulus in a composite [12]. The experimental data follows the predicted trend of increasing flexural modulus with GnP concentration. As this model assumes ideal dispersion and no agglomerate formation, the GnP-M25 composite data drops at 4 vol% due to worsening dispersion and more agglomerates present. Conversely, the GnP-M25-Pyrenealdehyde data shows a steeper slope with increasing concentration.

Table 4.4: Molecular weight between crosslinks calculated from DMA.

	Molecular Weight between Crosslinks (g/mol)		
Filler Concentration (vol%)	GnP-M25	GnP-M25-Pyrenealdehyde	Pyrenealdehyde – 100%
0	335 ± 66	335 ± 66	-
1.5	260 ± 1.1	271 ± 18	-
2.5	255 ± 0.54	261 ± 0.79	-
4	232 ± 57	308 ± 8.5	297 ± 12

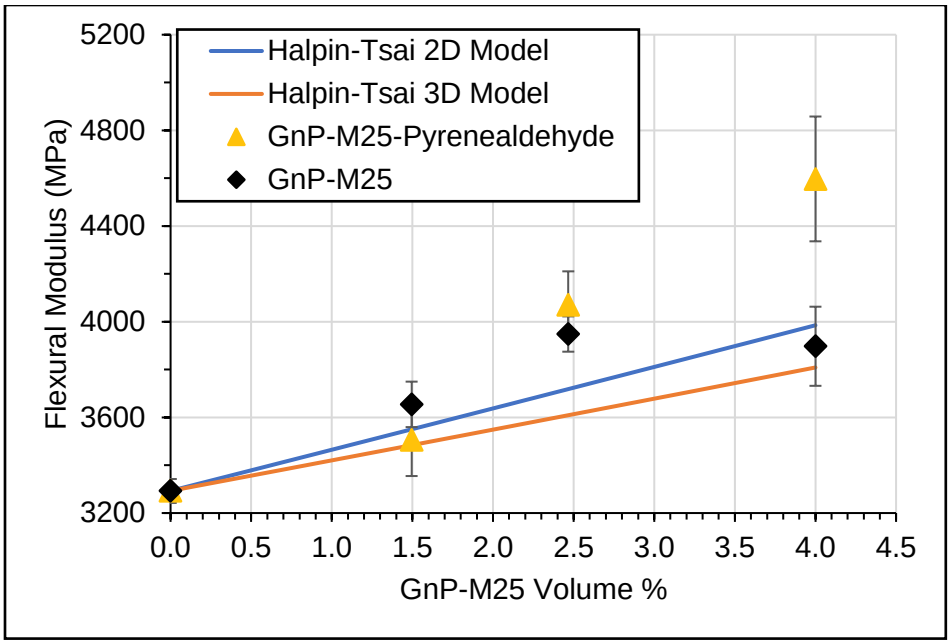

Figure 4.9: Halpin-Tsai model for flexural modulus.

The flexural strength of a GnP composite system is controlled by the strength of the GnP/epoxy interface along with dispersion factors. Improving this interface improves the flexural strength of the material due to enhanced stress transfer. However, shown in Figure 4.10a, the difference in flexural strength between both materials is minimal. At 1.5 vol%, GnP-M25-Pyrenealdehyde is 9.4% lower than GnP-M25, and at 4 vol%, it is 9.5% higher than GnP-M25. Increased surface area of GnP-M25-Pyrenealdehyde is shown to increase the flexural modulus and flexural strength to a lesser extent over the unmodified GnP-M25. Another influencing factor is the intercalation effect that can increase the GnP-M25 concentration. The toughness of both materials follows a similar trend. The covalent bond between the mPDA and 1-pyrenealdehyde does not increase the ductility of the interface. While strengthening the intermolecular forces at the interfacial layer at the GnP surface improves dispersion, the flexural strength and toughness do not experience a significant change.

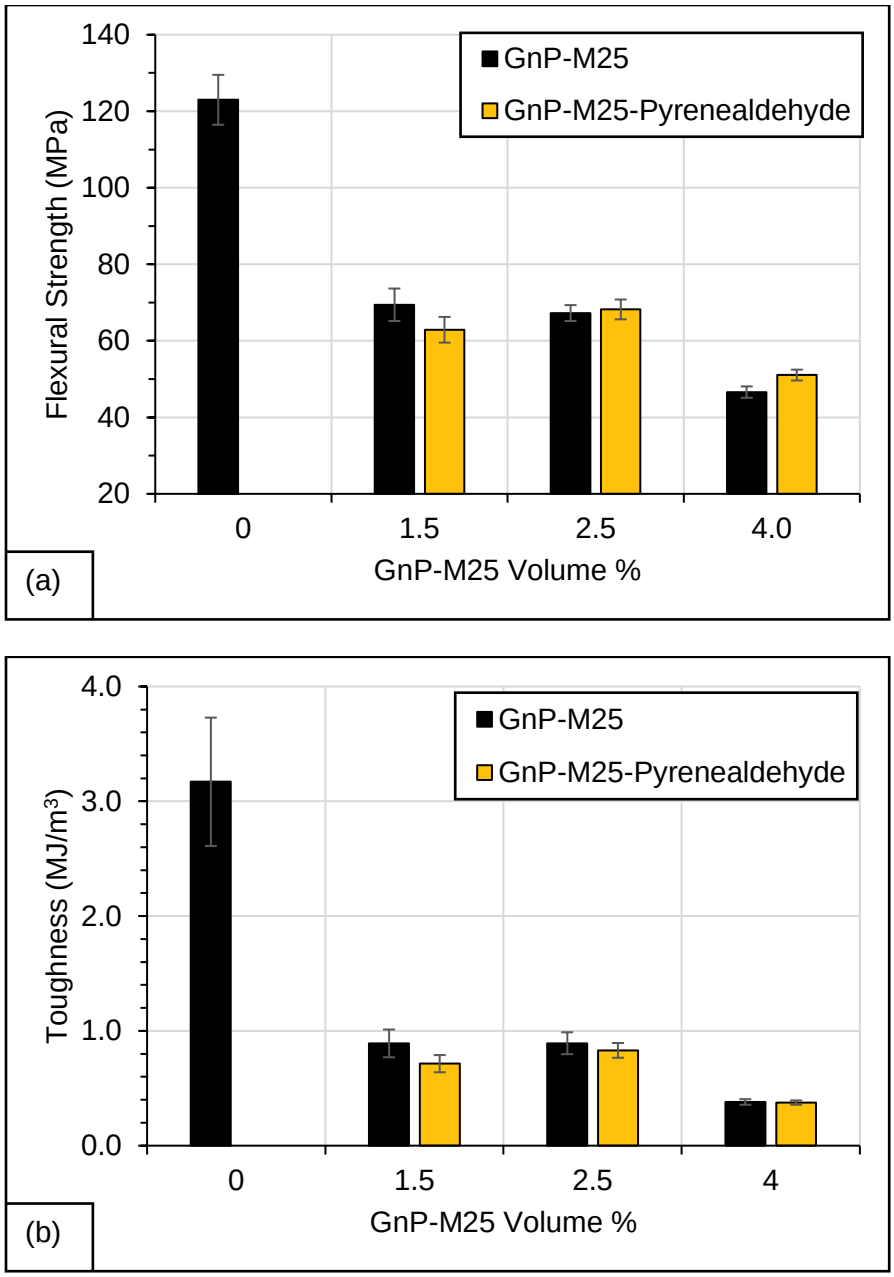

Figure 4.10: Flexural strength (a) and toughness (b) for GnP-M25 and GnP-M25-Pyrenealdehyde composites.

4.4.5 Thermal Properties

The glass transition temperature (T_g) of GnP nanocomposites is expected to increase with GnP concentration. This is shown at 1.5 and 2.5 vol% where the T_g increases by 53% over neat DGEBA/mPDA. At 4 vol% GnP-M25, both materials

experience a significant decrease in T_g. The unmodified GnP-M25 composite reverts to roughly the same value as neat DGEBA/mPDA, and the GnP-M25-Pyrenealdehyde composite falls 19% below GnP-M25. As T_g is measure of how easily the matrix chains can move, a lower T_g indicates that 4 vol% GnP-M25-Pyrenealdehyde does not restrict chain movement very effectively. In fact, this material allows the chains to move more easily than without GnP-M25 present. Even though the GnP surface interfacial layer has improved intermolecular forces, this effect seems to only make a stronger impact on the composite production. The layer of 1-pyrenealdehyde allows a higher degree of chain movement. Comparing with 1-pyrenealdehyde without GnP, the T_g is 38% higher than that of the neat epoxy. This further supports the assertion that the 1-pyrenealdehyde adsorption is the cause of decreased chain movement inhibition.

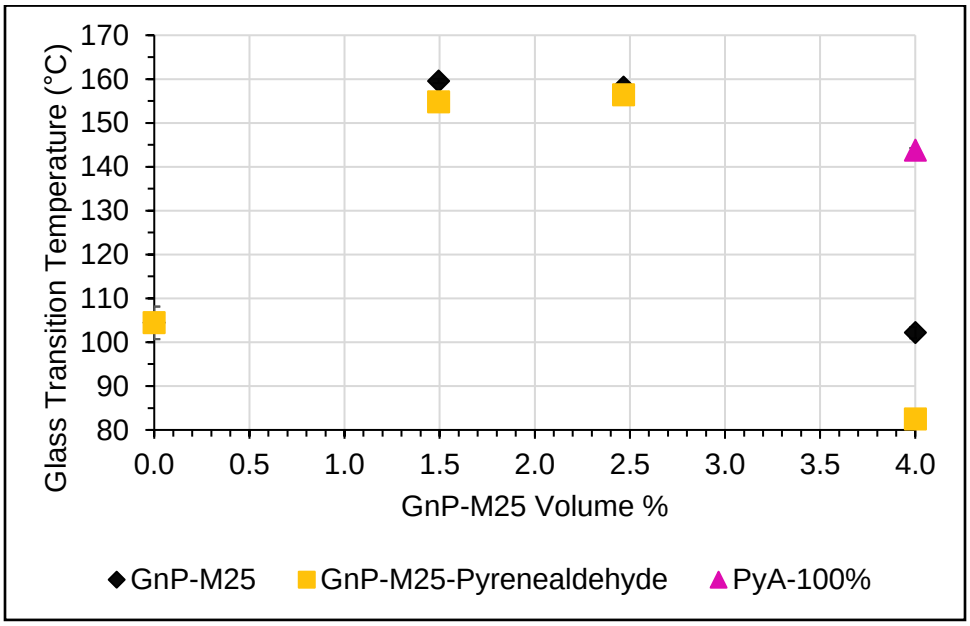

Figure 4.11: Glass transition temperature of composites using GnP-M25 (diamond), GnP-M25-Pyrenealdehyde (square), and 100% 1-pyrenealdehyde (triangle).

Another indication of the strength of the GnP/epoxy matrix interface is the magnitude of the tan δ peak. As a measure of composite damping, a lower magnitude

of tan δ represents more stress transfer to the GnP filler due to a stronger interface between the GnP and epoxy [26]. Shown in Figure 4.12, the tan δ peaks for GnP-M25 and GnP-M25-Pyrenealdehyde are practically the same at 1.5 and 2.5 vol%. However, the peak for GnP-M25-Pyrenealdehyde at 4 vol% is 59% higher than that for GnP-M25 indicating a lower magnitude of stress transfer. This result follows with the data where the 4 vol% GnP-M25-Pyrenealdehdye composite has a lower glass transition temperature.

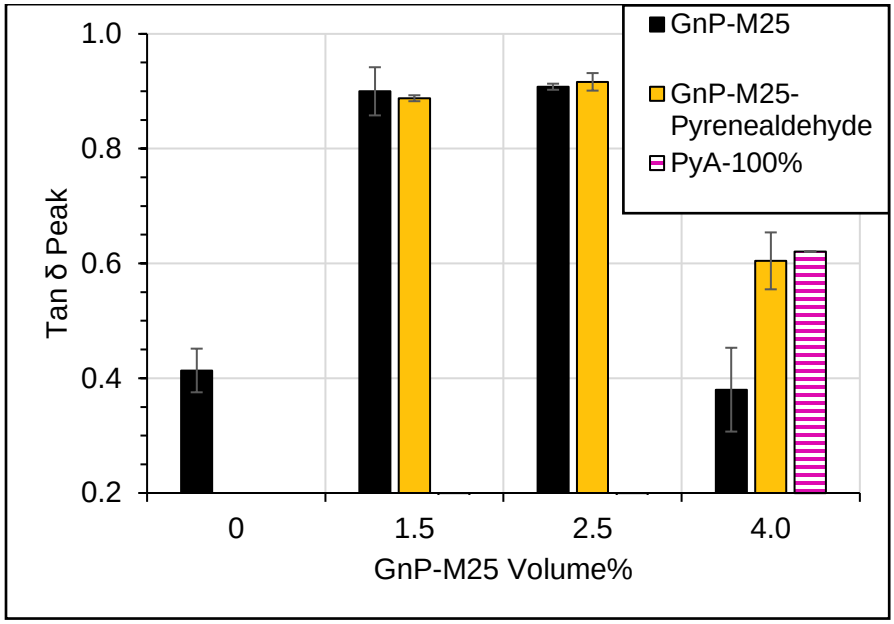

Figure 4.12: Tan δ peak magnitudes.

Further information on the quality of the GnP/epoxy matrix interface can be gleaned from the full width half maximum (FWHM) of the loss modulus peak. Since the loss modulus is a measure of energy dissipated as heat, a wider peak, or larger FWHM, signifies increased bulk chain movement inhibition. GnP-M25-Pyrenealdehyde shows essentially the same values of loss modulus FWHM as GnP-M25 at all concentrations. This supports that using 1-pyrenealdehyde as an adsorbate does not improve the ability of GnP-M25 to restrict chain movement through stronger intermolecular forces.

Similarly, 1-pyrenealdehyde without GnP does not improve the loss modulus FWHM.

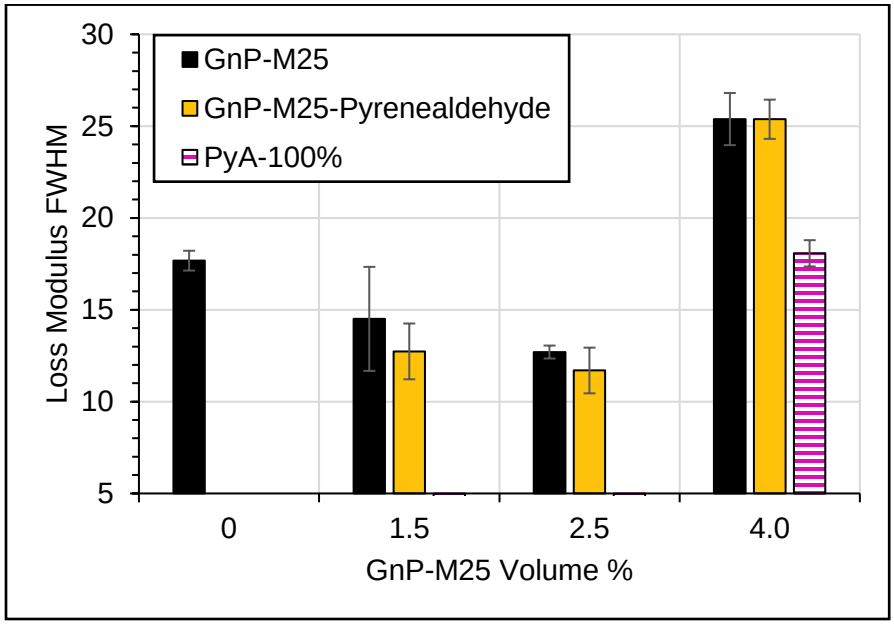

Figure 4.13: Full width half maximum of loss modulus peaks.

Viewing normalized loss modulus curves against normalized temperature superimposes the curves for each material for better analysis. As mentioned in Section 4.4.3, 1-pyrenealdehyde without GnP allows more homogeneous bulk chain movement due to its narrower peak. In the elastic region, both GnP materials increase the loss modulus and widens the peak towards lower temperatures following the same trend and at similar values. Therefore, the 1-pyrenealdehyde does not appear to affect the composite significantly in the elastic region. However, above the peak temperature, there is an additional peak for the GnP composites. With 1-pyrenealdehyde, this peak has a higher magnitude than without. Because there are stronger intermolecular forces at the interfacial layer at the GnP surface for GnP-M25-Pyrenealdehyde, the interface might have a slightly improved modulus. However, due to the previous analysis regarding tan δ and loss modulus peak width, this is an unlikely explanation. A more reasonable explanation matches with the increase in flexural modulus – an increase in

effective GnP concentration due to exfoliation.

Loss modulus peak temperature shifts indicate bulk chain movement initiation. 1.5 and 2.5 vol% GnP-M25-Pyrenealdehyde shift the peak temperature higher by ~50 °C. This shows that these composites require a much higher temperature to cause bulk chain movement. However, the 4 vol% GnP-M25-Pyrenealdehyde composite lowers the peak temperature ~30 °C. As a result, the higher volume of the 1-pyrenealdehyde interfacial layer facilitates bulk chain movement. Similarly with 4 vol% GnP-M25, increased agglomeration contributes to this effect. Again, 1-pyrenealdehyde without GnP does not exhibit the same properties, so these effects are due to the change in interface between GnP and epoxy.

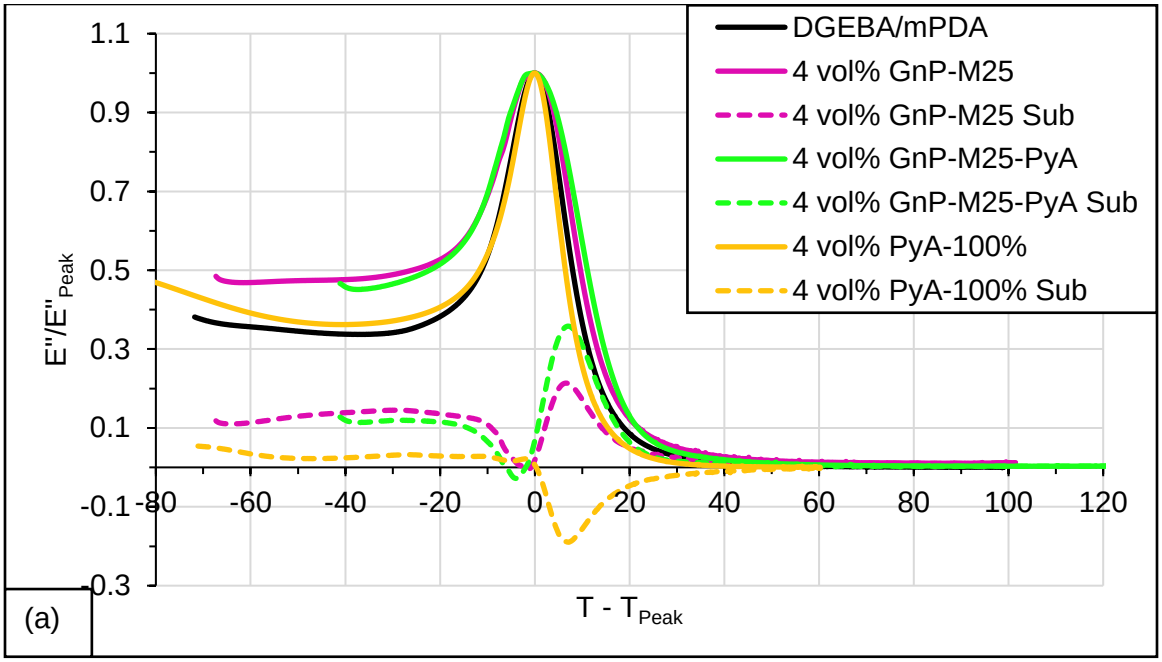

Figure 4.14: Normalized loss modulus curves for GnP-M25, GnP-M25-Pyrenealdehyde (PyA), and 100% PyA composites, (a) versus normalized temperature and (b), (c) versus actual increasing temperature.

Figure 4.14 (cont'd)

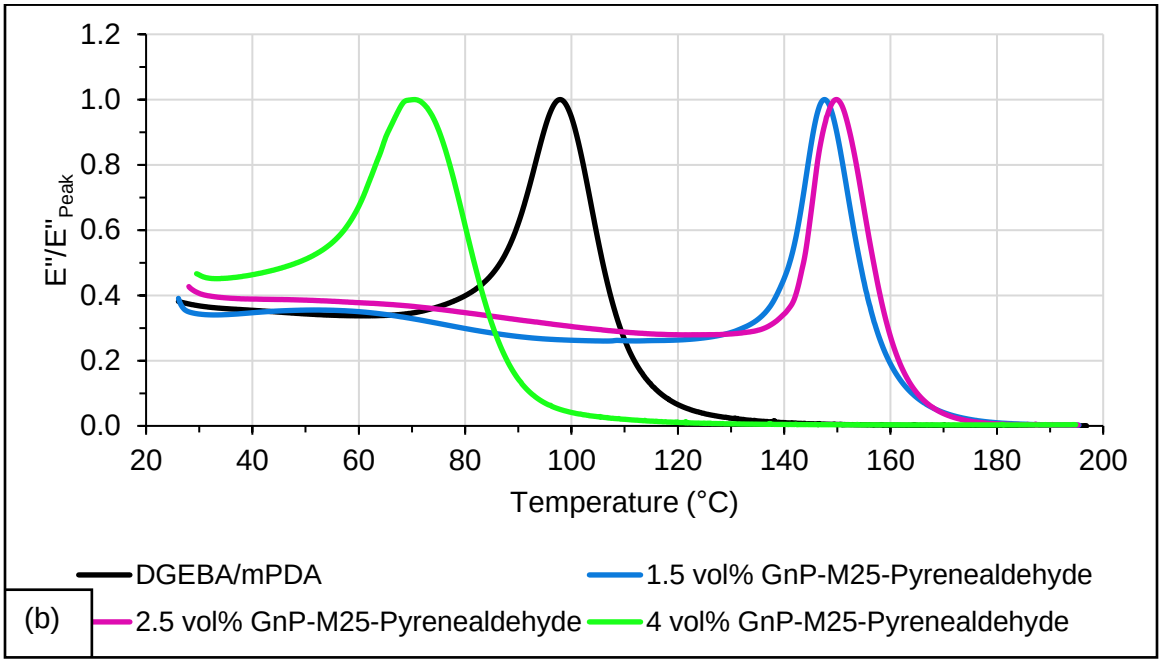

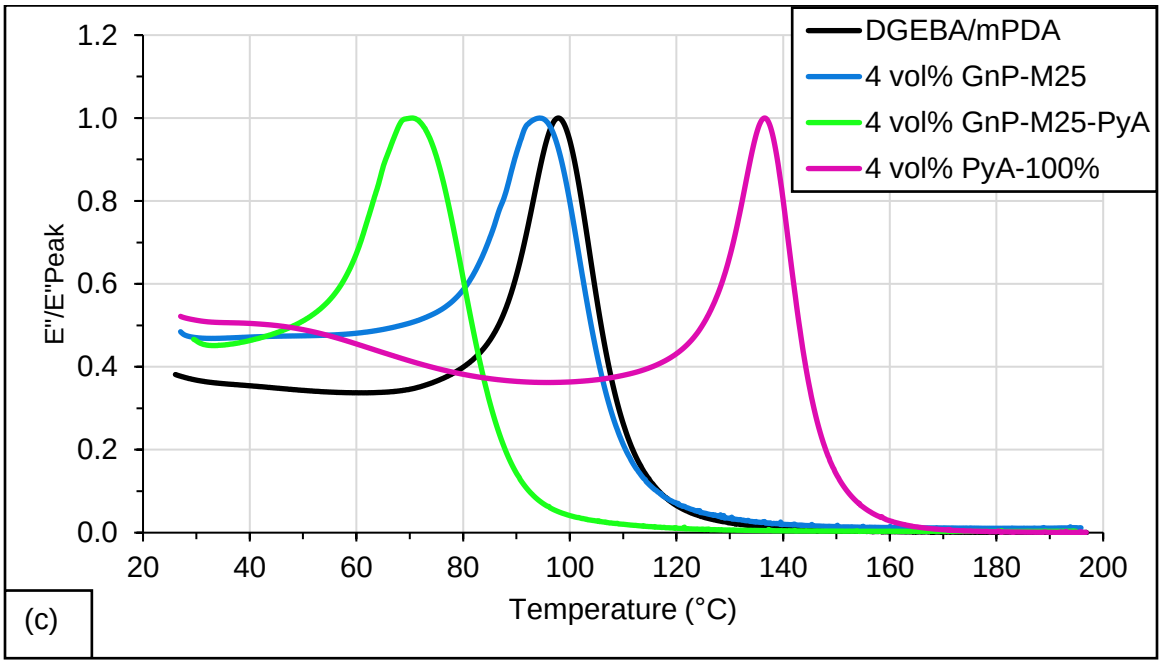

4.4.6 Thermal and Electrical Conductivity

Because GnP-M25 has a higher thermal conductivity than DGEBA/mPDA, it is expected that its incorporation will increase the composite's thermal conductivity. For both GnP-M25 and GnP-M25-Pyrenealdehyde, increasing concentration also increases

the composites' thermal conductivity. However, each concentration for GnP-M25-Pyrenealdehyde is at a lower value than the unmodified GnP-M25, with a max of 26% reduction at 1.5 vol%. Greater interfacial thermal resistance (high phonon scattering) directly causes a decrease in thermal conductivity [14]. The presence of an adsorbed layer of 1-pyrenealdehyde increases the interfacial thermal resistance, lessening the positive effects of the GnP-M25's high inherent thermal conductivity. The GnP is the dominating factor in improving this property as 1-pyrenealdehyde without GnP does not significantly affect thermal conductivity.

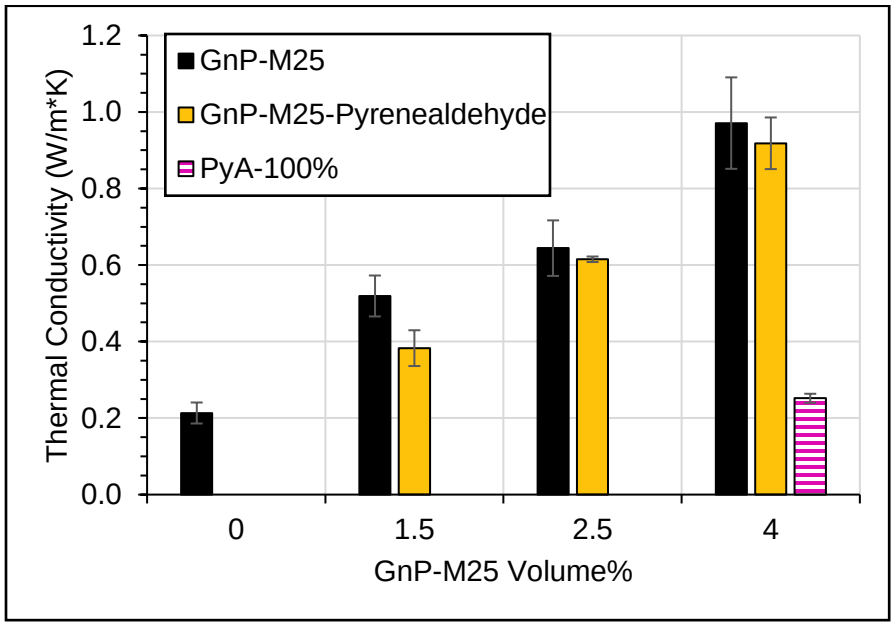

Figure 4.15: Thermal conductivity of GnP-M25 and GnP-M25-Pyrenealdehyde composites.

Similar to thermal conductivity, electrical conductivity of a composite is expected to increase with increasing GnP concentration due to its inherent high electrical conductivity (~108 S/m parallel to the surface) [19]. Four-point probe testing data shows unmodified GnP-M25 composites following this trend (Fig. 4.16). GnP-M25-Pyrenealdehyde composites also show an increase in electrical conductivity with

concentration as well. At 4 vol%, the GnP-M25-Pyrenealdehyde composite shows a 195% increase over GnP-M25 composites at the same concentration. Once the graphene nanoplatelets come into contact to form an unbroken network, the composite is at its percolation threshold. More well dispersed and distributed platelets are expected to decrease this percolation threshold. Shown in Table 4.6, the adsorbed 1-pyrenealdehyde decreased the percolation threshold 93% below the unmodified GnP-M25 composite. As stated previously, 1-pyrenealdehyde exfoliates the GnP-M25, effectively increasing the GnP concentration, which lowered the percolation threshold and improved the electrical conductivity.

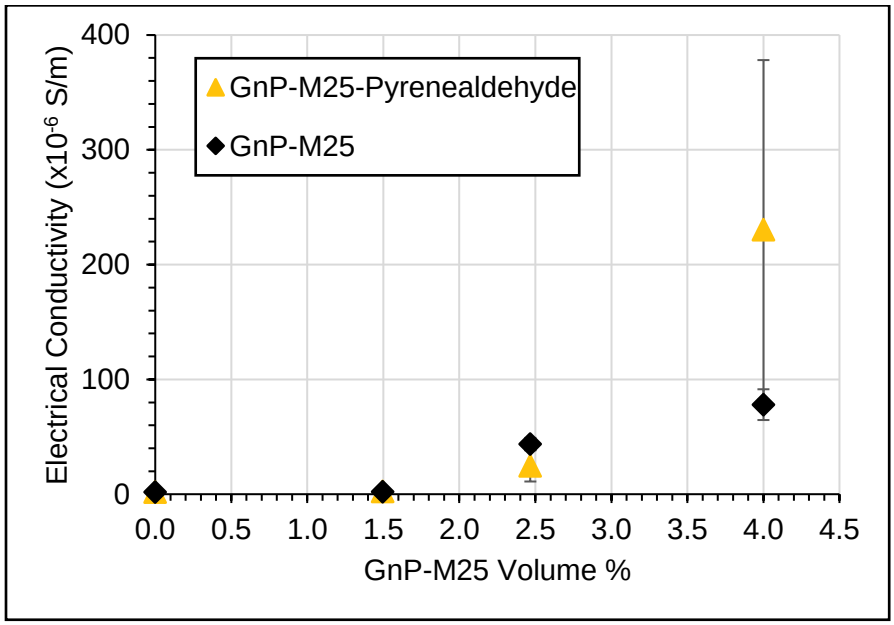

Figure 4.16: Electrical conductivity of GnP-M25 and GnP-M25-Pyrenealdehyde composites.

Table 4.5: Electrical conductivity measurements for GnP-M25 and GnP-M25-Pyrenealdehyde composites.

	Electrical Conductivity (x10^{-6} S/m)	
Filler Concentration (vol%)	GnP-M25	GnP-M25-Pyrenealdehyde
0	1.86 ± 0.07	1.86 ± 0.07
1.5	1.95 ± 0.09	2.31 ± 0.53
2.5	43.8 ± 5.26	24.7 ± 13.6
4	78.0 ± 13.4	230 ± 148

Table 4.6: Electrical percolation threshold for GnP-M25 and GnP-M25-Pyrenealdehyde composites.

Composite Filler	**Percolation Threshold (vol %)**
GnP-M25	1.41
GnP-M25-Pyrenealdehyde	0.01

4.5 Conclusion

1-Pyrenealdehyde was non-covalently adsorbed on the GnP-M25, resulting in changes in the composite's properties. Confirmed through Laser Raman and TGA, 1-pyrenealdehyde was adsorbed solely through physical interactions. In addition, it was shown that this molecule acts as an intercalant, fully or partially exfoliating the GnP resulting in higher effective concentrations of GnP-M25-Pyrenealdehyde than for the unmodified GnP-M25. Microscopic examination of the composites showed a higher amount of uniform sized platelets (lower agglomeration %) at consistent dispersion % over increasing concentration supports this as well.

The flexural modulus at 4 vol% for GnP-M25-Pyrenealdehyde is increased by 40% over unmodified GnP-M25 at the same concentration. On the other hand, flexural strength does not change noticeably across all concentrations. Higher effective GnP concentration and improved dispersion contributes to increasing flexural modulus.

However, a stronger interface between the GnP and epoxy is needed to significantly affect the flexural strength. The major difference between the two materials is the addition of hydrogen bonding to the van der Waals intermolecular forces at the GnP surface. While this assists in dispersion, the difference in interfacial strength is negligible on a larger scale.

Shown through normalized loss modulus data, 1-pyrenealdehyde without GnP does not follow the same trends as GnP-M25-Pyrenealdehyde. Used as an adsorbate, the composite epoxy chains are more easily moved in bulk as shown with a lower glass transition temperature. Similarly, despite the change intermolecular forces, there is a reduction in stress transfer to the GnP shown through a higher tan δ peak. The most significant effect on loss modulus is the presence of GnP within the composite. At 4 vol% GnP-M25-Pyrenealdehyde, the larger volume of the interfacial layer imparts a decrease in chain movement inhibition.

The thermal conductivity of the GnP-M25-Pyrenealdehyde composites were consistent with unmodified GnP-M25, if slightly lower. Adsorbates can interfere with phonon transfer, but as 1-pyrenealdehyde is very similar in structure to GnP, the difference is rather minimal. On the other hand, electrical conductivity for 4 vol% GnP-M25-Pyrenealdehyde is increased over GnP-M25 composites at the same concentration. This is in large part due to the improvement in GnP dispersion, agglomeration, and effective concentration.

BIBLIOGRAPHY

[1] Adeola, Adedapo O., and Patricia BC Forbes. "Optimization of the sorption of selected polycyclic aromatic hydrocarbons by regenerable graphene wool." Water Science and Technology 80.10 (2019): 1931-1943.

[2] ASTM Standard E1269, 2011, “Standard Test Method for Determining Specific Heat Capacity by Differential Scanning Calorimetry,” ASTM International, West Conshohocken, PA, 2011, DOI:10.1520/E1269-11R18, www.astm.org.

[3] ASTM Standard E1461, 2013, “Standard Test Method for Thermal Diffusivity by the Flash Method,” ASTM International, West Conshohocken, PA, 2013, DOI:10.1520/E1461-13R22, www.astm.org.

[4] ASTM Standard E2550, 2021, “Standard Test Method for Thermal Stability by Thermogravimetry,” ASTM International, West Conshohocken, PA, 2021, DOI: 10.1520/D0790-17, www.astm.org.

[5] ASTM Standard D790, 2017, “Standard Test Methods for Flexural Properties of Unreinforced and Reinforced Plastics and Electrical Insulating Materials,” ASTM International, West Conshohocken, PA, 2021, DOI:10.1520/E2550-21, www.astm.org.

[6] ASTM Standard D792, 2020, “Standard Test Methods for Density and Specific Gravity (Relative Density) of Plastics by Displacement,” ASTM International, West Conshohocken, PA, 2020, DOI: 10.1520/D0792-20, www.astm.org.

[7] Bogert, Marston Taylor, and Richard O. Roblin Jr. "The formation of cyclic acetals from aldehydes or ketones and alkylene oxides." Journal of the American Chemical Society 55.9 (1933): 3741-3745.

[8] Childres, Isaac, et al. "Raman spectroscopy of graphene and related materials." New developments in photon and materials research 1 (2013): 1-20.

[9] Choi, Eun Yeob, Lak Won Choi, and C. K. Kim. "Noncovalent functionalization of multi-walled carbon nanotubes with hydroxyl group-containing pyrene derivatives for their composites with polycarbonate." Carbon 95 (2015): 91-99.

[10] Ding, Yun-qiao, Yue-zhi Cui, and Tian-duo Li. "New views on the reaction of primary amine and aldehyde from DFT study." The Journal of Physical Chemistry A 119.18 (2015): 4252-4260.

[11] Eitan, A., et al. "Reinforcement mechanisms in MWCNT-filled polycarbonate." Composites Science and Technology 66.9 (2006): 1162-1173.

[12] Halpin, JC, and J. L. Kardos. "The Halpin-Tsai equations: a review." Polymer Engineering & Science 16.5 (1976): 344-352.

[13] Huang, Jing-Mei, et al. "An effective method to prepare imines from aldehyde, bromide/epoxide, and aqueous ammonia." The Journal of Organic Chemistry 76.9 (2011): 3511-3514.

[14] Huang, Xingyi, et al. "Thermal conductivity of graphene-based polymer nanocomposites." Materials Science and Engineering: R: Reports 142 (2020): 100577.

[15] King, Julia A., et al. "Mechanical properties of graphene nanoplatelet/epoxy composites." Journal of applied polymer science 128.6 (2013): 4217-4223.

[16] King, Julia A., et al. "Mechanical properties of graphene nanoplatelet/epoxy composites." Journal of Composite Materials 49.6 (2015): 659-668.

[17] Lee, Henry, and Kris Neville. Handbook of Epoxy Resins. Lu I Pub. Ser, 1984.

[18] Li, Bing, et al. "Polycyclic aromatic hydrocarbons adsorption onto graphene: a DFT and AIMD study." *Materials* 11.5 (2018): 726.

[19] Li, Yan, et al. "Mechanical, electrical and thermal properties of in-situ exfoliated graphene/epoxy nanocomposites." Composites Part A: Applied Science and Manufacturing 95 (2017): 229-236.

[20] Liu, Jia Daniel, et al. "Effect of crosslink density on fracture behavior of model epoxies containing block copolymer nanoparticles." Polymer 50.19 (2009): 4683-4689.

[21] Liu, Jingquan, et al. "Thermosensitive graphene nanocomposites formed using pyrene-terminal polymers made by RAFT polymerization." Journal of Polymer Science Part A: Polymer Chemistry 48.2 (2010): 425-433.

[22] Read, Oliver, et al. "Insights into the exfoliation mechanism of pyrene-assisted liquid phase exfoliation of graphene from lateral size-thickness characterisation." Carbon 186 (2022): 550-559.

[23] Silva, Pedro J. "New insights into the mechanism of Schiff base synthesis from aromatic amines in the absence of acid catalyst or polar solvents." PeerJ Organic Chemistry 2 (2020): e4.

[24] Sprung, Murray A. "A Summary of the Reactions of Aldehydes with Amines." Chemical Reviews 26.3 (1940): 297-338.

[25] Tyson, Bryan M., et al. "A quantitative method for analyzing the dispersion and agglomeration of nano-particles in composite materials." Composites Part B: Engineering 42.6 (2011): 1395-1403.

[26] Vennerberg, Danny, Zach Rueger, and Michael R. Kessler. "Effect of silane structure on the properties of silanized multiwalled carbon nanotube-epoxy

nanocomposites." Polymer 55.7 (2014): 1854-1865.

[27] Wang, Jun, Zaiming Chen, and Baoliang Chen. "Adsorption of polycyclic aromatic hydrocarbons by graphene and graphene oxide nanosheets." Environmental science & technology 48.9 (2014): 4817-4825.

[28] Xu, Liyan, and Xiaoning Yang. "Molecular dynamics simulation of adsorption of pyrene–polyethylene glycol onto graphene." Journal of colloid and interface science 418 (2014): 66-73.

[29] Zaman, Izzuddin, et al. "Epoxy/graphene platelets nanocomposites with two levels of interface strength." Polymer 52.7 (2011): 1603-1611.

[30] Zaman, Izzuddin, et al. "Interface modification of clay and graphene platelets reinforced epoxy nanocomposites: a comparative study." Journal of materials science 49.17 (2014): 5856-5865.

[31] Zheng, Wenge, Bin Shen, and Wentao Zhai. "Surface functionalization of graphene with polymers for enhanced properties." New progress on graphene research 10 (2013): 50490.

CHAPTER 5: CHANGES IN COMPOSITE MULTIFUNCTIONALITY USING PY-POP AS AN ADSORBATE ONTO GNP-M25

5.1 Abstract

A major issue in creating GnP composites is the poor interactions between GnP and the epoxy. This leads to poor dispersion and limits the property improvements desired by using GnP. Designing a molecule (Py-POP) to form a noncovalent bond with the GnP surface and a covalent bond with the epoxy resin during curing was utilized to improve the interface. GnP dispersion was improved through platelet agglomeration inhibition, which became more apparent at higher concentrations. Normalized loss modulus curves showed the effects of Py-POP adsorbed and signified that the Py-POP created a lower modulus interfacial layer at the GnP surface. Flexural modulus, flexural strength, and glass transition temperature were significantly improved over unmodified GnP composites at 4 volume percent of GnP. Similarly, the electrical conductivity of the GnP-M25-Py-POP composites were increased by ~19000% higher than unmodified GnP-M25 at 4 vol%.

5.2 Introduction

Graphene nanoplatelets (GnP), with a high surface to edge area ratio, do not adhere well to epoxy resins due to poor intermolecular bonding. The basal plane structure of the carbons in GnP do not readily participate in chemical bonding. To improve the GnP surface/epoxy interfacial attraction, a noncovalent pi bonding approach is beneficial to maintain the GnP structure and avoid reactions with GnP's inert surface. For strong adhesion, the high concentration of pi electrons in a pyrene moiety is more effective than a linear arrangement of pi electrons. The addition of a pyrene molecule to Jeffamine D2000 via an imine bond, creates a monofunctional

poly(oxypropylene), Py-POP.

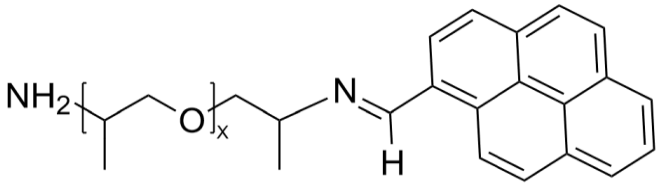

Figure 5.1: Molecular structure of Py-POP.

Both pyrene and GnP have structures of six-membered carbon aromatic rings. These structures exhibit π-π bonds out of plane, allowing for strong intermolecular bonding through π-π stacking. The pyrene moiety anchors the Py-POP molecule to the GnP surface and a primary amine on the opposite end of the molecule is available to participate in the curing process of the epoxy resin. Li et al. demonstrated through molecular simulations that the larger the total number of atoms present in the polycyclic aromatic hydrocarbon (PAH), the stronger the adsorption energy [14]. The largest PAH in this system is the graphene nanoplatelet. So, the adsorption energy is stronger for pyrene onto graphene than pyrene onto pyrene. As a result, it is expected that pyrene will preferentially create a monolayer onto the graphene surface. Through this improved interface between the GnP surface and crosslinked polymer matrix, there is expected to be an enhancement in the adhesion between the GnP and epoxy matrix as well as having a positive effect on the GnP dispersion and the composite's multifunctionality.

As shown by several studies, [1], [9], [16], [19], [25], polycyclic aromatic hydrocarbons readily adsorb onto the graphene surface. The adsorption depends strongly on the hydrophobicity of the solvent. Increasing solvent hydrophilicity yields increasing polycyclic aromatic hydrocarbon adsorption strength. In a molecular simulation study, the polycyclic aromatic hydrocarbons were shown to be able to

rearrange on the graphene surface due to similar adsorption energies across various configurations.

5.3 Materials and Methods

5.3.1 Materials

Graphene nanoplatelets, product name GnP-M25 (d = 25 μm, t ~ 7 nm, 5-10 layers) was provided by XG Sciences. 1-pyrenealdehyde, toluene, and isopropanol were purchased from Sigma Aldrich, used as received. Poly(oxypropylene) diamine known by its trade name Jeffamine D2000 (Hunstman) has an average molecular weight of 2000 g/mol and amine hydrogen equivalent weight of 514 g/eq. Preparation of Py-POP is described in Chapter 2. Bisphenol A diglycidyl ether (DGEBA), known by trade name Epon 828 was purchased from Miller-Stephenson. Meta-phenylene diamine (mPDA) was purchased from Sigma Aldrich. PELCO Conductive Liquid Silver Paint was used to create electrical contact points for electrical conductivity measurements.

5.3.2 Adsorption Method

GnP-M25 was ultrasonicated in isopropanol for 10 minutes in an ice bath to break up agglomerates. An excess of Py-POP was added to the mixture and mechanically stirred overnight via a stir bar. The mixture was then vacuum filtered through a 0.22 μm filter paper (PTFE) to remove the solvent and excess Py-POP. The GnP-M25-Py-POP was dried in a vacuum oven overnight to remove the residual solvent.

5.3.3 Composite Preparation Method

Four concentrations of GnP-M25 were used: 0, 3, 5, and 8 weight % (0, 1.5, 2.5, 4 volume %). The GnP-M25-Py-POP sample was added to isopropanol and

ultrasonicated for 10 minutes in an ice bath. DGEBA was added to the mixture, mechanically stirred to dissolve, and ultrasonicated 10 minutes in an ice bath while stirring with a stir bar. The isopropanol was removed from the mixture in a vacuum oven at 80 °C. After the solvent was removed, mPDA (14.5:100 weight ratio to DGEBA) was added at 75 °C to the GnP-M25-Py-POP/DGEBA mixture and stirred thoroughly. After degassing, the mixture was poured into flexural coupon silicone molds and cured using a cycle of 2 h at 75 °C then 2 h at 125 °C. The cured composites were polished to a flat surface before testing. All data will reference the GnP-M25 concentration for clarity, and it is noted that the addition of the adsorbates will increase the volume % of additives.

5.3.4 Characterization

Laser Raman spectroscopy was used to analyze the structure of GnP-M25 before and after adsorption of Py-POP using the LabRAM Aramis (Horiba). Laser wavelength was 532 nm. Spectra were recorded in two parts (1000 – 2000 cm^{-1} and 2000 – 3000 cm^{-1}) to reduce oxidation of the material.

Composite flexural coupons were tested using a three-point bending method according to the standard ASTM D790 using a Universal Testing System (Instron). Rectangular specimens were supported 2 inches apart, then force was applied to the middle of the specimen at a strain rate of 0.01 mm/mm/min until failure. Force applied and extension of deflection measured were used to calculate flexural modulus and flexural strength.

The TA Instruments TGA Q500 machine was used for thermogravimetric analysis (TGA) of the samples' thermal stability. Heating rate was set at 10 °C/min to 500 °C in a nitrogen atmosphere. Decomposition onset temperature was determined

using ASTM E2550.

Dynamic mechanical analysis (DMA) was performed using a TA DMA Q800 machine. Testing conditions were single-cantilever method, temperature ramp to 200 °C at a rate of 3 °C/min, set at a frequency of 1 Hz, and set at an amplitude of 30 μm. Glass transition temperature was defined as the temperature at the peak of the tan δ curve. Polymer density was measured according to the standard ASTM D792.

A Carl Zeiss Auriga Dual Column FIB scanning electron microscope was used to capture cross-sectional images of polymer composites. These images were used to qualitatively analyze GnP dispersion. Using the image processing software ImageJ, a quantitative measurement of dispersion and agglomeration was calculated.

Flexural testing coupons were used to measure electrical conductivity via a Four-point probe method. Coupons were cut to 30 mm in length, polished surfaces to be flat, and oxygen plasma treated for 10 minutes at 300 W. Opposite ends were coated in a layer of silver paint. Two contacts points were placed using silver paint 15 mm apart in the middle of the composite coupon surface. A heat gun was used to dry the silver paint. A Keithley 2000 multimeter was used to apply a 1 μA current from one end to the opposite end of the sample. Voltage was measured between the two contact points.

Thermal conductivity was calculated by measuring the composites thermal diffusivity and heat capacity. The thermal diffusivity was measured via laser flash method using a Netzsch LFA 447 according to ASTM 1461-13. Flexural coupon samples were cut to fit in the machine, surfaces polished flat, and coated with a graphite layer. A TA DSC Q2000 was used to measure heat capacity according to ASTM E1269-11. Samples were ramped to -10 °C at 20 °C/min, held isothermally for 5 minutes,

ramped to 50 °C at 20 °C/min, and held isothermally for 5 minutes. Heat capacity was taken at 25 °C.

5.4 Results and Discussion

5.4.1 Adsorption of Py-POP onto GnP-M25

Effects of the adsorption of Py-POP onto GnP-M25 were compiled through various characterization techniques. The Laser Raman spectra show that Py-POP only interacts with the GnP surface through physisorption. Graphene has inherent peaks that describe its structure. The G peak (~1580 cm^{-1}) represents in-plane vibrational mode of the carbon conjugated double bond structure through the stretching of sp2 atoms in rings and chains [8]. As shown in Table 5.1, the G peaks for unmodified GnP-M25 and GnP-M25-Py-POP appear at 1574 cm^{-1} and 1576 cm^{-1}, respectively. A redshift in the G peak is generally attributed to an increase in number of layers but can be explained by the local effects of the adsorbed pyrene moiety.

Another important peak, the D peak (~1350 cm^{-1}), which, in simple terms, corresponds to the disorder or defects of the graphene. A pristine graphene surface will show no D peak because the sp^2 carbon structure is uninterrupted. The more sp^2 carbons that are converted to sp^3, the more intense the D peak will be. For both the unmodified GnP-M25 and the GnP-M25-Py-POP, the D peak is virtually nonexistent. GnP-M25 is expected to have no functional groups or holes on the basal plane. Since the D peak does not change with the adsorption of Py-POP, this indicates that Py-POP is only interacting with GnP-M25 via physisorption rather than any reactions that would disrupt the graphene structure. For a more direct comparison, the intensity ratio between the D and G peaks are used, which shows a very similarly low value for both

materials.

The third important peak to focus on is the 2D peak (~2700 cm^{-1}). This peak is an overtone of the D peak that represents the number of layers of graphene present. The fewer layers of graphene, the stronger the 2D peak. Comparing the 2D to G peak intensity ratios, GnP-M25-Py-POP shows a value an order of magnitude larger than unmodified GnP-M25. Due to the pyrene present on one end of the polymer chain, and pyrene's ability to intercalate between the graphene layers, it is possible that there is a small amount of graphene exfoliation that has occurred. Pyrene has been shown to be an intercalate for graphene [22].

Table 5.1: Laser Raman peak intensity ratios.

Peak Intensity Ratios	**GnP-M25**	**GnP-M25-Py-POP**
D:G	0.01	0.013
2D:G	0.0016	0.019

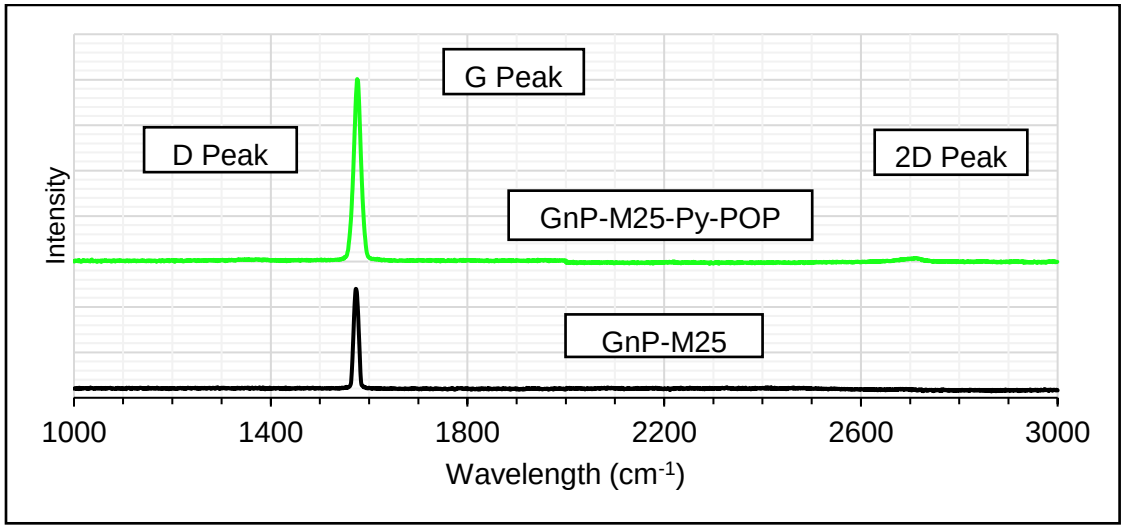

Figure 5.2: Laser Raman Spectra for GnP-M25 (bottom) and GnP-M25-Py-POP (top).

TGA can be used to measure the mass of Py-POP adsorbed. Based on the surface area of the GnP, the theoretical maximum monolayer adsorption of pyrene onto

a platelet of GnP-M25 is 248 mg pyrene/g GnP-M25. Since GnP-M25 does not experience significant weight loss below 500 °C, the weight lost for GnP-M25-Py-POP corresponds solely to the adsorbed material, Py-POP. Average adsorbate measured mass is 713 mg Py-POP/g GnP-M25. Measured molecular weight from mass spectrometry can directly relate this to the mass of pyrene moieties within the Py-POP, giving an adsorption of 75 mg pyrene moieties/g GnP-M25. For Py-POP, the pyrene moieties adsorbed correlates to 30% of the theoretical maximum adsorption of pyrene molecules. Steric effects of the connected poly(oxypropylene) amine chain tail limit the Py-POP adsorption.

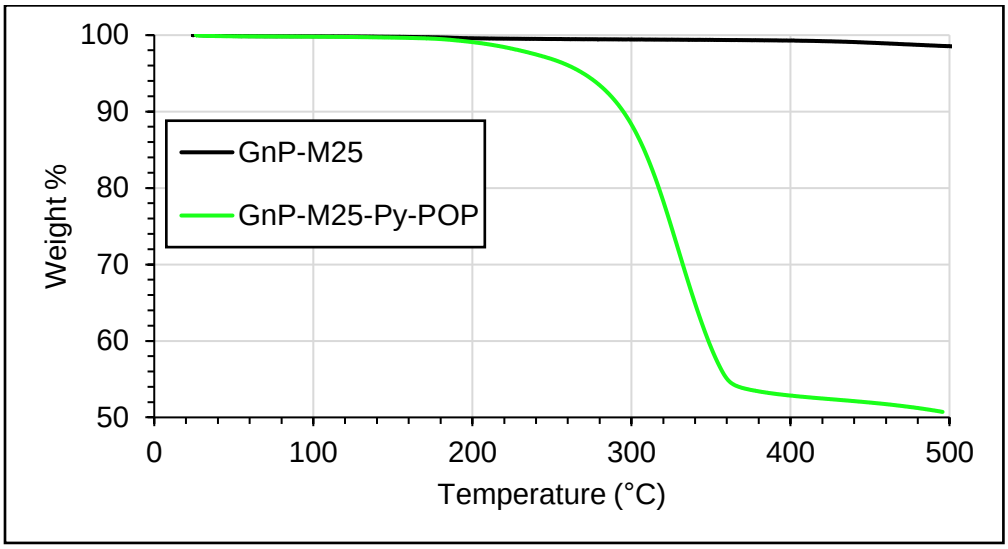

Figure 5.3: Weight loss analysis through TGA on GnP-M25 and GnP-M25-Py-POP in a N_2 atmosphere.

5.4.2 GnP Dispersion

Figure 5.4 depicts the cross-section images of GnP-M25 and GnP-M25-Py-POP composites taken on the SEM. These images were used analyze dispersion and agglomeration qualitatively and quantitatively at each concentration. The white lines and groups present in the images are the GnP. Qualitatively, there is a distinct difference in

the images as the GnP concentration increases. Each sample shows GnP that is dispersed with agglomerates present.

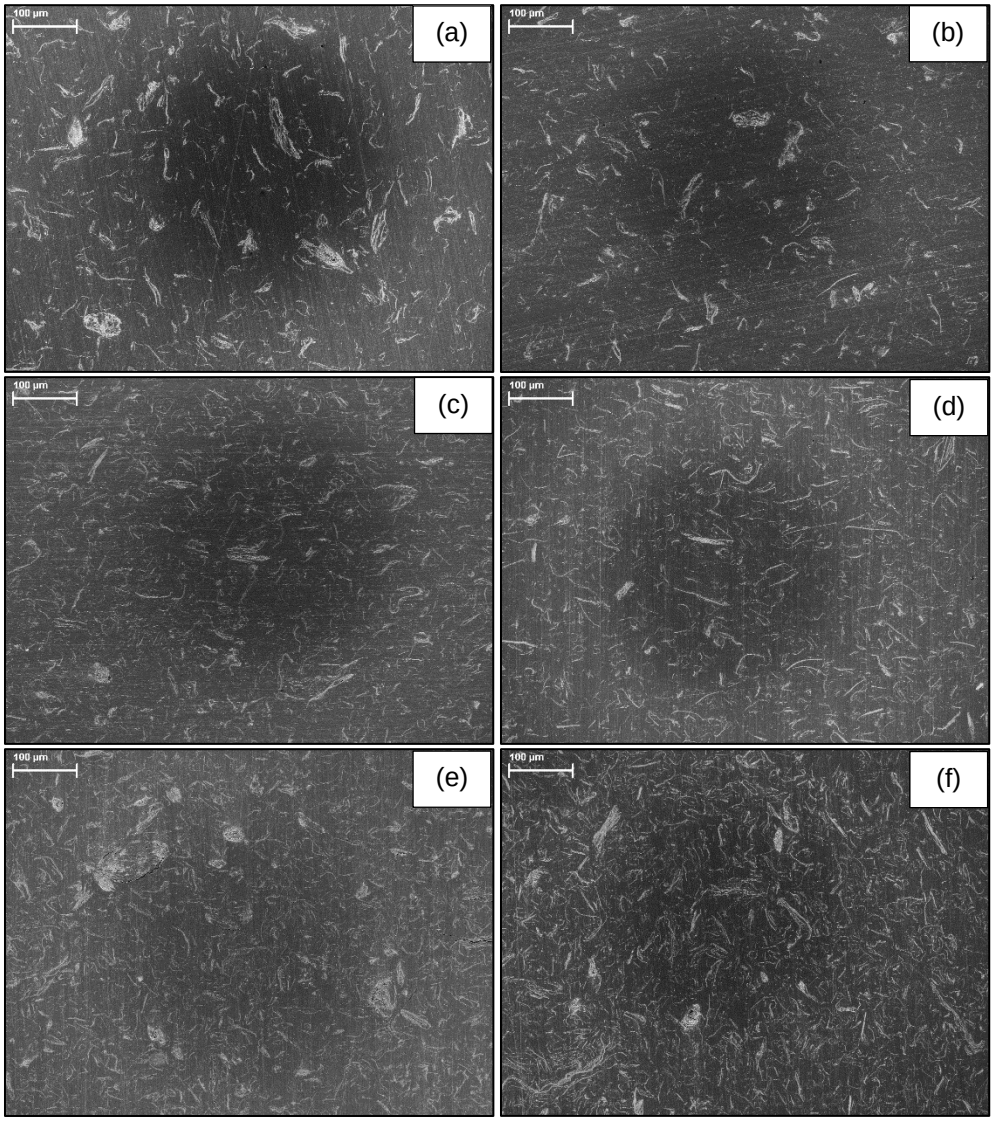

Figure 5.4: SEM cross sectional images for GnP-M25 composites at (a) 1.5 vol%, (c) 2.5 vol%, and (e) 4 vol%, and GnP-M25-Py-POP composites at (b) 1.5 vol%, (d) 2.5 vol%, and (f) 4 vol%.

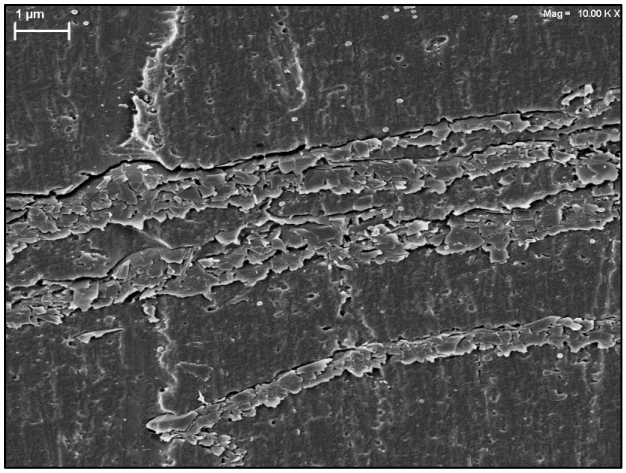

Figure 5.5: 4 vol% GnP-M25-Py-POP composite cross section.

However, it is difficult to compare the two composite materials for exact differences in dispersion and agglomeration. To assess these differences more accurately in GnP dispersion due to an adsorbate, an image analysis technique was used. Dispersion and agglomeration of GnP are very important factors that affect multiple composite properties. Tyson et al. [23] shows a method to quantify the dispersion and agglomeration of fillers in a composite using cross-section image analysis. By applying a set of gridlines to the cross-section image (taken in an SEM), two variables can be measured: distance between the platelets and width of platelets. To calculate the dispersion % for the composite, the distances between platelets are collated and a lognormal distribution curve is fit to the data. The closer the curve is to the mean value, the better dispersed the GnP is. So, a dispersion % value is taken as the integral of the lognormal distribution curve within 20% of the mean. With this method, a higher dispersion % value indicates a more uniformly distributed GnP composite. Figure 5.6a summarizes the dispersion % for GnP-M25 and GnP-M25-Py-POP composites. In each concentration, both materials have a very similar dispersion %.

However, this method of quantifying dispersion also needs to consider agglomeration %. Rather than measuring distance between platelets, agglomeration is a measure of the thickness of GnP groups in the composite. In this case, a smaller value indicates more uniform GnP group sizes and less agglomerates. Both calculations show a more accurate picture of the quality of dispersion within each composite. As expected, agglomeration % is highest at the highest GnP concentration. At all concentrations, GnP-M25-Py-POP shows a lower agglomeration % than GnP-M25 composites. Also, at 4 vol%, GnP-M25-Py-POP composites have 3.4% less agglomerate % than GnP-M25 composites. While dispersion % for both materials are comparable at each concentration, a lower agglomeration % for GnP-M25-Py-POP implies better dispersion overall.

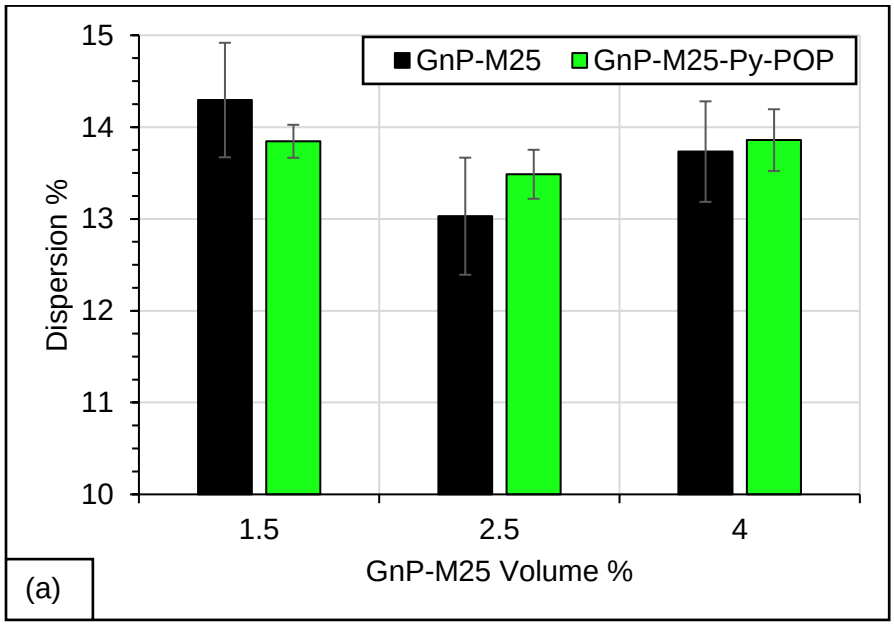

Figure 5.6: Dispersion percent, (a), and agglomeration percent, (b), calculated from SEM cross-sectional images.

Figure 5.6 (cont'd)

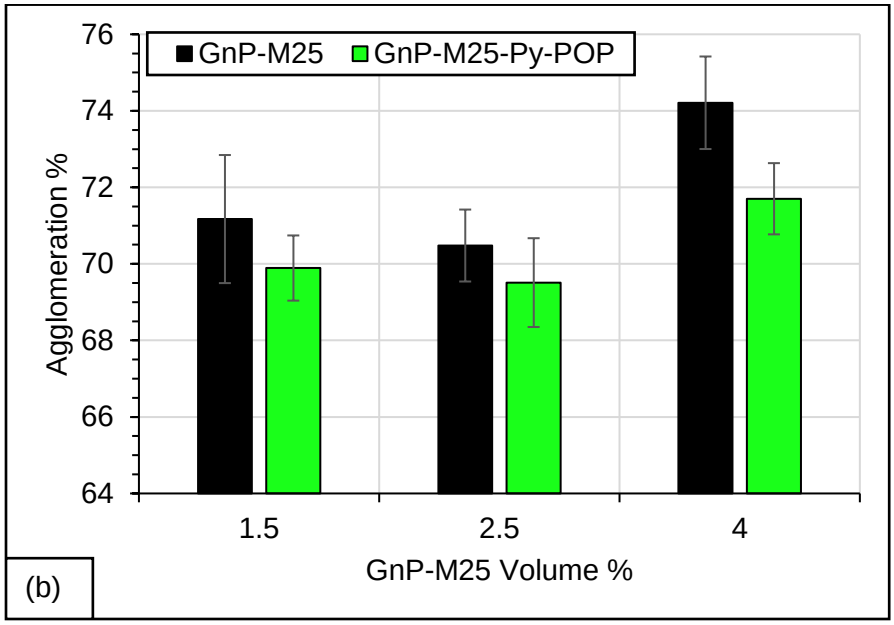

5.4.3 Py-POP Effect on Epoxy Matrix Properties

For better understanding of the interactions within the epoxy system, composites containing the adsorbates without GnP-M25 were tested. The mass of Py-POP used corresponds to 20, 50, and 100% of the experimental adsorption onto 4 vol% GnP-M25 from Section 5.4.1. These tests assist in determining what effects are caused by the adsorbate itself or its interaction as an interface between the GnP and epoxy.

The glass transition temperatures for composites including 20, 50, and 100% adsorbed Py-POP do not vary significantly from each other – only an average of 4 °C. As a result, the 100% Py-POP value was used for analysis. The neat DGEBA/mPDA and 100% Py-POP samples have a T_g of ~104 and ~128 °C, respectively. The inclusion of this amount of Py-POP generates chain mobility inhibition, due to the combination of reacting at one end with the epoxy during curing and allowing the rest of the chain to entangle with the crosslinks since the pyrene end is unreactive.

Comparisons between the loss modulus (E") curves of these materials also

contribute to understanding how the Py-POP interacts with the DGEBA/mPDA matrix. To do this, the loss modulus curves were normalized with respect to the peak loss modulus value (E''/E''_{Peak}) and peak temperature ($T - T_{Peak}$). In this way, the differences in curve shape can be analyzed directly. Similarly, each normalized curve is subtracted by the normalized curve for neat DGEBA/mPDA to show changes due to the added Py-POP [10]. The 20 and 50% Py-POP samples show broadening at temperatures above T_{Peak}. This indicates a reduction in chain mobility within the material. The 100% Py-POP material shows higher loss modulus below T_{Peak} but follows the neat DGEBA/mPDA closely as the temperature increases. Comparing the normalized loss modulus curves with respect to increasing temperature, the 20 and 50% Py-POP curves shift upward towards ~10 °C, and the 100% Py-POP increases by ~20 °C over the neat epoxy. This difference in curves can be attributed to a more homogeneous mixture of Py-POP at the highest concentration. At 20 and 50% Py-POP, the data suggests that there are Py-POP rich “pockets” within the DGEBA/mPDA structure, resulting in two loss modulus peaks. In summary, Py-POP has a chain restriction effect due to entangling of the pyrene end. Also, a higher volume of Py-POP allows for better dispersion throughout the epoxy.

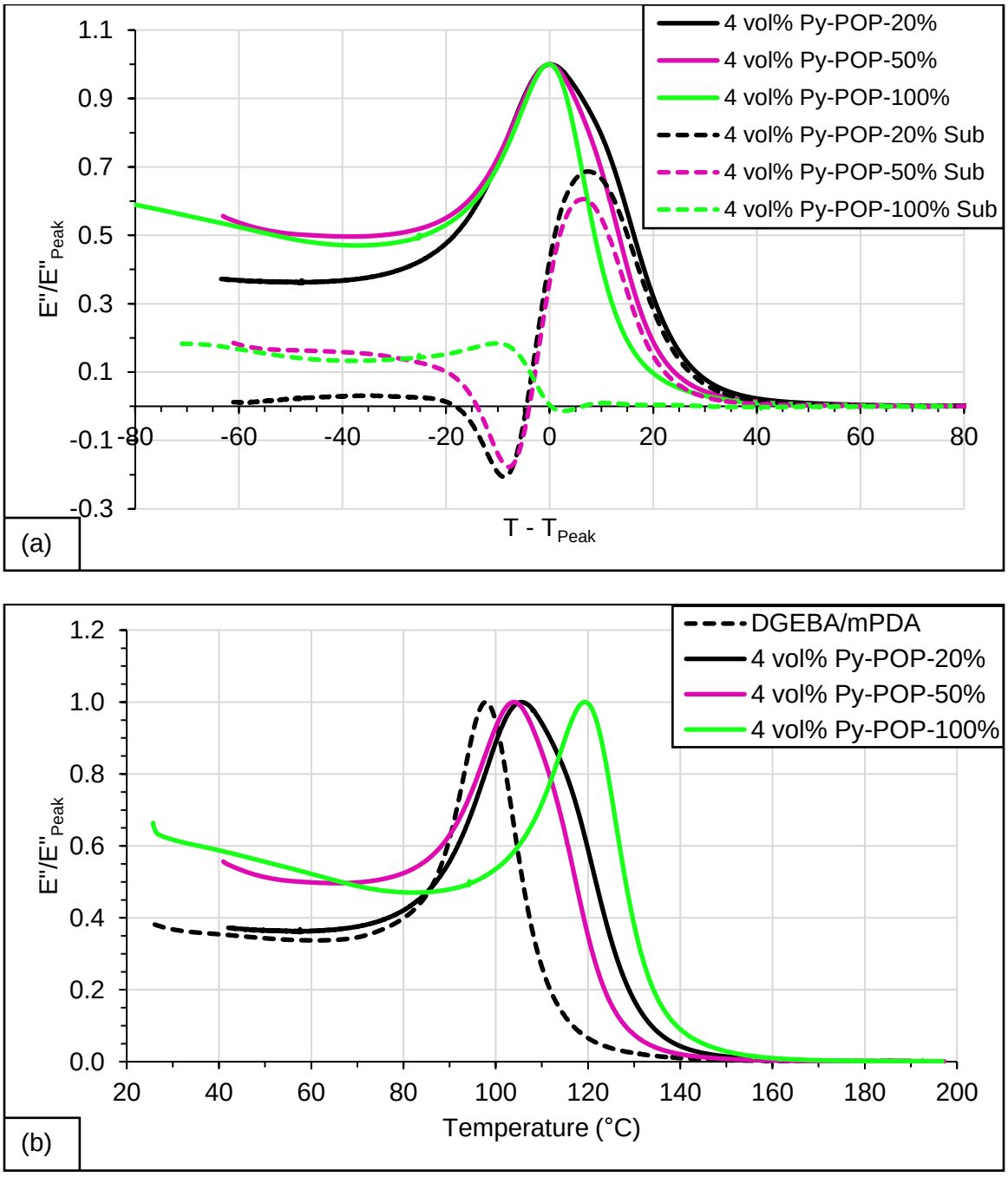

Figure 5.7: Normalized loss modulus curves of Py-POP composites (a) versus normalized temperature and (b) versus increasing temperature.

The electrical conductivity results for these materials showed no difference from the neat epoxy. Because the electrical conductivity is very low for these materials, the actual numbers found are not entirely accurate as they maxed out the maximum voltage

drop that could be measured. Nonetheless, these results showed that the Py-POP by itself does not generate a significant effect on the composites' electrical conductivity.

Another property that was considered was thermal conductivity. The 100% Py-POP material showed an increase of 25% over the neat epoxy. However, this is a very minor increase since the value for the neat epoxy is small. Comparing with the 4 vol% GnP-M25 composite, the increase due to the Py-POP becomes virtually insignificant.

Table 5.2: Thermal conductivity.

Samples	**Thermal Cond. (W/m*K)**	**Thermal Cond. Error (W/m*K)**
Neat DGEBA/mPDA	0.213	0.027
100% Py-POP	0.267	0.008
4 vol% GnP-M25	0.971	0.120

5.4.4 Mechanical Properties

To investigate the effects of the adsorbate Py-POP on GnP-M25, three separate concentrations of GnP-M25 were used. Figure 5.8 compares the flexural modulus of unmodified GnP-M25/DGEBA/mPDA composites with GnP-M25-Py-POP/DGEBA/mPDA composites. It is expected, with ideal dispersion, that increasing GnP concentration will increase flexural modulus. However, the results show that flexural modulus increases from 1.5 to 2.5 vol% GnP-M25, and plateaus at 4 vol%. As stated previously, the intermolecular forces present between unmodified GnP-M25 and DGEBA are limited to van der Waals interactions. As a result, the platelets are more likely to agglomerate than maintain dispersion, especially in a highly concentrated mixture. For the GnP-M25-Py-POP/DGEBA/mPDA composite, the flexural modulus progressively increases with concentration. In contrast with unmodified GnP-M25, the GnP-M25-Py-POP composite continues to increase in flexural modulus at the highest concentration.

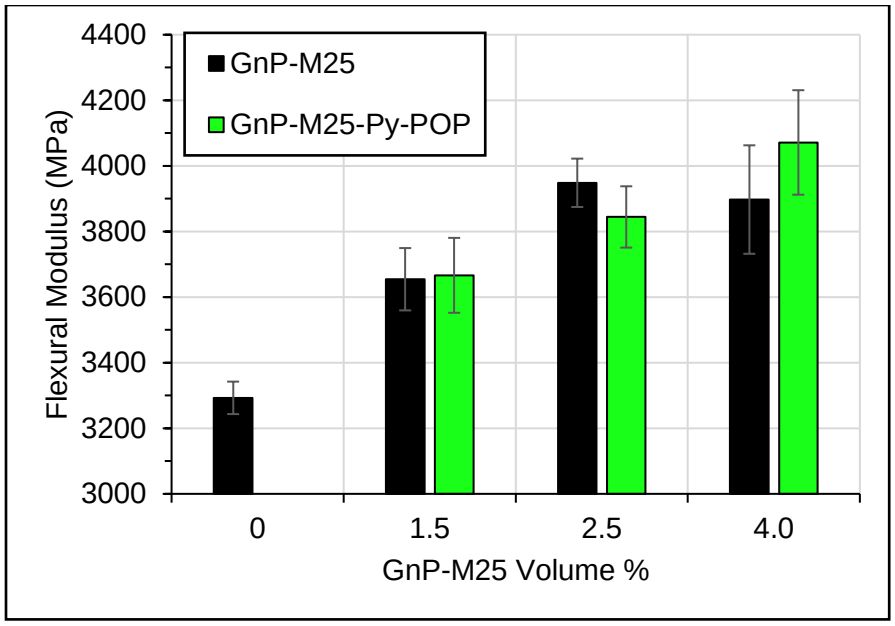

Figure 5.8: Flexural modulus for GnP-M25 and GnP-M25-Py-POP composites.

For comparison, Table 5.3 shows the percent increase in flexural modulus over neat DGEBA/mPDA samples at three GnP concentrations. The flexural modulus of neat DGEBA/mPDA material is 3293 MPa, indicating that addition of GnP-M25 is beneficial for the composite's flexural modulus.

Where unmodified GnP-M25 will tend to agglomerate at high concentrations, the adsorbed Py-POP introduces mechanisms that resist this agglomeration effect. By covering the platelets with Py-POP, re-stacking of the GnP is sterically hindered due to the POP chains. Following this, the primary amine group participates in the curing reaction of the epoxy, forming covalent bonds into the crosslink network. This linkage strengthens the interface between the epoxy and the GnP surface, improving the stress transfer between the two. As a result, the flexural modulus increases. However, the positive effects of this interaction seem to only make a noticeable difference at the highest concentration. While the epoxy/GnP interface is strengthened, the Py-POP creates an interfacial layer that has a lower modulus than the bulk epoxy due to the

higher concentration of Py-POP present.

Table 5.3: Flexural modulus percent increase over neat DGEBA/mPDA.

Composite Filler	**1.5 vol%**	**2.5 vol%**	**4 vol%**
GnP-M25	11.0	19.9	18.4
GnP-M25-Py-POP	11.3	16.8	23.7

Table 5.4: Molecular weight between crosslinks calculated from DMA.

	Molecular Weight between Crosslinks (g/mol)		
Filler Concentration (vol%)	GnP-M25	GnP-M25-Py-POP	Py-POP – 100%
0	335 ± 66	335 ± 66	-
1.5	260 ± 1.1	259 ± 11	-
2.5	255 ± 0.54	249 ± 6.0	-
4	232 ± 57	222 ± 25	301 ± 5.8

Table 5.4 depicts the molecular weight between crosslinks (MW_C) for the GnP composites in question. These values were calculated using their measured densities and storage modulus in the rubbery region at 180 °C [21]. As expected, MW_C decreases with increasing concentration of GnP-M25 due to the platelets impeding chain propagation. As a result, there is a higher number of crosslinks per area. Practically, the two materials show the same MW_C at all concentrations. These results point towards the positive effect of an improved interface between the GnP surface and crosslink network. The flexural modulus at 4 vol% for GnP-M25-Py-POP is higher than GnP-M25 composites even though their MW_C (and by direct relationship, crosslink density) are the same. Furthermore, the MW_C of Py-POP without GnP-M25 is similar to the neat epoxy. By itself, the Py-POP has little impact on the MW_C.

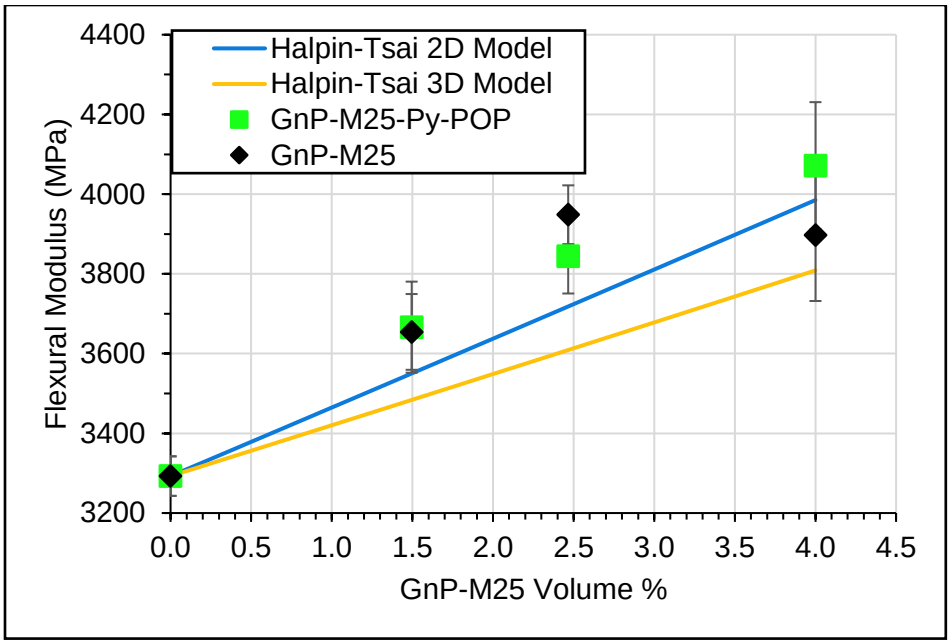

Figure 5.9: Halpin-Tsai model for flexural modulus.

A common model to predict the modulus of composite materials is the Halpin-Tsai equation [12]. The model representing 2D randomly oriented filler more closely predicts the flexural modulus than the 3D randomly oriented filler model. Since GnP is a 2D material, this is a logical estimation. The GnP-M25-Py-POP composite experimental data shows the same trendline as the Halpin-Tsai equation, just at larger values.

The flexural strength of the composites is indicated by the maximum stress applied to the coupon before fracturing. The GnP-M25-Py-POP composites showed an improvement in flexural strength of 18 and 14% over the unmodified GnP-M25 composites at 1.5 and 4 vol%, respectively. The interfacial layer of the Py-POP on the GnP surface has a lower modulus than the bulk epoxy. In turn, this assists in preventing failure at the GnP-epoxy interface. So, the composite can withstand a higher stress load before breaking.

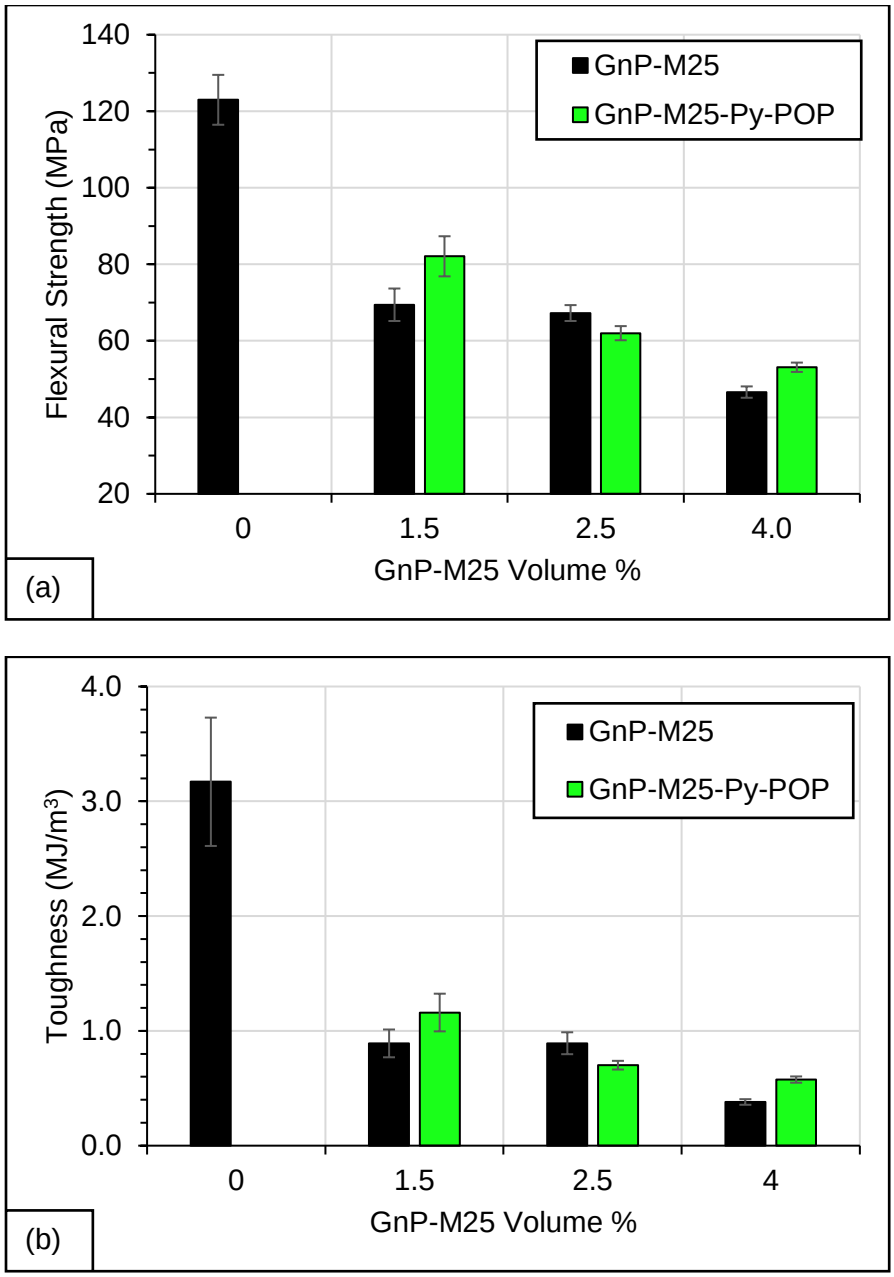

Figure 5.10: (a) Flexural strength and (b) toughness of GnP-M25 and GnP-M25-Py-POP composites.

The addition of unmodified GnP-M25 shows similar values of flexural strength at 1.5 and 2.5 vol%. At 4 vol%, there is a loss of 31% with respect to 2.5 vol% GnP-M25. The flexural strength of neat DGEBA/mPDA is 123 MPa, so addition of unmodified GnP-M25 causes a reduction of at least 44%. Adding fillers like GnP are expected to reduce

flexural strength as the nanoparticles act as fracture sites. With adsorbed Py-POP, the flexural strength was improved over GnP-M25 by 18% at 1.5 vol% and by 14% at 4 vol%. Improving the poor interface directly improved the flexural strength but is still lower than the neat DGEBA/mPDA due to the presence of GnP-M25. Both materials show a trend of decreasing flexural strength with increasing GnP-M25 concentration. Similarly, the GnP-M25-Py-POP composites have higher toughness than the GnP-M25 counterpart.

5.4.5 Thermal Properties

The glass transition temperatures were taken from the peak of the tan δ curves from DMA testing. Addition of GnP into the epoxy system disrupts the mobility of the matrix chains, thus increasing T_g. A clear example of this interaction is a 53% increase in T_g going from 0 to 1.5 vol% GnP-M25. However, with increasing GnP-M25 content, the T_g does not increase further. The value dips to a comparable value as the neat epoxy. At higher concentration, agglomeration is more likely to occur, reducing the effective GnP surface area. Therefore, there will be a weaker effect of chain movement inhibition. The significant (~35%) reduction of T_g for GnP-M25 composite from 2.5 to 4 vol% can be attributed this effect. For the GnP-M25-Py-POP composite, there is a 16.5% decrease in T_g from 2.5 to 4 vol%. The adsorbed Py-POP assists in reducing the number and size of formed agglomerates, resulting in a better dispersed composite. Additionally, the strengthened GnP/epoxy interface will improve chain movement inhibition. The Py-POP at a similar volume as the adsorbate on 4 vol% GnP-M25-Py-POP results in a T_g very similar to the material with GnP-M25. Because the Py-POP will only react with the epoxy on one end, the other untethered chain can entangle with the

rest of the epoxy matrix. This entanglement effect will similarly increase chain movement restriction to increase T_g.

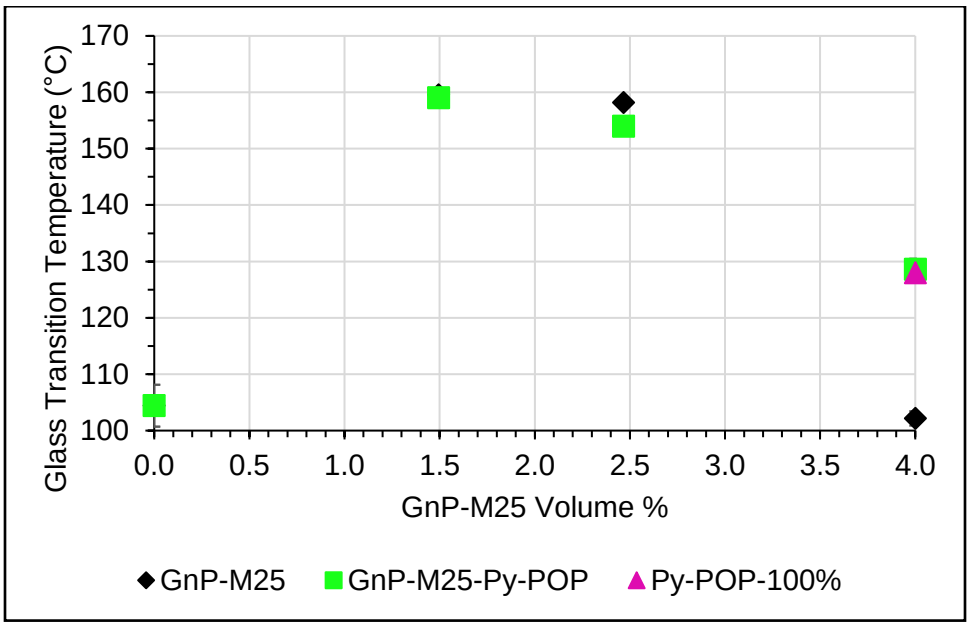

Figure 5.11: Glass transition temperature of composites using GnP-M25 (diamond), GnP-M25-Py-POP (square) and Py-POP (triangle).

Tan δ curves can also be compared to understand the effect of the GnP filler. Tan δ, or the damping parameter, is representative of energy loss in the system due to chain movement. Any fillers present will take on some of the stress load, effectively lowering the magnitude of damping experienced by the composite. In other words, the polymer chains will be less likely to move as the higher modulus filler is being affected instead. Consequently, an improvement of the filler/polymer interface will improve this stress transfer, leading to a reduction in the tan δ peak magnitude. An interfacial improvement can be seen at 2.5 vol%. The GnP-M25-Py-POP tan δ peak is 15% lower than unmodified GnP-M25 composite at this concentration, which can be contributed to both an improved GnP/polymer interface and possibly better dispersion (effectively an increase in GnP concentration).

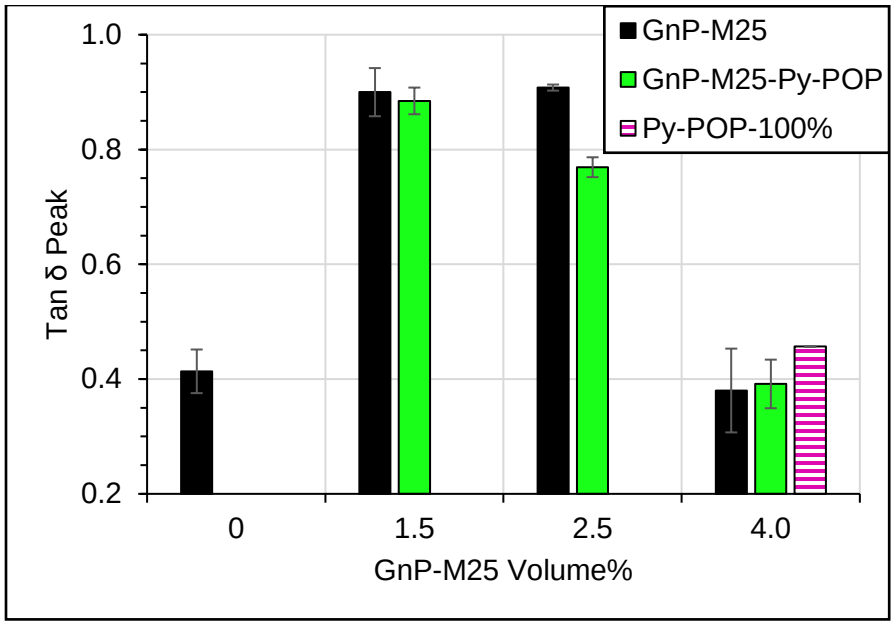

Figure 5.12: Tan δ peak magnitudes.

At 4 vol%, tan δ peaks for both materials are reduced significantly down to a similar value to the neat epoxy, which indicates increased movement restriction of the polymer chains [24]. Theoretically, higher concentration of stiff fillers should increase T_g. However, the T_g does not increase at 4 vol% with a reduced tan δ peak. At the highest concentration of GnP-M25 considered, there are expected to be a higher number and larger agglomerates present, effectively reducing the overall GnP surface area. Lower GnP surface area, in turn, will have less of an effect on the composite properties. In a well dispersed composite at the same concentration, the T_g is expected to increase. At 4 vol%, the GnP-M25-Py-POP composite has a T_g 27 °C higher than the GnP-M25 composite. Additionally, the presence of Py-POP without GnP-M25 has very little effect on the tan δ peak, resulting in a peak value similar to that of the neat epoxy. This supports that the adsorbed Py-POP improves the interface between the GnP surface and epoxy network over unmodified GnP-M25.

Loss modulus represents energy dissipated as heat caused by interfacial friction.

Incorporation of GnP will broaden the loss modulus peak due to chain inhibition and will increase with GnP concentration. As shown in Fig. 5.13, the loss modulus peak is the broadest for all materials at 4 vol%. In addition, GnP-M25-Py-POP shows a 20% broader peak than the GnP-M25 composite. These results are evidence that the GnP-M25-Py-POP is inhibiting the epoxy chain movement to a greater extent than GnP-M25. This follows since the T_g at 4 vol% is higher for the GnP-M25-Py-POP composite.

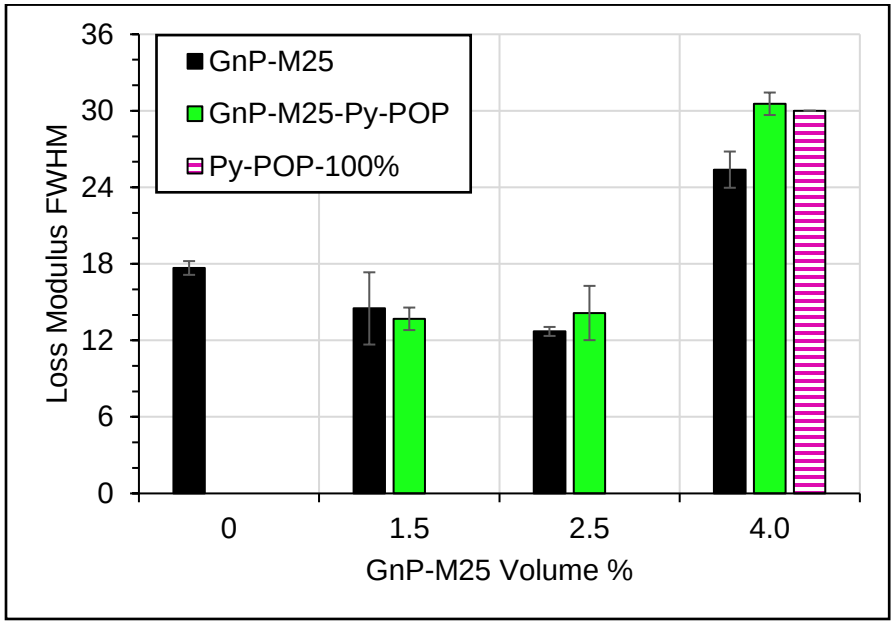

Figure 5.13: Full width half maximum (FWHM) of loss modulus peaks for GnP-M25 and GnP-M25-Py-POP composites.

Analyzing the normalized loss modulus curves grants further insight into the interfacial reaction between the GnP and epoxy with Py-POP. Using a normalized temperature for the x axis, the differences in the shape of the normalized loss modulus curve are easier to visualize. All of the samples shown in Fig. 5.14a exhibit increased E" in the elastic region and broadening of the E" peak. Below T_{Peak}, GnP-M25-Py-POP widens the E" peak by the largest amount versus the other materials. The subtracted curves for GnP-M25-Py-POP and Py-POP follow a very similar trend below T_{Peak}, which

differs from GnP-M25. Py-POP at the surface of GnP-M25 generates a lower modulus layer that will experience more chain movement (increasing E”) below the temperature necessary for the bulk epoxy. Since GnP-M25 without Py-POP does not experience this same trend, this effect is attributed to the presence of Py-POP. Above T_{Peak}, Py-POP does not impede chain movement, so the E” curve resembles the neat epoxy. Conversely, GnP-M25 restricts chain movement and widens the E” curve towards higher temperatures. The combination of these two materials results in the effect shown for GnP-M25-Py-POP. There is broadening of the E” curve towards higher temperatures due to the presence of GnP-M25, but because of the lower modulus layer at the GnP surface, this effect is lessened.

The temperature at the E” peak also indicate changes in the composite. Shifts to higher temperatures imply that the polymer chains are restricted and require higher temperatures to initiate bulk movement. As shown in Figure 5.14b, 1.5 vol% GnP-M25-Py-POP increases the E” peak temperature by ~50 °C. However, increasing GnP-M25-Py-POP concentration further results in a decreasing peak E” temperature. So, at 4 vol%, there is an increase of ~20 °C over the neat epoxy. As discussed previously, the Py-POP interfacial layer at the GnP surface is a lower modulus than the bulk epoxy. So, increasing the volume of GnP-M25-Py-POP will induce a greater effect. 4 vol% GnP-M25 composites exhibit a slight decrease in E” peak temperature with respect to the neat epoxy due to GnP agglomeration and chain network interruption. At 4 vol%, GnP-M25-Py-POP and Py-POP show very similar E” peak temperatures.

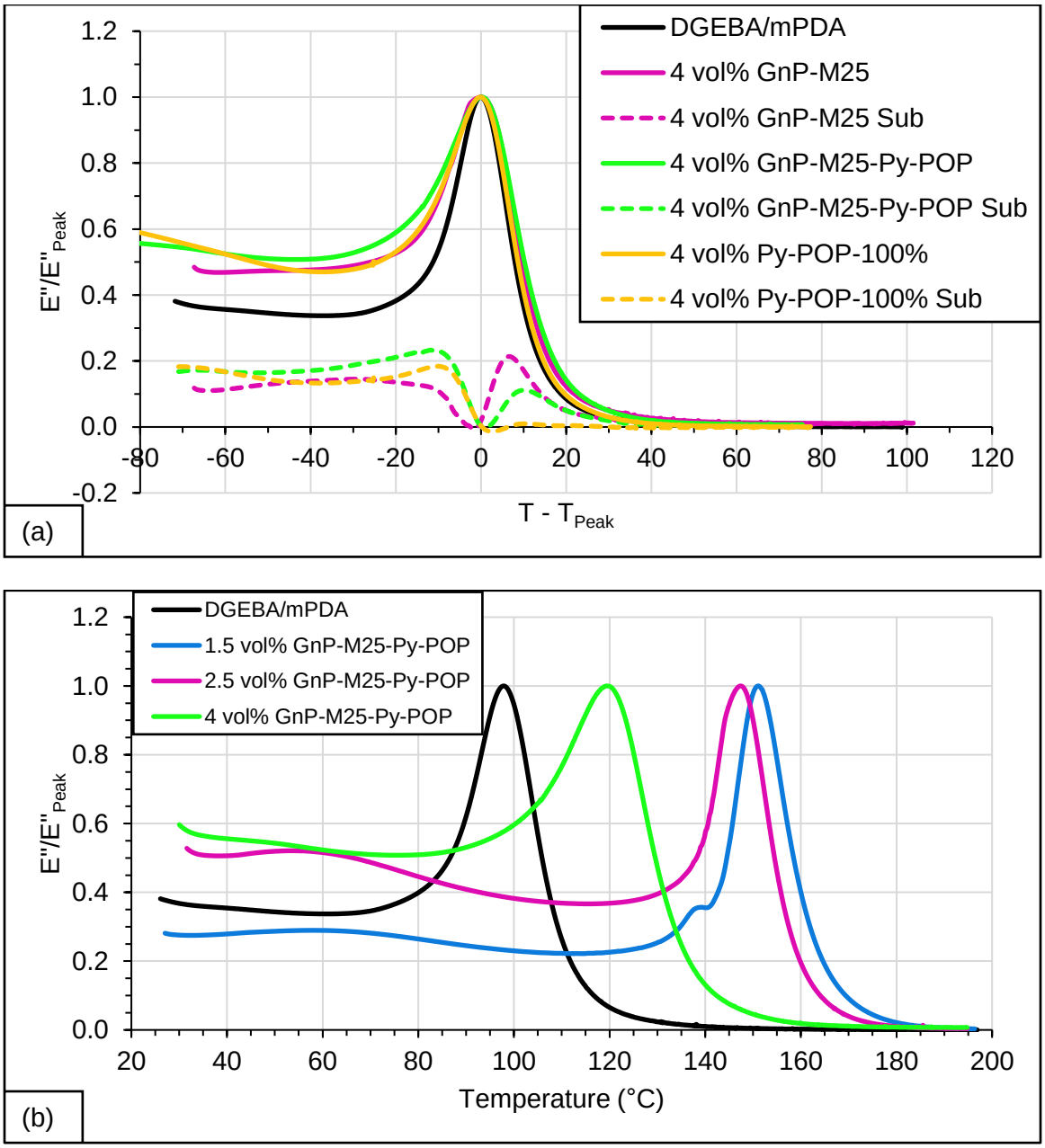

Figure 5.14: Normalized loss modulus curves for GnP-M25, GnP-M25-Py-POP, and 100% Py-POP composites.

Figure 5.14 (cont'd)

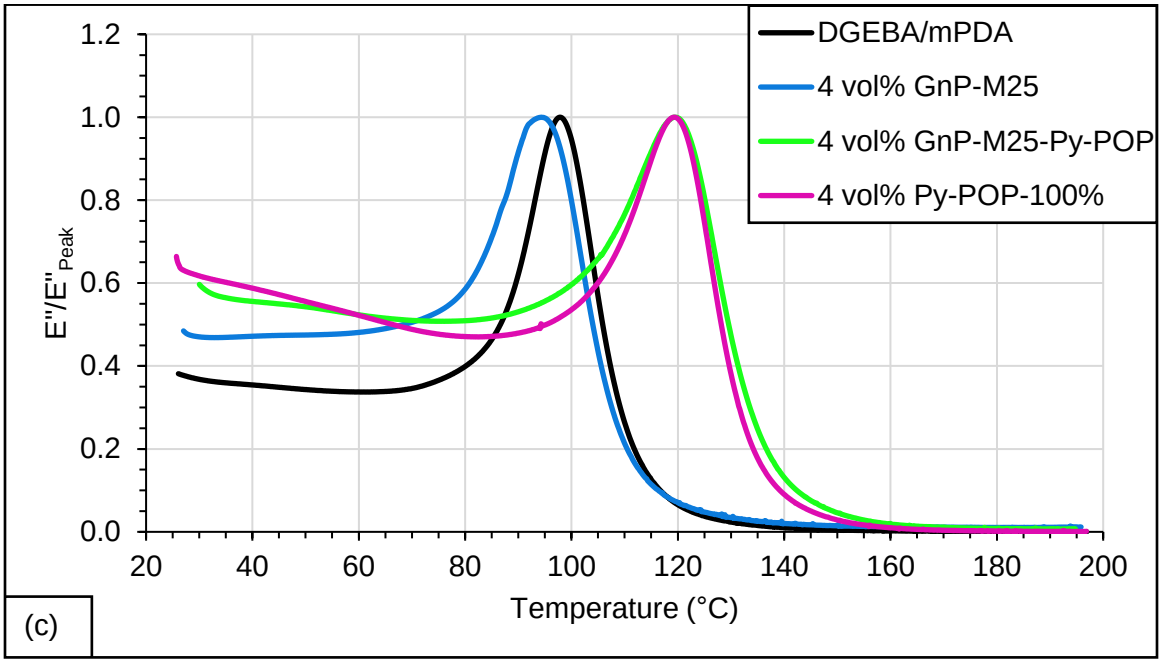

5.4.6 Electrical and Thermal Conductivity

Incorporating GnP-M25 into DGEBA/mPDA is expected to improve the thermal conductivity of the composite. Similarly, with increasing GnP concentration, the composites' thermal conductivity will also increase due to the increase in GnP/polymer interfacial area. With the exception at 2.5 vol%, the thermal conductivity of GnP-M25-Py-POP composites is lower than that of GnP-M25 composites. There is a decrease of 27% at 1.5 vol% and 17% at 4 vol%. The limiting factor for improving thermal conductivity in this case is the interfacial thermal resistance [13]. One method to reduce the resistance is by functionalizing the graphene surface; however, any molecules covalently or non-covalently bonded to the graphene surface will cause phonon scattering, reducing the overall thermal conductivity. Despite this, the GnP-M25-Py-POP shows a trend in increasing thermal conductivity with concentration. In addition, incorporating Py-POP without GnP-M25 does not cause a significant increase in

thermal conductivity. This further supports that the GnP-M25 is the dominating factor in increasing thermal conductivity.

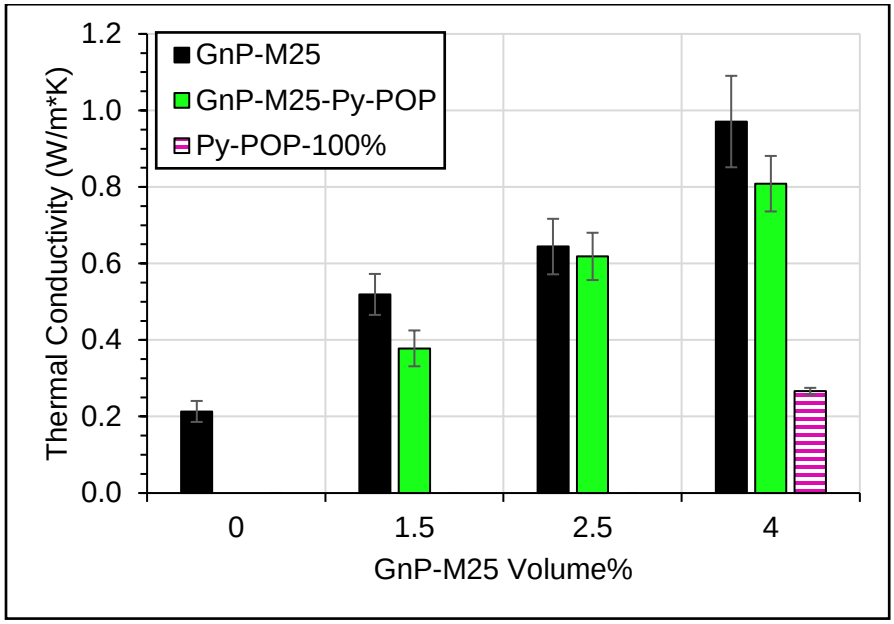

Figure 5.15: Thermal conductivity of GnP-M25 and GnP-M25-Py-POP composites.

Isolated graphene is reported to have an electrical conductivity of ~10^8 Sm^{-1} [17]. Incorporating GnP-M25 into an epoxy is expected to increase the electrical conductivity of the composite over the neat polymer. Shown in Figure 5.16, the electrical conductivity of the GnP-M25-Py-POP composite increases at a much greater rate with concentration than the unmodified GnP-M25 composite. This improvement is very apparent at 2.5 and 4 vol%. These results are indication of an improved interface between the graphene surface and epoxy. With only weak intermolecular forces connecting the GnP-M25 and epoxy matrix, the electrical conductivity is essentially limited by the dispersion and percolation of the platelets. So, if the dispersion is not uniform throughout the composite, the electrical conductivity will not show as drastic an increase. For the GnP-M25-Py-POP composites, a combination of improved dispersion, reduced agglomeration, and enhanced GnP surface/epoxy interface is likely the cause for such a

considerable increase in the electrical conductivity. The π-π stacking between the GnP surface and pyrene moiety allows for a higher efficiency of electron transfer. This interaction overcomes the need for platelet percolation to increase electrical conductivity. Since Py-POP is covalently bonded with the epoxy matrix, there is not another step for the current to pass through that will further impede the flow. The π-π stacking introduces an easy pathway for the current to travel between the GnP and epoxy matrix. Py-POP without GnP-M25 resulted in electrical conductivity indistinguishable from the neat epoxy material.

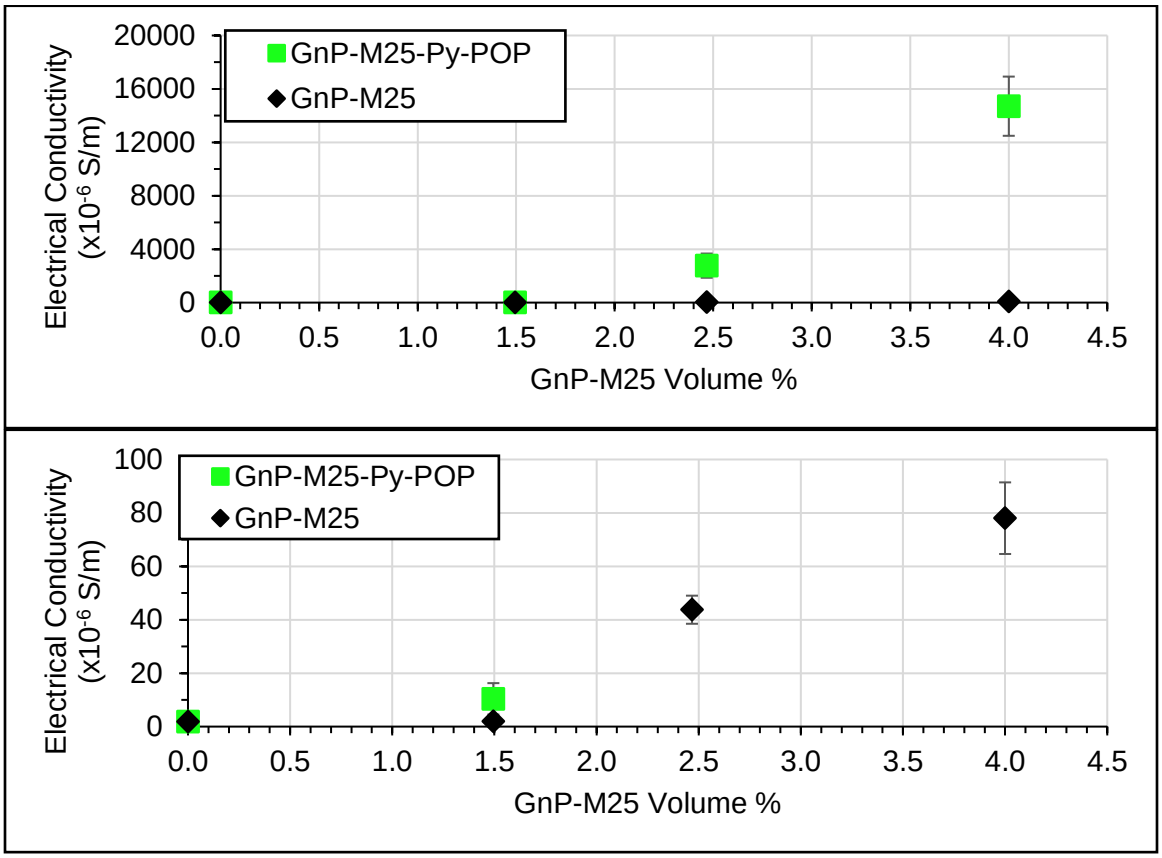

Figure 5.16: Electrical conductivity of GnP-M25 and GnP-M25-Py-POP composites. (a) Full range to show GnP-M25-Py-POP, (b) zoomed in to see trend of GnP-M25.

Table 5.5: Electrical conductivity for GnP-M25 and GnP-M25-Py-POP composites.

	Electrical Conductivity ($x10^{-6}$ S/m)	
Filler Concentration (vol%)	GnP-M25	GnP-M25-Py-POP
0	1.86 ± 0.07	1.86 ± 0.07
1.5	1.95 ± 0.09	10.4 ± 5.88
2.5	43.8 ± 5.26	2768 ± 907
4	78.0 ± 13.4	14704 ± 2220

The electrical percolation threshold can be estimated from the electrical conductivity measurements [17]. As shown in Table 5.6, the percolation threshold for GnP-M25-Py-POP is 18% lower than for GnP-M25. The primary factors affecting percolation threshold are particle size, shape, orientation, and distribution. Better dispersed and larger aspect ratio GnP will show a lower percolation threshold, and since there is no expected change in GnP size, this is evidence for improved dispersion.

Table 5.6: Electrical percolation threshold for GnP-M25 and GnP-M25-Py-POP composites.

Composite Filler	**Percolation Threshold (vol %)**
GnP-M25	1.41
GnP-M25-Py-POP	1.15

5.5 Conclusion

Non-covalent bonding Py-POP to the GnP surface has made significant changes in the resulting composite properties. This adsorption was confirmed to be an exclusively physical interaction by Laser Raman and TGA. As shown in the normalized loss modulus curves, the Py-POP at the GnP surface creates an interfacial layer that is softer (lower modulus) than the bulk epoxy. The presence of Py-POP improves the dispersion over unmodified GnP composites by reducing the agglomeration of platelets. Improving dispersion of GnP is an effective method of enhancing the multifunctionality

of the composite.

The flexural modulus is improved over unmodified GnP-M25 composites at 4 vol%. GnP-M25-Py-POP flexural modulus shows a trend of increasing with GnP concentration. For unmodified GnP-M25, the flexural modulus increases but plateaus or slightly decreases at 4 vol%. At this loading, agglomeration becomes a larger issue, which is apparent for GnP-M25, but this problem is minimized with adsorbed Py-POP. However, due to the lower modulus interfacial layer, the increase in flexural modulus of the composite does not experience a dramatic increase. For flexural strength, the presence of Py-POP and the improvement in the GnP/epoxy interface it brings also increases the flexural strength over the unmodified GnP-M25 composites. Similarly, the glass transition temperature for GnP-M25-Py-POP at this concentration is ~30 °C higher than GnP-M25 due to the improved interface and dispersion.

Finally, the improved GnP surface/epoxy interface greatly increases the electrical conductivity of the composite. At 4 vol%, the GnP-M25-Py-POP composite is ~19000% larger than the GnP-M25 composite. This work gives evidence to support that improving the GnP surface/polymer interface can improve a composite's properties. This is shown through improved dispersion, mechanical, thermal, and electrical properties.

BIBLIOGRAPHY

[1] Adeola, Adedapo O., and Patricia BC Forbes. "Optimization of the sorption of selected polycyclic aromatic hydrocarbons by regenerable graphene wool." Water Science and Technology 80.10 (2019): 1931-1943.

[2] ASTM Standard E1269, 2011, “Standard Test Method for Determining Specific Heat Capacity by Differential Scanning Calorimetry,” ASTM International, West Conshohocken, PA, 2011, DOI:10.1520/E1269-11R18, www.astm.org.

[3] ASTM Standard E1461, 2013, “Standard Test Method for Thermal Diffusivity by the Flash Method,” ASTM International, West Conshohocken, PA, 2013, DOI:10.1520/E1461-13R22, www.astm.org.

[4] ASTM Standard E2550, 2021, “Standard Test Method for Thermal Stability by Thermogravimetry,” ASTM International, West Conshohocken, PA, 2021, DOI: 10.1520/D0790-17, www.astm.org.

[5] ASTM Standard D790, 2017, “Standard Test Methods for Flexural Properties of Unreinforced and Reinforced Plastics and Electrical Insulating Materials,” ASTM International, West Conshohocken, PA, 2021, DOI:10.1520/E2550-21, www.astm.org.

[6] ASTM Standard D792, 2020, “Standard Test Methods for Density and Specific Gravity (Relative Density) of Plastics by Displacement,” ASTM International, West Conshohocken, PA, 2020, DOI: 10.1520/D0792-20, www.astm.org.

[7] Björk, Jonas, et al. "Adsorption of aromatic and anti-aromatic systems on graphene through π− π stacking." The Journal of Physical Chemistry Letters 1.23 (2010): 3407-3412.

[8] Childres, Isaac, et al. "Raman spectroscopy of graphene and related materials." New developments in photon and materials research 1 (2013): 1-20.

[9] Choi, Eun Yeob, Lak Won Choi, and C. K. Kim. "Noncovalent functionalization of multi-walled carbon nanotubes with hydroxyl group-containing pyrene derivatives for their composites with polycarbonate." Carbon 95 (2015): 91-99.

[10] Eitan, A., et al. "Reinforcement mechanisms in MWCNT-filled polycarbonate." Composites Science and Technology 66.9 (2006): 1162-1173.

[11] Gupta, V. B., et al. "The temperature-dependence of some mechanical properties of a cured epoxy resin system." Polymer Engineering & Science 25.13 (1985): 812-823.

[12] Halpin, JC, and J. L. Kardos. "The Halpin-Tsai equations: a review." Polymer Engineering & Science 16.5 (1976): 344-352.

[13] Huang, Xingyi, et al. "Thermal conductivity of graphene-based polymer nanocomposites." Materials Science and Engineering: R: Reports 142 (2020): 100577.

[14] King, Julia A., et al. "Mechanical properties of graphene nanoplatelet/epoxy composites." Journal of applied polymer science 128.6 (2013): 4217-4223.

[15] King, Julia A., et al. "Mechanical properties of graphene nanoplatelet/epoxy composites." Journal of Composite Materials 49.6 (2015): 659-668.

[16] Li, Bing, et al. "Polycyclic aromatic hydrocarbons adsorption onto graphene: a DFT and AIMD study." *Materials* 11.5 (2018): 726.

[17] Li, Yan, et al. "Mechanical, electrical and thermal properties of in-situ exfoliated graphene/epoxy nanocomposites." Composites Part A: Applied Science and Manufacturing 95 (2017): 229-236.

[18] Liu, Jia Daniel, et al. "Effect of crosslink density on fracture behavior of model epoxies containing block copolymer nanoparticles." Polymer 50.19 (2009): 4683-4689.

[19] Liu, Jingquan, et al. "Thermosensitive graphene nanocomposites formed using pyrene-terminal polymers made by RAFT polymerization." Journal of Polymer Science Part A: Polymer Chemistry 48.2 (2010): 425-433.

[20] Nan, Ce-Wen, Yang Shen, and Jing Ma. "Physical properties of composites near percolation." Annual Review of Materials Research 40.1 (2010): 131-151.

[21] Nielsen, Lawrence E. "Cross-linking–effect on physical properties of polymers." Journal of Macromolecular Science, Part C 3.1 (1969): 69-103.

[22] Read, Oliver, et al. "Insights into the exfoliation mechanism of pyrene-assisted liquid phase exfoliation of graphene from lateral size-thickness characterisation." Carbon 186 (2022): 550-559.

[23] Tyson, Bryan M., et al. "A quantitative method for analyzing the dispersion and agglomeration of nano-particles in composite materials." Composites Part B: Engineering 42.6 (2011): 1395-1403.

[24] Vennerberg, Danny, Zach Rueger, and Michael R. Kessler. "Effect of silane structure on the properties of silanized multiwalled carbon nanotube-epoxy nanocomposites." Polymer 55.7 (2014): 1854-1865.

[25] Wang, Jun, Zaiming Chen, and Baoliang Chen. "Adsorption of polycyclic aromatic hydrocarbons by graphene and graphene oxide nanosheets." Environmental science & technology 48.9 (2014): 4817-4825.

[26] Xu, Liyan, and Xiaoning Yang. "Molecular dynamics simulation of adsorption of

pyrene–polyethylene glycol onto graphene." Journal of colloid and interface science 418 (2014): 66-73.

[27] Zaman, Izzuddin, et al. "Epoxy/graphene platelets nanocomposites with two levels of interface strength." Polymer 52.7 (2011): 1603-1611.

[28] Zaman, Izzuddin, et al. "Interface modification of clay and graphene platelets reinforced epoxy nanocomposites: a comparative study." Journal of materials science 49.17 (2014): 5856-5865.

[29] Zheng, Wenge, Bin Shen, and Wentao Zhai. "Surface functionalization of graphene with polymers for enhanced properties." New progress on graphene research 10 (2013): 50490.

CHAPTER 6: SUMMARY AND FUTURE WORK

6.1 Summary

The research discussed in this dissertation focused improving the interface between the graphene nanoplatelet (GnP) surface and epoxy resin. Three molecules were chosen to noncovalently interact with the GnP surface to influence this interface. One molecule, 1-pyrenealdehyde, exhibited strong noncovalent interactions with the GnP surface and relatively weak interactions with the epoxy, the second, poly(oxypropylene) diamine, showed weak noncovalent interactions with GnP but covalently bonded with the epoxy, and the third, α-isopropyliminopyrene-ω-amino-poly[oxy(2-methylethylene)] (Py-POP), strongly interacted with the GnP surface and covalently bonded with the epoxy. The third molecule was synthesized for this work. Changes in mechanical, thermal, and electrical properties and quality of dispersion of GnP nanocomposites were investigated.

Chapter 2 discussed the synthesis of an interfacial molecule that formed a strong noncovalent interaction with the GnP surface and covalently bonded with the epoxy resin. Starting with a poly(oxypropylene) diamine (Jeffamine D2000), one primary amine end was capped with a pyrene moiety using 1-pyrenealdehyde. This product, labeled Py-POP, was a poly(oxypropylene) chain with a primary amine at one end and a pyrene molecule at the other. FTIR results indicated the presence of the imine bond formed from the aldehyde and amine condensation reaction. Mass spectrometry further determined the purity of the product by showing low concentrations of each reagent and di-pyrene molecules.

In Chapter 3, Jeffamine D2000 was adsorbed to the GnP-M25 surface through

noncovalent interactions. Although the intermolecular interactions are limited to weak van der Waals forces, thermogravimetric analysis indicated the presence of adsorbed D2000. The adsorbed D2000 can react with the epoxy during the curing process through the primary amine groups. The D2000 interfacial layer on the GnP decreased the flexural modulus of the GnP-M25-D2000 composite compared with the unmodified GnP material. Due to the flexibility of the D2000 molecule, the glass transition temperature decreased as well. Through improved quality of dispersion of the GnP, the electrical conductivity was increased at the highest GnP loading.

Chapter 4 discussed adsorbing 1-pyrenealdehyde to the GnP-M25 basal plane. Both materials have a six-membered carbon aromatic ring structure, creating strong bonds between them through π-π stacking. This resulted in adsorption coverage at 78% of the theoretical maximum monolayer of pyrene. The flexural modulus of 4 vol% GnP-M25-Pyrenealdehyde increased 40% over the unmodified GnP composite due to the intercalative nature of pyrene and improved GnP dispersion. However, the flexural strength showed no change with the adsorbed 1-pyrenealdehyde because the interfacial interactions between the GnP surface and epoxy were not significantly altered. Because GnP and 1-pyrenealdehyde have extremely similar structures, there was a negligible change in interactions with the epoxy once the 1-pyrenealdehyde was adsorbed, leading to small changes in the composite properties. Improved dispersion and exfoliation due to 1-pyrenealdehyde adsorption was determined to be the cause of enhanced properties.

Lastly, Chapter 5 discussed the effects of noncovalently adsorbed Py-POP on the GnP-M25 surface. The pyrene-terminated end adsorbed strongly to the GnP

surface, and the primary amine end reacted with the epoxy. Because of the low modulus interfacial layer of Py-POP on the GnP, the flexural modulus did not increase above the unmodified GnP composites significantly. This strong linkage led to improved flexural strength and glass transition temperature, which correlates to improved interfacial interactions. Along with better quality of dispersion, this interfacial Py-POP layer improved the electrical conductivity of the composite by ~19000% at 4 vol% GnP-M25.

6.2 Future Work

6.2.1 Optimizing Adsorption of Py-POP

As discussed in Chapter 5, the amount of Py-POP adsorbed to the GnP surface correlates to roughly 30% of theoretical maximum pyrene coverage. While steric effects limit the adsorption, increasing the amount of Py-POP adsorbed is expected to increase the noticeable effects on the composite at lower GnP concentration. Investigating different polar solvents for the adsorption step is one way to optimize Py-POP adsorption. GnP-M25 contains oxygen functional groups along its edges, but at a relative concentration that is very small compared with the basal plane surface area. These edge groups could influence the efficiency of Py-POP adsorption. Passivating or removing the oxygen edge groups can eliminate any interactions with the Py-POP molecules.

6.2.2 Varying Structure of Filler Materials

Varying the molecular weight of the poly(oxypropylene) chain can affect the composite properties. Longer or shorter chains of Py-POP would change the volume of the interfacial layer between the GnP surface and epoxy. A larger or smaller interfacial

volume of lower modulus material, such as Py-POP, can influence the overall composite properties through difference in quality of dispersion, mechanical, and thermal properties.

Another route of future work involves investigating the effects of the size of the anchor polycyclic aromatic hydrocarbon (PAH). Previous simulation studies have shown that increasing the size of the PAH increases the adhesion energy. So, it would be valuable to understand the significance of the adhesion strength between the PAH and GnP surface in terms of composite properties.

Varying the size of the GnP is another variable that would be important to investigate. Increasing the GnP surface area also increases the theoretical maximum adsorption of interfacial molecules, resulting in a larger effect at lower GnP concentration. Smaller sized GnP requires less volume for a higher percentage of adsorption, which can also induce greater effects on the composite.